

COMBUSTION IN A GAS STREAM

Studies in "flame spreading" and "flame stability".

by

N. R. L. Maccallum, B.Sc.

ProQuest Number: 13848981

All rights reserved

INFORMATION TO ALL USERS

The quality of this reproduction is dependent upon the quality of the copy submitted.

In the unlikely event that the author did not send a complete manuscript and there are missing pages, these will be noted. Also, if material had to be removed, a note will indicate the deletion.



ProQuest 13848981

Published by ProQuest LLC (2019). Copyright of the Dissertation is held by the Author.

All rights reserved.

This work is protected against unauthorized copying under Title 17, United States Code
Microform Edition © ProQuest LLC.

ProQuest LLC.
789 East Eisenhower Parkway
P.O. Box 1346
Ann Arbor, MI 48106 – 1346

CONTENTS.

	<u>Page No.</u>
Preface	1
Chapter 1 Theory of Flame Spreading	4
Chapter 2 Preliminary Study of Flame Spreading in a Ramjet	28
Chapter 3 Measurements of Combustion Efficiency in a Ramjet using Flame Spreaders	48
Chapter 4 Development of Apparatus for Small Scale Flame Spreading Experiments	63
Chapter 5 Flame Blow-off from Rectangular Burners	90
Chapter 6 Conclusions and Suggestions for further research	106
Appendix I One dimensional flow in a ramjet combustion chamber	112
Appendix II Flow through a Capillary Meter	120
Appendix III The Calibration and Use of Soap Bubble Meters, Wet Gas Meters, and Dry Gas Meters.	128
Appendix IV Laminar Flow in a Channel of Rectangular cross-section.	134
Bibliography	138
List of Tables	144
List of Figures	145
List of Symbols	148
Published Papers.	

PREFACE

In many steady flow combustion systems in which homogeneous mixtures of fuel and air are burned the flame is anchored on some form of stabiliser. Downstream from the stabiliser the flame spreads across the current of fuel-air mixture. The flame-spreading process governs the overall rate of combustion, and is a matter of importance in certain practical propulsion devices such as the ramjet. The nature of the process and the factors which affect it are therefore worthy of serious investigation, and form the subject of this thesis. Already there is a growing literature on flame spreading. This is reviewed in Chapter 1.

The author began his study of the subject in May 1952 when invited by Professor Small to join the combustion research team of the University of Glasgow. The subject had been proposed by Mr. P. Lloyd of the National Gas Turbine Establishment, Pyestock, and on his suggestion the author spent the summers of 1952 and 1953 on experimental work at Pyestock. An exploratory series of experiments on flame spreading in a ramjet was first carried out, and is described in Chapter 2. In these preliminary experiments an investigation was made of the operation of flame spreaders. These are physical arrangements such as baffles, inclined fingers, etc., which are inserted in the fuel-air stream and

are intended to hasten the flame spreading process. The influence of the geometry of the device on the overall combustion efficiency was studied systematically in a second series of experiments reported in Chapter 3.

These full scale experiments suggested that before the flame spreading process is fully understood a more detailed knowledge is required of (a) the flow of pilot gases in the wake of the finger and (b) the ignition of a secondary flame by a pilot source. The second of these was chosen for further study. In Chapters 4 and 5 the results are presented of work which has been completed as a preparation for small scale experiments in this field.

One of the techniques developed for the small scale experiments involves the use of an Ionisation Probe. In designing a burner for its calibration the author found that the literature on flame blow-off was misleading in its references to rectangular burners, and a substantial part of this thesis (Chapter 5) is developed from this. The work has led to new knowledge which has been published (see below).

The main conclusions of the work described in this thesis and suggestions for further research are given in Chapter 6.

Publications.

A review of "Flame Spreading Characteristics in Combustion" has been prepared for publication in Combustion Researches and Reviews, 1956, A.G.A.R.D., Butterworths

Scientific Publications, London. This review is based on the literature survey given in Chapter 1, but it also includes mention of some of the results of the flame spreading experiments described in Chapters 2 and 3.

A paper entitled "Flame blow-off from Rectangular Burners" has been accepted for publication by the Editor of Fuel. This paper, which is based on Chapter 5, corrects and extends the hitherto accepted authority (Grumer, Harris and Schultz, 1953) on this subject.

A contribution on "Electronic Probe Measurements in Flames" has been made to the discussion at the Joint Conference on Combustion held in London in October 1955 under the auspices of the Institution of Mechanical Engineers.

Preprints of these three publications are included as an appendix to the thesis.

Acknowledgements.

The author wishes to thank Professor James Small and Dr. J. Barr of the University of Glasgow for their encouragement and guidance, and to acknowledge the facilities granted to him by the former. He also wishes to acknowledge the help given to him by Mr. G. O. Goudie, formerly of the University of Glasgow, in obtaining some of the experimental observations referred to in Chapter 2 and in Appendix III.

CHAPTER I.

THEORY OF FLAME SPREADING.

- 1.1 Introduction.
- 1.2 Laminar flame propagation.
- 1.3 Flame spreading in laminar flow
 - 1.31 Flame stabilisation on bunsen burners.
 - 1.32 Flame spreading.
- 1.4 Flame spreading in turbulent flow.
 - 1.41 Flame stabilisation by bluff bodies.
 - 1.42 Flame stabilisation by cans.
 - 1.43 Flame stabilisation by independent pilots.
 - 1.44 The concept of turbulent burning velocity.
 - 1.45 The use of the turbulent burning velocity in calculating flame spreading in enclosed burners.
 - 1.46 Flame spreading in a ramjet.
- 1.5 Discussion.

CHAPTER 1.

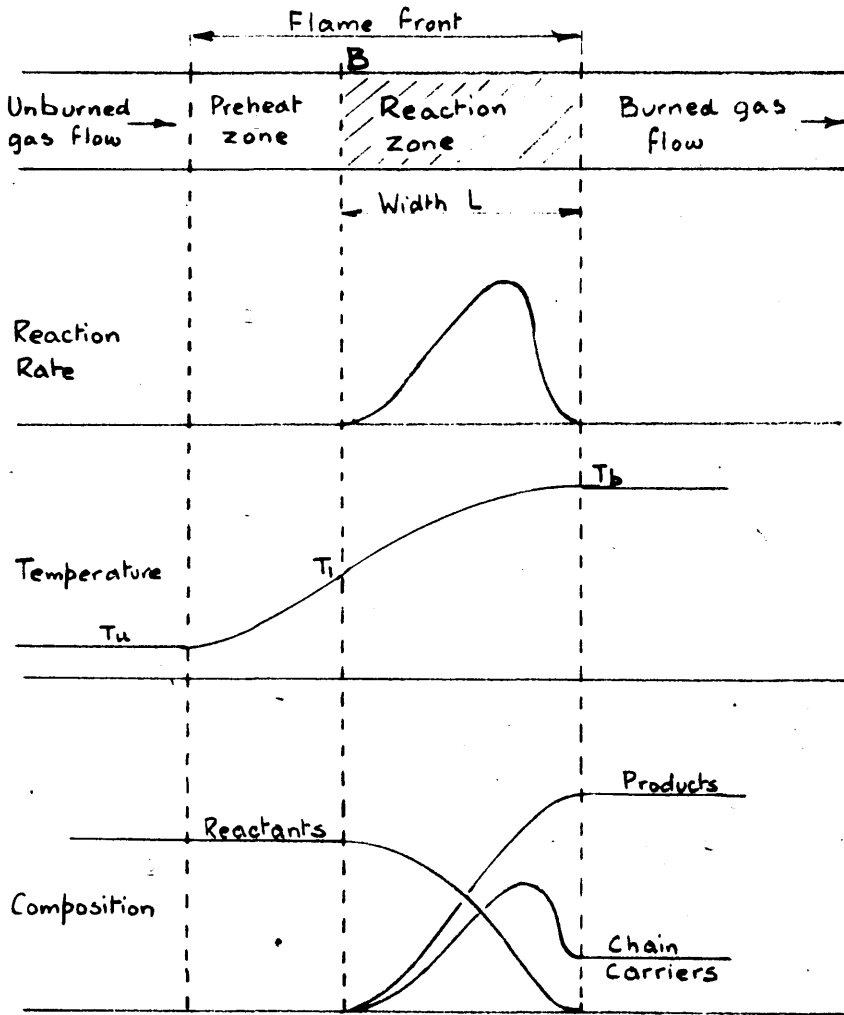
1.1 Introduction

The subject of this thesis is the manner in which a flame "spreads" from a pilot, or source, into a moving homogeneous stream of fuel and air. The literature relevant to the flame spreading process is reviewed briefly in this Chapter. Since flame spreading can take place only if a flame is successfully stabilised, a discussion of the mechanism of flame stabilisation is also given for the various flame spreading systems which are considered. In the review given below, the combustion systems in which flame spreading takes place are divided into two groups. The first group (paragraph 1.3) consists of those systems in which the flow is laminar. An example of this type is the inner cone of a laminar bunsen flame. In the second group (paragraph 1.4) are included the high velocity systems in which the flow is turbulent. This section includes turbulent bunsen-type flames, and the typical ramjet combustion system.

However, before these two groups of combustion systems are discussed, the fundamental concept of laminar flame propagation, and the associated property of laminar burning velocity, are considered. These concepts are discussed at this stage because it is upon them that some of the "flame spreading" theories are based.

FIG. 1 FLAME PROPAGATION

Qualitative structure of stationary wave.
Based on Lewis and von Elbe (1951, p231)



1.2 Laminar Flame Propagation.

When a suitable source of ignition is provided in an explosive gas mixture a reaction wave, originating at the ignition source, passes through the gas. If this reaction wave propagates by the processes of diffusion and heat transfer it is known as a combustion or deflagration wave. However, in some cases a very fast moving wave may develop, maintained by the energy of the chemical reaction of the highly compressed medium in the wave. This second type of wave is referred to as a detonation wave. Only the first of these two types of waves, the combustion wave, is applicable to the study of flame spreading in steady flow systems, and it alone is considered below.

If, during the propagation of such a combustion wave, the motion of the gas is laminar, this is said to be an example of laminar flame propagation. The velocity of the **wave** front relative to the unburned gas is referred to as the laminar burning velocity.

Structure of a laminar flame.

If a co-ordinate system is chosen so that the reaction wave is stationary, and the gas flows through the wave in a direction normal to the wave front, then profiles may be drawn representing the probable structure of the wave (see Fig. 1). The profiles are based partly on calculations made by Lewis and von Elbe (1951, p.347) on the decomposition of ozone, and partly on measurements of temperatures in flame

fronts (Gaydon and Wolfhard, 1948; Dixon-Lewis and Wilson, 1951).

In the "preheat" zone the gas temperature rises from the temperature of the approaching unburned gas, T_u , to the temperature level T_1 . The heat required for this temperature rise is supplied by conduction from the hot gases in the reaction zone. The exothermic reaction becomes appreciable when the gases reach the temperature T_1 , which is the so called "ignition temperature". Reaction then continues until the final temperature T_b is attained.

Laminar burning velocity.

Using the model shown in Fig. 1, and making some gross assumptions an expression may be obtained for the laminar burning velocity. Firstly the heat flow into the fresh gas by conduction at the plane B is equated to the heat necessary to raise the temperature of the approaching gas from T_u to T_1 .

$$k \left(\frac{dT}{dx} \right)_B = c_p S_L \rho (T_1 - T_u) \quad \dots\dots\dots \text{Eqn. 1.1}$$

where k is the thermal conductivity of the fresh gas, assumed to be independent of temperature, c_p is the specific heat at constant pressure of the fresh gas, also assumed to be independent of temperature, S_L is the laminar burning velocity and ρ is the density of the cold gas.

An approximate relationship for the temperature gradient may be estimated from the shape of the temperature profile -

$$\left(\frac{dT}{dx}\right)_B \approx \frac{2 (T_b - T_1)}{L} \dots\dots\dots\text{Eqn. 1.2}$$

where L is the width of the reaction zone.

The mean rate of heat release in the reaction zone per unit volume, Q , may be substituted for the width of the reaction zone, L , using the relation -

$$Q L = c_p S_L \rho (T_b - T_u) \dots\dots\dots\text{Eqn. 1.3}$$

Combining the above three equations leads to the following relationship for the laminar burning velocity -

$$S_L \approx \frac{1}{c_p \rho} \left(\frac{2 k Q}{T_b - T_u} \cdot \frac{T_b - T_1}{T_1 - T_u} \right)^{\frac{1}{2}} \dots\dots\dots\text{Eqn. 1.4}$$

The above equation 1.4 has only a limited range of application.

If it is assumed that the reaction within the reaction zone is bimolecular, or uni-molecular then the equation may be

used to predict the influence of pressure on the burning

velocity, e.g. for a bimolecular reaction the average

reaction rate is proportional to the square of the pressure,

the density is proportional to the pressure and so according

to equation 1.4 the burning velocity is independent of the

pressure. By a similar treatment it is predicted that the

burning velocity varies inversely as the square root of the

pressure when the reaction is uni-molecular. However, as

stated by Friedman (1953), the equation cannot be used to

calculate the absolute burning velocity of a given mixture

because no adequate means are known of obtaining either the

average heat release in the reaction zone, or the value of the

ignition temperature.

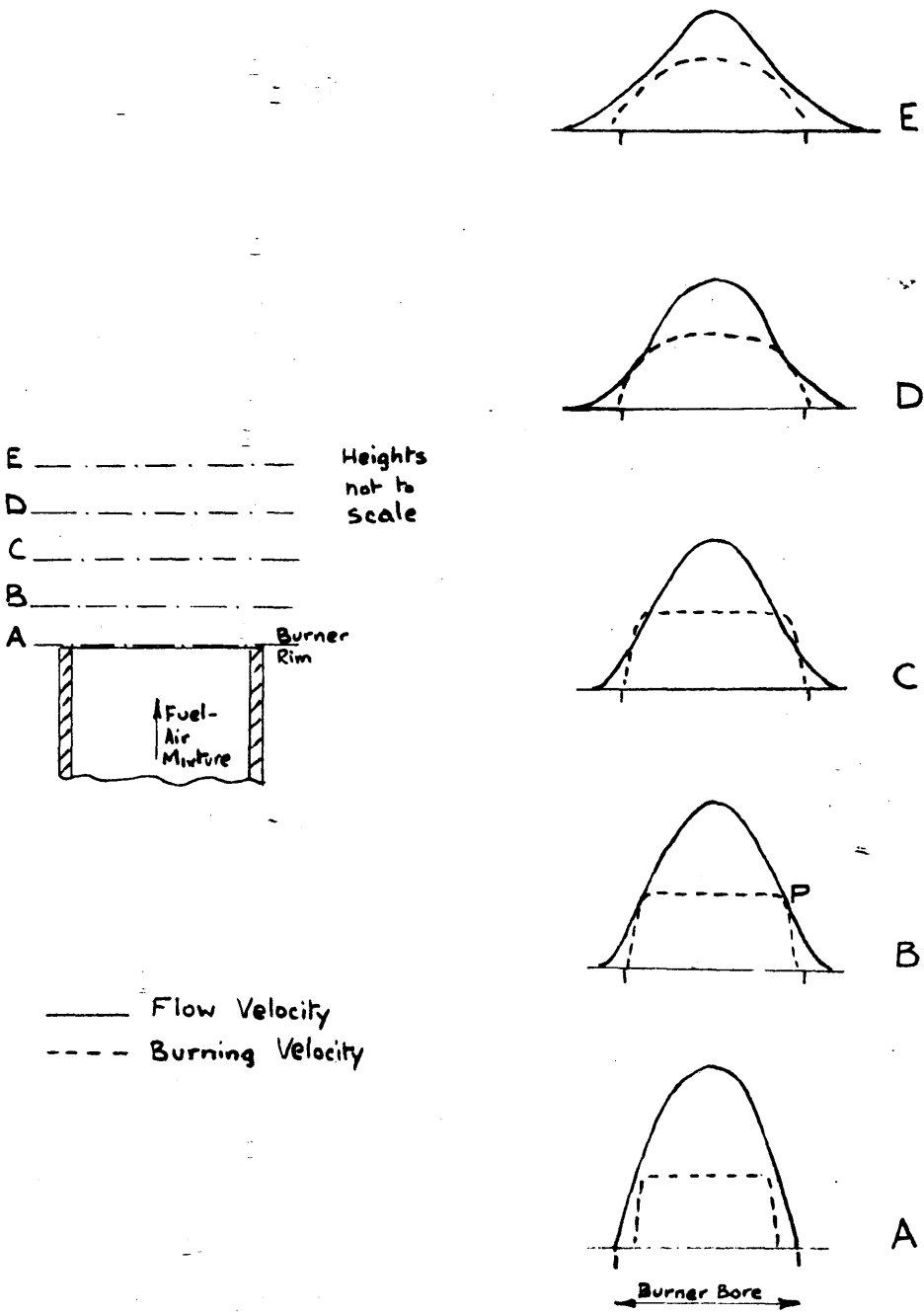
The thermal theory of flame propagation, which is outlined in its most simple form above, does not give an obvious explanation for some experimental results on the influence of hydrogen on the burning velocity of carbon monoxide (Jahn, cited by Tanford and Pease, 1947a). These results have been explained by the diffusion theories of Tanford (1947, 1949) and Tanford and Pease (1947b) who considered the influence of chain carriers on burning velocity. Here again however, the theory predicted only comparative, and not absolute values of burning velocity.

It is seen that the theories indicated above cannot yet be used to predict absolute values of the laminar burning velocity. However, a considerable body of experimental data has been obtained on the burning velocities of most of the common fuel-air and fuel-oxygen mixtures. Several methods have been used in obtaining these burning velocity measurements, including the bunsen cone method, the soap bubble method, the constant volume bomb and the flat flame burner. A recent review of these methods has been given by Linnett (1954).

1.3 Flame spreading in laminar flow.

An illustration of flame spreading in laminar flow is given by the inner cone of the simple laminar bunsen flame. As indicated in the Introduction above, the anchoring of a

FIG 2 STABILISATION OF A FUEL-WEAK FLAME ON A BUNSEN BURNER



bunsen flame will first be considered, followed by a discussion of the flame spreading.

1.31. Flame stabilisation on bunsen burners.

Consider a flame located in a flow system through which a homogeneous mixture of fuel and air is passing. Assume that the flame front is initially at right angles to the direction of flow. If now at some point the burning velocity exceeds the local flow velocity, then at that point the flame will move upstream. Likewise if the burning velocity at some point is less than the local flow velocity, then the flame there will be driven back. In general the flame will tend to assume a shape such that the local burning velocity is always equal to the component of the local flow velocity normal to the flame front. The flame will be maintained in a stable position only if the burning velocity at one point is exactly equal to the local flow velocity, at all other points the flow velocity being greater than the burning velocity.

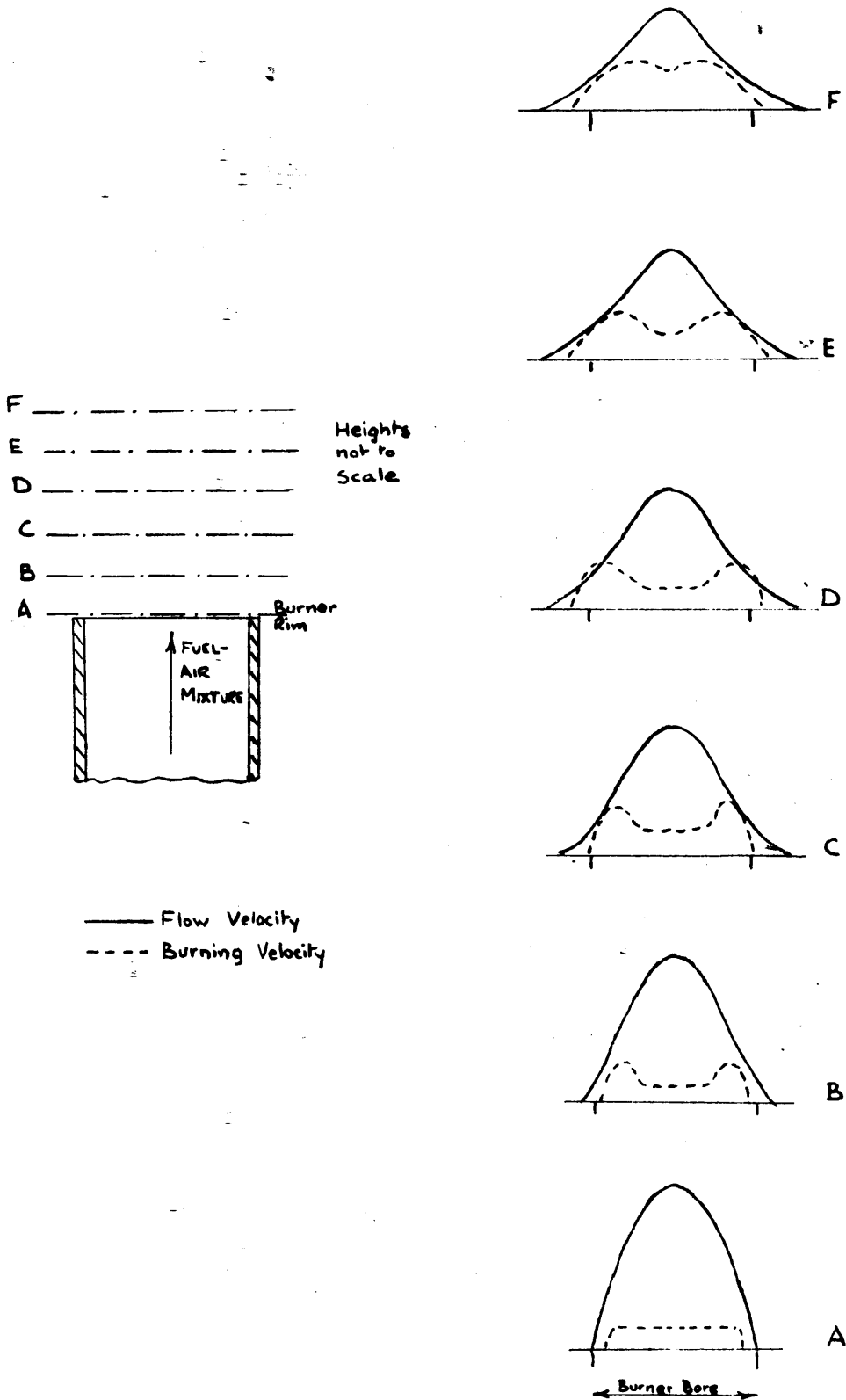
Stabilisation of fuel-weak flames.

The principle discussed above will now be applied to the case of a flame anchored in the jet issuing from a cylindrical tube, e.g. a bunsen burner. The fuel concentration in the mixture is less than the stoichiometric concentration. The flow velocity distributions at the burner rim (A), and at four heights above the rim (B, C, D and E) are given in Fig. 2.

At the burner exit A the velocity profile will be parabolic if the approach length in the burner is sufficiently great. At increasing distances from the rim the velocity distribution gradually flattens and broadens, due to momentum transfer with the surrounding air. An indication of the distribution of the laminar burning velocity at each of the heights is superimposed on the flow velocity profiles in Fig. 2. Close to the burner rim the burning velocity drops to zero due to the loss of chain carriers and heat to the burner wall. As the height above the rim is increased, this quenching effect is diminished. However, as the height increases, diffusion of ambient air into the fuel-air mixture takes place and weakens the mixture strength close to the boundary, tending to decrease the burning velocity.

At height A the flow velocity everywhere exceeds the burning velocity and therefore no flame can be stable in this position. At height B an equality exists at point P between the burning and the flow velocities and so a flame may be anchored at this height. On a further increase of height a region is reached (C) in which at one or more points the burning velocity exceeds the flow velocity. A flame lighted in this position will move upstream until the stable position at height B is reached. However, on further increasing the height a position is eventually reached at which diffusion has so reduced the burning velocity in the boundary region that a flame will be blown downstream (height E).

FIG. 3 STABILISATION OF A FUEL-RICH FLAME ON A BUNSEN BURNER



Between this region and the region where a flame moves upstream (height C) there is a position of unstable equilibrium (height D).

If a flame is anchored at position B, as indicated above, and if the flow velocity is increased, the fuel concentration remaining the same, then the height to the new position of stable equilibrium, B, is increased. The position of unstable equilibrium, D, is lowered, and on a sufficient increase in the flow rate a condition is reached in which the heights to planes B and D coincide. When this occurs the flame is on the point of "blow-off".

Stabilisation of fuel-rich flames.

When the surrounding atmosphere is air (or oxygen) an additional process enters into the mechanism of anchoring of fuel-rich flames, as compared with the mechanism, described above, of anchoring fuel-weak flames. This process, which is the increase of the burning velocity due to the diffusion of air, is illustrated in Fig. 3. In this case height C is the position of stable equilibrium.

It should be noted that in certain fuel-rich mixtures it is possible for a flame to be anchored in a "lifted" position, which may be several diameters above the burner exit.

The above outlines of the mechanism of flame stabilisation are based on the publications of Lewis and von Elbe (1951, Chapter VII), Wohl, Kapp and Gazley (1949) and others.

Correlation of blow-off limits.

From the discussion given above it is apparent that flame anchoring in a bunsen burner depends on a balance at one point between the flow velocity, and the burning velocity, and that this balance point lies close to the boundary of the stream. Since the flow velocity at a point close to the boundary is roughly proportional to the boundary velocity gradient, Lewis and von Elbe (1943) proposed that the stability limits of burners of various dimensions may be correlated by the wall velocity gradient. This correlation has been applied very successfully by Lewis and von Elbe themselves and others.

This correlation for flames anchored on tubes in which the flow is laminar has also been found to apply to stability limits of burners in which the flow is turbulent (Bollinger and Williams, 1947; Wohl, Kapp and Gazley, 1949). In this case the boundary velocity gradient is calculated from the Blasius Equation.

The correlation of blow-off limits by the boundary velocity gradient has also been applied to burners of rectangular cross-section. This work is described in Chapter 5 of this thesis.

1.32 Flame spreading.

The shape of the flame front in a bunsen flame has been predicted roughly by Lewis and von Elbe (1943).

They calculated the shape from a knowledge of the velocity distribution and by assuming that the laminar burning velocity is constant along the entire length of the flame front. The major discrepancies between the theoretical and the observed flame shapes occur at the tip of the flame, and at the flame base. At the flame tip the burning velocity is, in general, altered, due to the influences of heat conduction and diffusion in the vicinity of the sharply curved combustion wave. At the flame base the burning velocity is decreased due to quenching by the burner, as mentioned in the preceding paragraph on flame stabilisation on bunsen burners. Nevertheless, over most of the flame front the burning velocity is, in fact, constant, and in that region the experimental and theoretical flame profiles are in good agreement.

Thus, for the simple case of a laminar bunsen burner, it may be predicted with reasonable accuracy whether a flame will, or will not, be anchored under given flow conditions. If the flame is anchored, the shape it assumes may also be predicted, allowance being made for flow redistribution and quenching effects where necessary. The laminar burning velocity is an important parameter in these calculations.

1.4 Flame spreading in turbulent flow.

Here again the procedure is adopted of considering flame stabilisation and flame spreading separately. It must be noted however, that, in high velocity systems, there are strong interactions between the flame spreading zone and the

region of flame stabilisation (Longwell, 1955). Examples of this effect are discussed below in the sections on flame stabilisation.

One method of flame stabilisation, as illustrated by the anchoring of a bunsen flame, has already been discussed. However the flow velocities at which flames can be anchored in this way are limited, particularly in fuel-weak mixtures. In the high velocity systems, which are considered in this section, the flame is normally stabilised by a bluff body, or a can, or an independent flame pilot.

- 1.41 Flame stabilisation by bluff bodies.

Surveys of the literature on this subject have recently been given by Longwell (1953) and Zukoski and Marble (1955).

While the mechanism by which the fresh gases are ignited in the anchoring zone is still not completely defined. (Williams and Shipman, 1953), several workers have suggested models which offer some explanation of the experimental results. Scurlock (1948) suggested that the recirculation zone behind the stabiliser acts as a source of heat which ignites the passing fresh gas. Blow-off occurs when insufficient heat can be transferred from the hot recirculation zone into the cold unburned gas to maintain ignition. A similar model, in which the mass flow into the wake is critical, has been proposed by de Zubay (1950). Longwell, Frost and Weiss (1953) have applied the concept of homogeneous combustion to the

recirculation zone. Spalding (1953) has analysed three different models of anchoring - stabilisation by a jet of hot gases, by recirculation and by standing vortices, in each case the same expression being obtained for the condition of the blow-off. A wake mixing model has been considered by Lees (1954).

All the theories mentioned above predict that the group U_{BO}/D^n will correlate, as a function of the fuel-air ratio, the blow-off results for different sizes of stabilisers at any one pressure. U_{BO} is the flow velocity at blow-off, D is the stabiliser characteristic dimension, and n is an index. Longwell, Frost and Weiss, Spalding and Lees predict that the index n should be unity.

It has been found that the values of the exponent n which give the best agreement with the various sets of experimental data vary from 0.45 to 1.0. An explanation of this apparent inconsistency has been given by Zukoski and Marble (1955). They have shown that a transition takes place in the wake boundary at a value of the Reynolds Number, based on the stabiliser width, of about 10^4 . At that flow rate, the wake boundary immediately downstream of the stabiliser, which at lower flows had been laminar, becomes turbulent. Considering only the blow-off results taken at Reynolds Numbers of greater than 10^4 Zukoski and Marble have found all the results, except those of Longwell, Chenevey, Clark and Frost (1949), to be correlated by an exponent value

of 0.5. Longwell's results, which require an exponent of 1.0, were taken at Reynolds Numbers of the order of 10^6 , and it may be that, as Longwell (1955) and Zukoski and Marble suggest, in this higher range of Reynolds Number a third regime of wake structure exists.

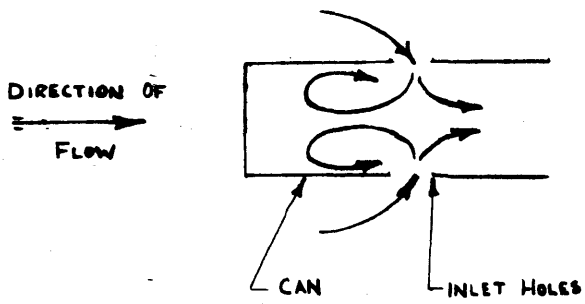
Spalding (1953) suggested from theoretical considerations that the blow-off velocity is proportional to the square of the laminar burning velocity. Calculations (Spalding, 1954) based on the published blow-off results are seen to be in agreement, in the higher range of Reynolds Number, with this relationship.

De Zubay (1950) has found that the blow-off velocity is almost directly proportional to the absolute pressure. This result is in agreement with the theories of Spalding (1953) and the second order reaction rate theory of Longwell, Frost and Weiss (1953).

From the summary given above it is seen that, with the aid of correlations of the type given by Spalding (1954), the blow-off velocity, for given conditions of mixture strength, pressure and stabiliser dimension, may be predicted with a fair degree of accuracy.

In the blow-off experiments which have been referred to above, care was taken to avoid flow and pressure fluctuations. Scurlock (1948) has demonstrated that induced turbulence, due to, say, a grid in the flow approaching the stabiliser, has a deleterious effect on the stability limits. A reduction in the

FIG. 4 FLAME STABILISATION BY A CAN



stability limits may also be caused if, in an effort to achieve complete combustion, the flame holder is placed a considerable distance before the chamber outlet (Longwell, 1955; Barrere and Mestre, 1954). Under these conditions pulsations in the flame front have consistently been observed by Dunlap (1950), even at flow velocities of 50 ft/sec., and less. These reductions in stability limits demonstrate the interaction in high velocity systems between the flame spreading zone and the stabilising zone.

1.42 Flame stabilisation by cans.

The flow through a typical can stabiliser is illustrated in Fig. 4.

The stability limits of cans have not been studied as thoroughly as those of the simple bluff bodies. Longwell (1955) indicates that the blow-out limits at one fuel/air ratio may be correlated by the term A/VP^2 where A is the mass flow rate into the recirculation zone, V is the volume of the recirculation zone and P is the pressure. Other recently published experiments (Probert, 1955) on the stability of a can having a single row of gas inlet holes suggest the correlating group - $q/D^{2.4} p^{1.5}$, where q is the mass flow rate through the can inlet holes, and D is the can diameter (all the cans were geometrically similar). In comparing these two correlating groups it must be remembered that one group is based on the mass flow into the recirculation zone, while in the other the measured quantity is the total mass flow rate

through the inlet holes.

A can, having three rows of inlet holes, was used as the stabiliser in the pilot of the combustion system which is described in Chapter 2 (see Figs. 6a, 8). This system was used to study the influence of "flame spreaders" on the overall combustion efficiency. The flame spreaders were attached to the downstream end of the pilot, and consisted of a number of flat fingers which crossed the annular space through which the main fuel-air mixture passed. It was found that the use of suitable finger arrangements resulted in considerable improvement in the combustion efficiency performance (see Chapter 3). However, it was also found that, if the number, width and inclination of the fingers which formed the flame spreader were increased beyond certain limits, a situation resulted in which combustion was extinguished before the system could be brought to choked tailpipe conditions (the finger inclination is the angle between the finger and the axis of the duct). This would appear to be another example of the interaction of flow fluctuations and combustion stability.

In each of the theoretical analyses of flame stabilisation which have been mentioned in paragraphs 1.41 and 1.42, it was assumed that there was no loss of heat from the combustion zone. That heat loss from the zone of anchoring by radiation for example, can be important, particularly at low pressures, has been shown by Spalding and Tall (1954).

1.43. Flame stabilisation by independent pilots.

Independent hydrogen-oxygen pilots have been used by Wilkerson and Fenn (1953) in studies of the influence of mixing rate on the combustion efficiency in ramjets. Here again it is reported (Fenn, 1955) that when the mixing rate became excessive, combustion was extinguished.

1.44 The concept of turbulent burning velocity.

It has been demonstrated in paragraph 1.3 above that the concept of a laminar burning velocity proved valuable in the study of flame spreading in a laminar bunsen flame.

Similarly it was thought that a "turbulent" burning velocity would aid the analysis of a flame burning in a turbulent stream. The first attempt to predict this turbulent burning velocity in terms of the turbulence characteristics was made by Damkohler (1940). He considered two extreme cases, firstly, the case where the scale of turbulence is large compared with the flame thickness, which appears to correspond most closely to the situation met in practice, and secondly, the case where the scale is small compared with the flame thickness. For the large scale turbulence it was considered that the turbulence merely caused a wrinkling of the flame front, and, by assuming that the individual sections of the flame front continue to propagate at the laminar flame speed, Damkohler predicted that the turbulent burning velocity is roughly proportional to the intensity of the turbulence in

the approach flow. For the case of the small scale turbulence it was assumed that the flame front is not distorted and that the increase in the burning velocity is due to an acceleration of the transport processes within the flame. In this way Damkohler obtained -

$$\frac{S_T}{S_L} = \left(\frac{\epsilon}{\nu} \right)^{\frac{1}{2}} \quad \dots\dots\text{Eqn. 1.5}$$

where S_T and S_L are the turbulent and laminar burning velocities respectively,

ϵ is the eddy diffusivity in the approach stream and ν is the kinematic viscosity.

The concept that a flame in large scale turbulence consists of rapidly fluctuating laminar flames has also been used by Karlovitz, Denniston and Wells (1951), and Karlovitz (1954), who predicted the turbulent burning velocity from the manner in which burning volumes of gas are moved backwards and forwards by the turbulence. Their treatment led to the equations -

$$S_T = S_L + u' \quad \dots\dots\dots\text{Eqn. 1.6}$$

for weak turbulence, $u' \ll S_L$, where u' is the intensity of turbulence and

$$S_T = S_L + (2 S_L u')^{\frac{1}{2}} \quad \dots\dots\dots\text{Eqn. 1.7}$$

for strong turbulence, $u' \gg S_L$.

When the intensities of turbulence in the gas stream approaching an open bunsen type flame were substituted in equation 1.7, the turbulent burning velocities predicted by

the equation were found to be considerably less than the experimental values. Reasonable agreement was obtained only when a turbulence intensity, thought to represent the intensity of "flame-generated" turbulence, was used in the equation in place of the turbulence in the approach stream.

This estimation and use of the intensity of "flame-generated" turbulence by Karlovitz represents a considerable advance in the "wrinkled flame front" theories of turbulent flames. However it has been suggested by Longwell, Frost and Weiss (1953) that, within a given volume, an insufficient number of laminar flame sheets can be obtained to yield the probable local heat release rates observed in the $1\frac{7}{8}$ inch diameter ramjet of Mullen, Fenn and Garmon (1951). Although Longwell made an assumption as to the space occupied by the burned gases which may have led him to underestimate the number of flame fronts possible, it does appear that there is a definite limitation to the "wrinkled laminar flame front" theories, beyond which they are no longer valid.

An alternative concept of the structure of a turbulent flame has recently been proposed by Summerfield, Reiter, Kebely and Mascolo (1955). They suggest that a turbulent flame is a zone of distributed reaction in which there are smooth spatial variations of the time-average values of temperature and composition, somewhat similar to a broadened laminar flame, the structure of which was indicated in Fig. 1. The transport processes within this "distributed reaction zone" flame are

controlled by the stream turbulence. It is claimed that this distributed reaction model has been confirmed by a series of experiments which consisted of filtered flame photographs, spectroscopic studies, temperature traverses and ionisation probe measurements. While the results of the first three techniques seem to favour this structure as opposed to the wrinkled laminar flame models of Karlovitz and his colleagues (1951), it is thought by the writer that the reported ionisation probe measurements can be explained by either model (c.f. paragraph 4.43). On the basis of the distributed reaction zone model, and by comparison with the laminar flame structure, Summerfield and his associates obtained the following similarity equation -

$$\frac{S_T d_T}{\epsilon} = \frac{S_L d_L}{\nu} \dots\dots\dots \text{Eqn. 1.8}$$

where S_T and S_L are the turbulent and laminar burning velocities respectively,

d_T is the thickness of the flame zone in a turbulent flame

d_L is the thickness of the flame zone in a laminar flame

ϵ is the eddy diffusivity in the approach stream

and ν is the kinematic viscosity.

A number of measurements of the turbulent burning velocity, and of the turbulent flame zone thickness were made with different turbulence producing grids in the approach flow, and at various flow velocities. In spite of the crudeness of some of the methods used, the group on the left hand side of equation 1.8 gave a reasonable correlation of the results.

This distributed reaction zone model proposed by Summerfield and his colleagues may prove very useful, particularly in the high velocity, high turbulence range of conditions. A difficulty in the application of the theory as it stands is that the left hand side of the equation contains two terms that are characteristics of the turbulent flame - the burning velocity and the flame thickness. Gas sampling traverses, of the type shown by Wohl, Shore, von Rosenberg and Weil (1953) and Longwell (1955), may prove helpful in providing information on the thickness of the turbulent flame.

It may be noted that Damkohler (1940), in his analysis of the influence of small scale turbulence on a flame front, conceived a flame structure which is quite similar to the model used by Summerfield.

1.45 The use of the turbulent burning velocity in calculating flame spreading in enclosed burners.

In burners of constant cross-sectional width the propagation of a flame across the fuel-air stream causes considerable redistribution of the flow velocities. By assuming a continuous flame front and a constant value of the turbulent burning velocity, Scurlock (1948), Tsien (1951), and others have provided relationships from which the flame shape and flow paths may be calculated. Conversely, the relationships may be used to determine values of turbulent burning velocity from observed flame shapes (Scurlock, 1948).

It is doubtful whether the assumptions as to a continuous

flame front and a constant burning velocity are valid in the enclosed combustion systems in which the approach velocity is greater, say, than 100 ft/sec. Flame spreading in these high velocity systems, which are typified by a ramjet combustion chamber, is discussed below.

1.46 Flame spreading in a ramjet.

Flame spreading in a $1\frac{7}{8}$ inch ramjet has been studied by Wilkerson and Fenn (1953), the effectiveness of the spreading being represented by the combustion efficiency at the chamber outlet. All the efficiency measurements were taken with choked flow at the burner exit. An independent hydrogen-oxygen pilot was used and it was found that the efficiency with any one geometric system increased considerably when the pilot heat input was increased from 0.5 to 4.5% of the possible heat release within the chamber. This result cannot be explained by the wrinkled flame front theories of turbulent burning velocity. The distributed reaction zone theory (equation 1.8) cannot yet be applied to these conditions owing to the lack of data on the thickness of the turbulent flame. However, a satisfactory explanation of these results has been given by Wilkerson and Fenn themselves, who considered the combustion chamber to be a region of homogeneous combustion. The temperature T at a characteristic point in the chamber was assumed to be given by the expression -

$$T = T_u + C h K \quad \dots\dots\dots\text{Eqn. 1.9}$$

where T_u is the temperature of the unburned gas,

C is a constant

h is the pilot heat input (as a percentage of the total heat release)

and K is a factor measuring the rate of mixing of the pilot heat with the main stream.

The factor K was determined by observing the temperature distribution with only the hot pilot gases and cold air entering the chamber, the main fuel supply being stopped. Since all measurements were taken using a stoichiometric fuel-air mixture the combustion efficiency, η_c , was then assumed to be a function only of the temperature at the characteristic point, given by -

$$\eta_c = B e^{-\frac{E}{\bar{R} T}} \quad \text{.....Eqn. 1.10}$$

where B is a constant,

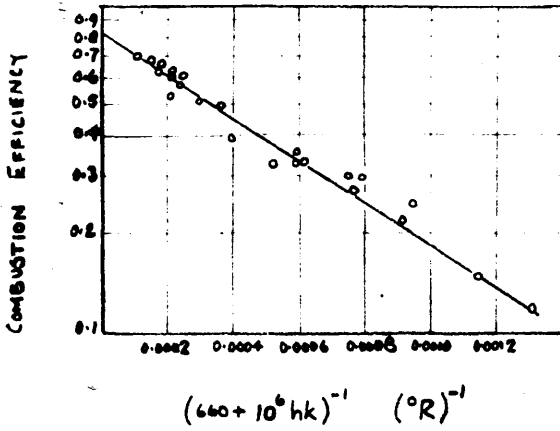
E is the activation energy

and \bar{R} is the universal gas constant.

When a suitable value of the constant C , in equation 1.9 was chosen, a good correlation of the results was obtained.

With the same apparatus Wilkerson and Fenn studied the influence of mixing rate on the combustion efficiency. Different mixing regimes were obtained by placing orifices of diameters ranging from $1\frac{1}{2}$ inch to $1\frac{3}{4}$ inch within the $1\frac{7}{8}$ inch diameter duct carrying the main stream. The orifices were placed at a distance of just over 1 inch upstream from the pilot exit. The mixing factor, K , was measured for each of the

FIG. 5 INFLUENCE OF MIXING AND OF PILOT HEAT
ON COMBUSTION EFFICIENCY
(From Wilkerson and Fenn, 1953)



geometries used. When the pilot heat was maintained at a constant fraction of the total heat input, it was found that an increase in the mixing factor, K , which was achieved by using a smaller diameter of orifice, was accompanied by an increase in the combustion efficiency. Equations 1.9 and 1.10 which had correlated the influence of pilot heat on the combustion efficiency, were also found to correlate the influence of mixing rate on the combustion efficiency. These correlations are given in Fig. 5. While Wilkerson and Fenn appreciate that their treatment is oversimplified, it nevertheless provides a satisfactory explanation of their results.

The use of devices, such as the orifices employed by Wilkerson and Fenn, which increase the rate of mixing by imparting general turbulence to the main stream, represents one method of achieving improved flame spreading. In the apparatus described in Chapters 2 and 3 of this thesis, the flame spreading was improved by the use of a system of fingers placed across the main stream, the roots of the fingers being level with the pilot exit. It has been shown by gas sampling that mass transfer of pilot gases takes place along the wakes of the fingers, and it appears that when the main fuel supply is introduced these fingers act, at least partially, as flameholders.

1.5 Discussion.

In low speed systems it appears that the flame spreading is controlled by the burning velocity (laminar or turbulent).

In the conditions met in a ramjet combustion chamber in which the flow is choked at the burner exit, the combustion appears to be more homogeneous, and the mixing processes become important. It has been observed that increasing the mixing rate improves the flame spreading. However, if the mixing rate is increased beyond a certain limit, a decrease in the stability, leading to extinction, can occur.

The theoretical analysis of the influence of mixing on the combustion rate which has been made by Berl, Rice and Rosen (1955) is relevant to this problem. They have shown that much higher heat release rates can be obtained with optimum mixing, than are obtained with only slight mixing. They have also shown that, when extremely rapid mixing takes place, the time required to burn a given volume of mixture becomes excessive.

CHAPTER 2.

PRELIMINARY STUDY OF FLAME SPREADING IN A RAMJET.

- 2.1 Introduction.
- 2.2 Open jet apparatus.
 - 2.21 Visual observations and flame photographs.
 - 2.22 Gas sampling.
- 2.3 Tailpipe apparatus.
 - 2.31 Method of calculation of combustion efficiency
 - 2.32 Experimental method and discussion of results.
- 2.4 Conclusions.

CHAPTER 2.2.1 Introduction.

The experiments described in this Chapter were the first to be carried out in the research project. They were intended to clarify the existing concepts of flame spreading and to give guidance to the design of future experiments.

Since it is hoped to apply the methods of flame spreading to ramjet and gas turbine combustion chambers it was thought that these preliminary experiments would be most useful if carried out on an apparatus operating under conditions similar to those encountered in, say, a ramjet combustion chamber. Such an apparatus requires considerable supplies of fuel and compressed air, and since the facilities available at Glasgow University were limited, it was decided to carry out these initial experiments at the National Gas Turbine Establishment, Pyestock.

Two experimental rigs were prepared, one an "Open Jet Apparatus", and the other a "Tailpipe Apparatus". The Tailpipe Apparatus was equivalent to the combustion system of typical 5 inch diameter ramjet, while the Open Jet Apparatus was essentially a similar chamber but with the tailpipe removed to allow observation of the flame patterns.

The air supply for the rigs was provided by two Rolls-Royce Nene Jet Engines fitted with air bleeds. Because of the difficulty of maintaining an adequate supply of a gaseous fuel, and because ramjet engines, in practice, normally operate on

Fig. 6a OPEN JET APPARATUS

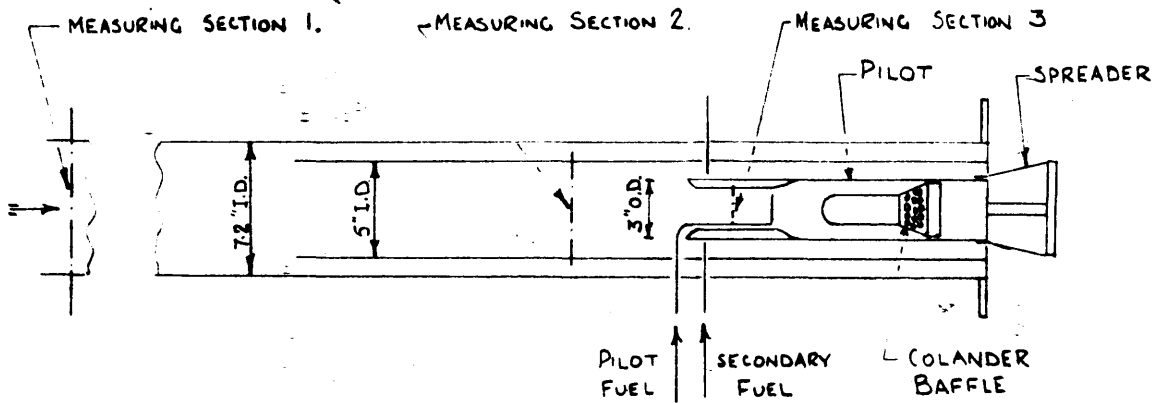
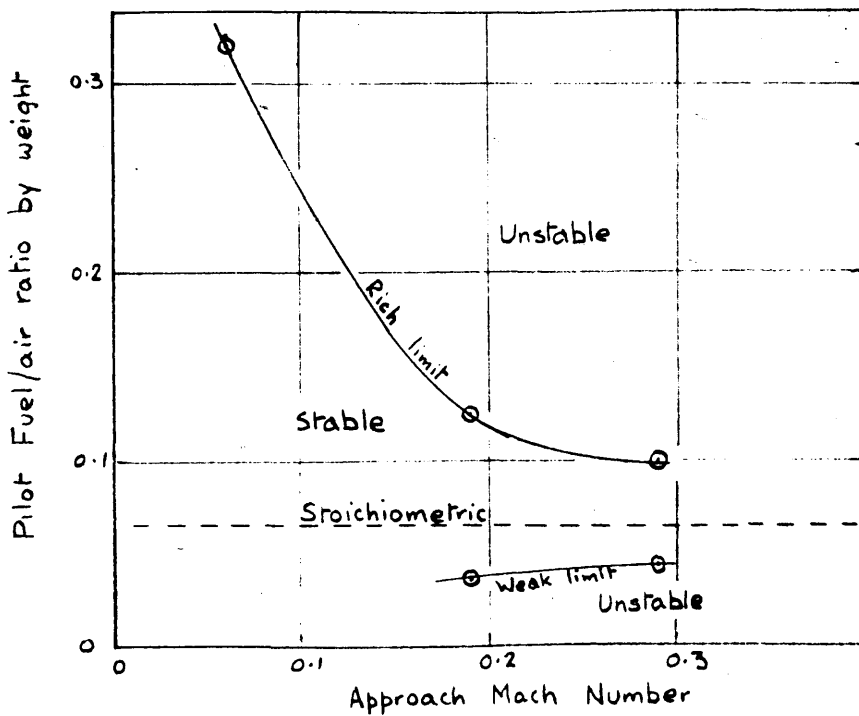


Fig. 6b PILOT STABILITY LIMITS



liquid fuels, a liquid fuel, "Ramjet Kerosine", was used in the experiments.

2.2 Open Jet Apparatus.

This apparatus consisted of a 3 inch diameter pilot, 16 inches long, placed within a 5 inch diameter duct, the whole being carried in an outer duct of diameter 7.2 inch. A sketch of the apparatus is given in Fig. 6a. The system within the 5 inch duct was equivalent to a small ramjet burner. About 12% of the air entering the 5 inch diameter duct passed through the pilot. This air will be referred to as "Pilot Air". The remainder of the air within the 5 inch diameter duct flowed through the annular space between this duct and the pilot. This air will be referred to as "Secondary Air". A stream of jacketing air flowed through the annulus between the 7.2 inch diameter duct and 5 inch diameter duct. The object of this jacketing air stream was to prevent the vorticity due to the motion of the gas stream relative to the ambient air affecting the flame until well downstream of the end of the pilot.

Fuel was supplied independently to the pilot and secondary streams using upstream injection and natural air blast atomisation. At values of Mach Number upstream of the pilot of up to about 0.3 (Measuring Section 2), and under suitable pilot fuel flows a flame was stabilised behind the colander baffle (or can). A few stability limits of the pilot were observed and these are plotted in Fig. 6b. As expected,

the flow of secondary fuel had little effect on the pilot stability limits in this apparatus.

When secondary fuel was supplied the flame issuing from the pilot spread across the secondary stream as shown in Photographs Nos. 11, 16 and 21 of Fig. 7. The object of the flame spreaders examined was to increase the rate at which the flame propagated into the secondary stream, resulting in higher combustion efficiencies for a given length of combustion chamber, or shorter combustion chambers for the same combustion efficiency. Flame spreaders consisting of various numbers of fingers could be attached to the downstream end of the pilot, the fingers traversing the annular space through which the secondary stream passed (see Photographs No. 1 and 2 etc. of Fig. 7.)

The air flow within the 5 inch duct was measured by a pitot-static tube mounted at Measuring Section 2. This pitot static tube was calibrated using a traversing pitot - static tube placed at Measuring Section 1, the 5 inch - 7.2 inch annulus being blanked off. A traversing total head tube at Measuring Section 3 with associated static pressure wall taps was used to measure the flow of pilot air.

Both pilot and secondary fuel flows were measured by rotameters. The nominal calibration of each rotameter was checked over a range of fuel flows by weighing the quantity of kerosine passed in a given time.

At the air inlet temperatures used (about 130°C) the fuel entering the combustion zone had not evaporated. No measurements were made of the fuel distribution nor of the droplet size.

2.21 Visual observations and flame photographs.

The structure of the flame as it propagated into the secondary stream was observed visually with each of the following spreader systems:-

Three fingers, 1 in. wide at inclinations of 31° , 18° .

Four fingers, $\frac{1}{2}$ in. wide " " " 60° , 45° , 31°
 18° , 10° .

Eight fingers, $\frac{1}{2}$ in. wide " " " 31° , 18° , 10° .

Eight fingers, $\frac{1}{4}$ in. wide " " " 31° , 18° .

The "inclination" is taken to be the angle between the finger and the axis of the burner.

Observations were made over a range of average Mach Numbers upstream of the pilot (Measuring Section 2) between 0.12 and 0.28. The pilot fuel/pilot air ratio was maintained approximately constant at 0.062 by weight (stoichiometric 0.067), except at the lowest values of the approach Mach Number. When the approach Mach Number was 0.12 a considerable number of yellow streaks appeared in the pilot flame, possibly caused by poor atomisation of the fuel resulting from the lower air velocities. To minimise this streaking the pilot fuel/air ratio was reduced at this velocity

FIG. 7. FLAME APPEARANCE IN FLAME SPREADING SYSTEMS

Approach Mach No. 0.12

Pilot Fuel/air ratio 0.051 by weight; Secondary fuel/air ratio zero

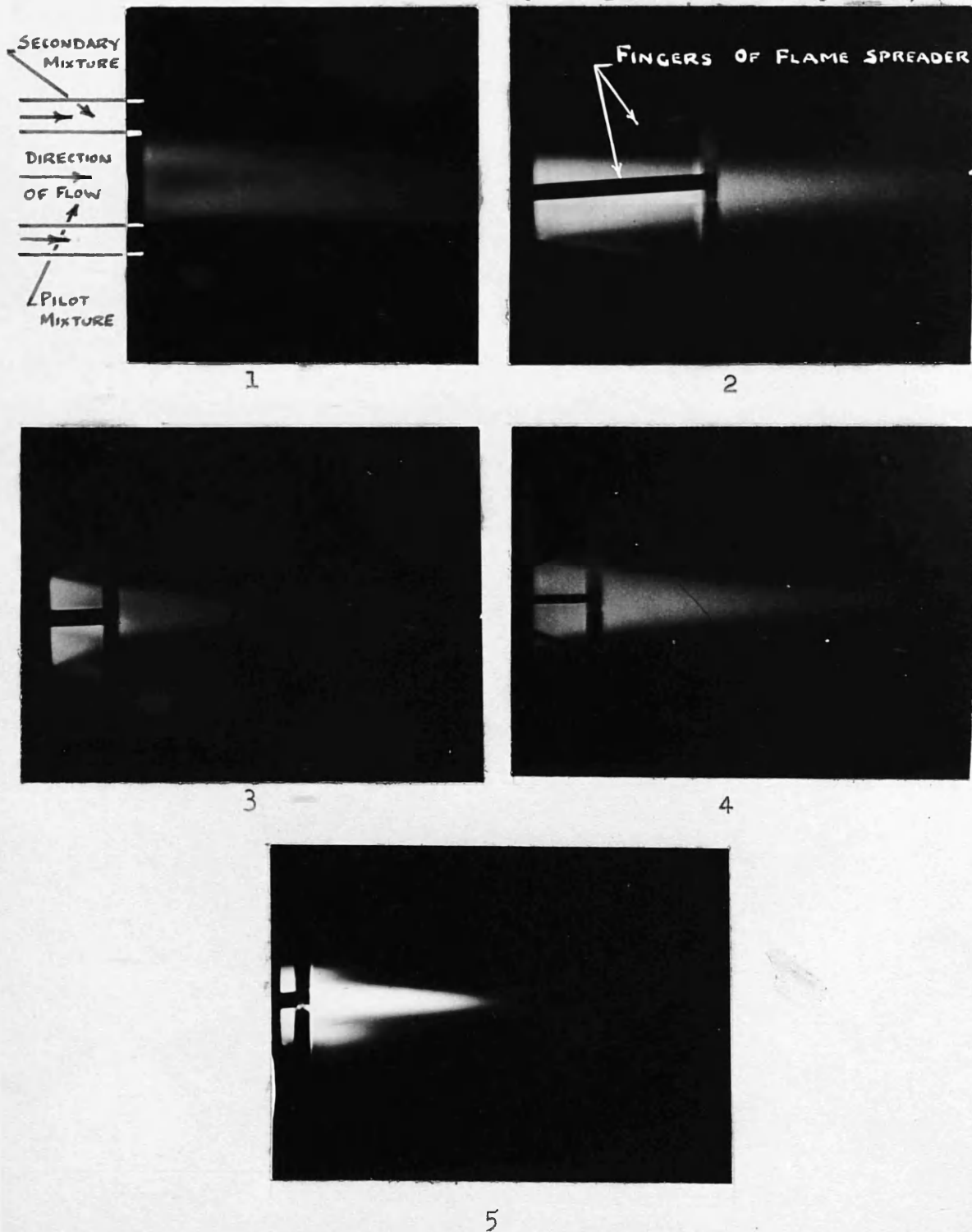
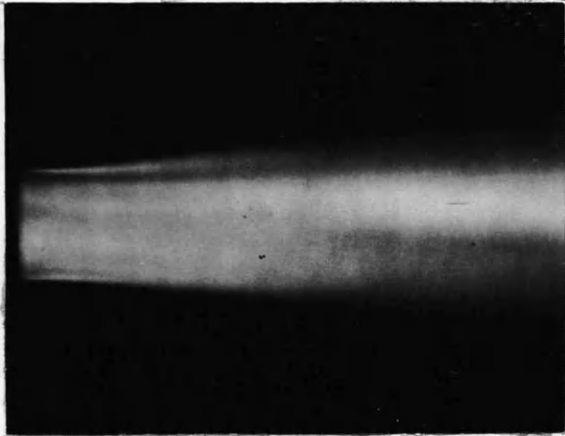


FIG. 7 Cont'd.

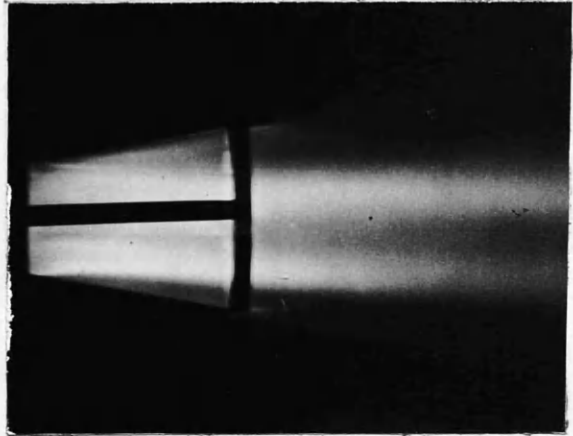
FLAME APPEARANCE IN FLAME SPREADING SYSTEMS

Approach Mach No. 0.12

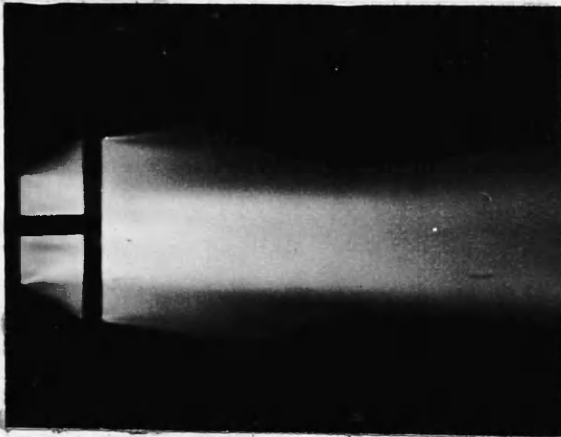
Pilot fuel/air ratio 0.051 by weight;
Secondary fuel/air ratio 0.027 by weight.



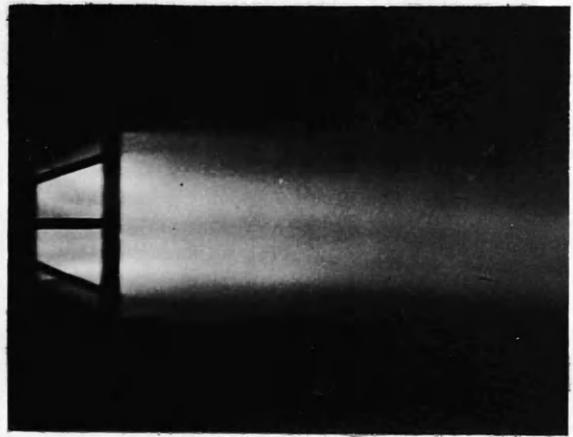
6



7



8



9



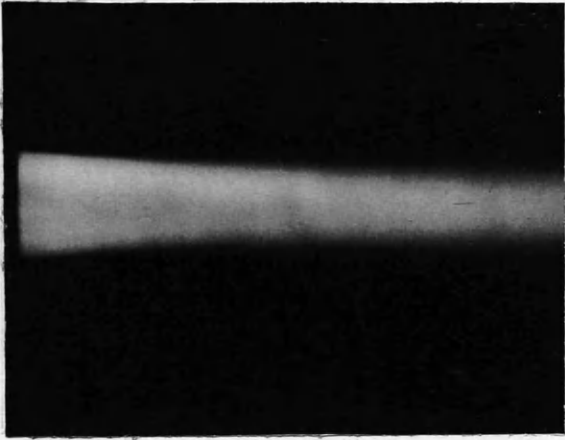
10

FIG. 7 Cont'd.

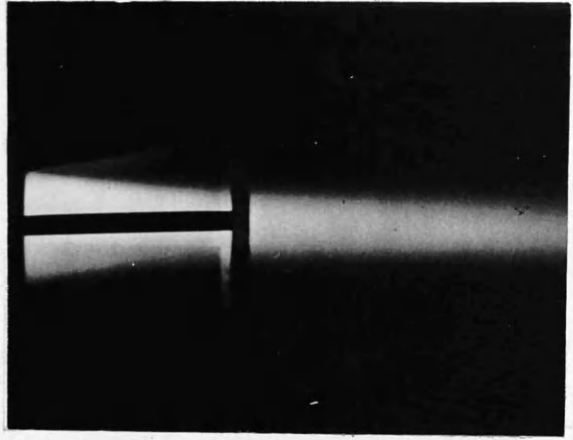
FLAME APPEARANCE IN FLAME SPREADING SYSTEMS

Approach Mach No. 0.28

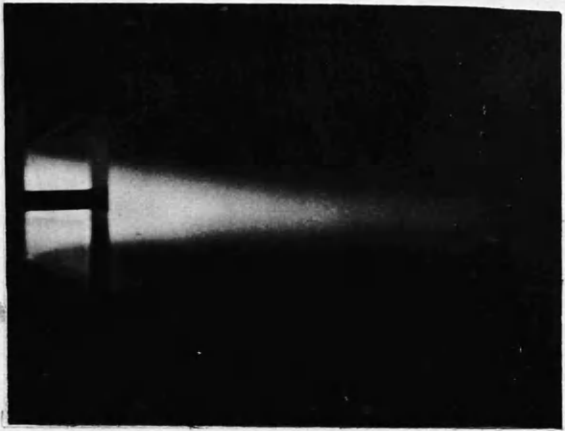
Pilot fuel/air ratio 0.062 by weight;
Secondary fuel/air ratio zero.



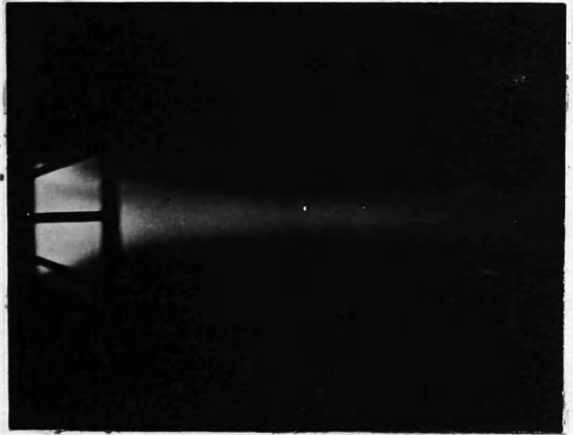
11



12



13



14



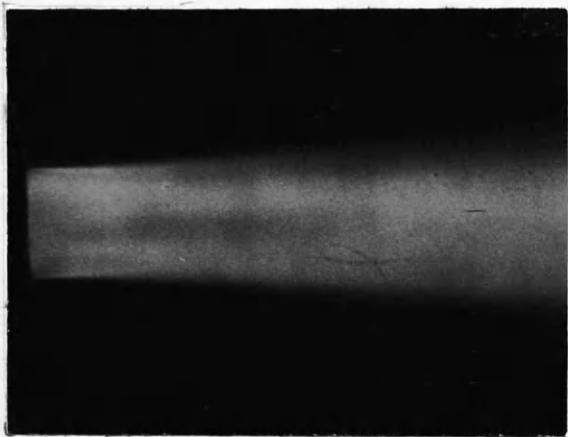
15

FIG. 7 Cont'd.

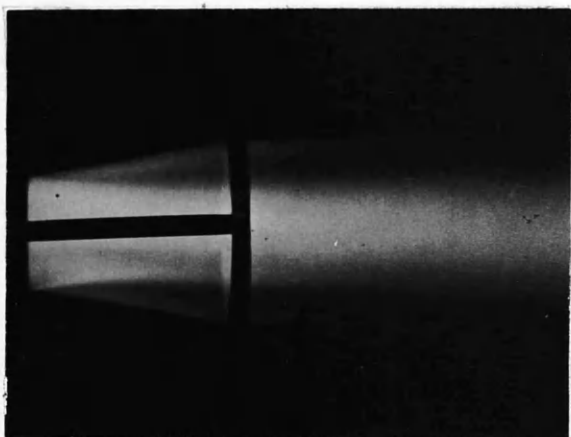
FLAME APPEARANCE IN FLAME SPREADING SYSTEMS

Approach Mach No. 0.28

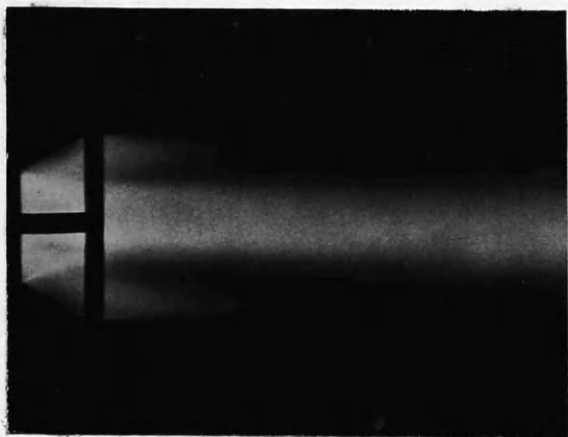
Pilot fuel/air ratio 0.062 by weight;
Secondary fuel/air ratio 0.028 by weight.



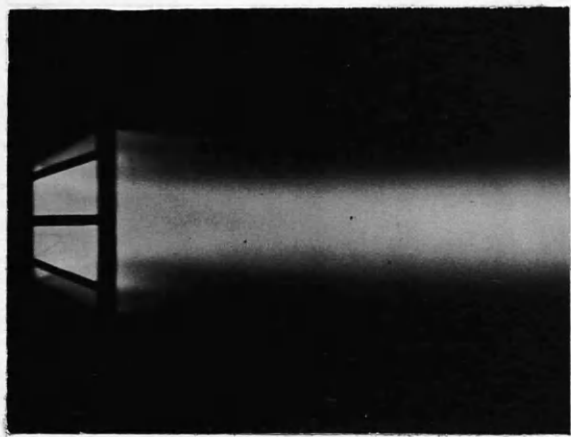
16



17



18



19



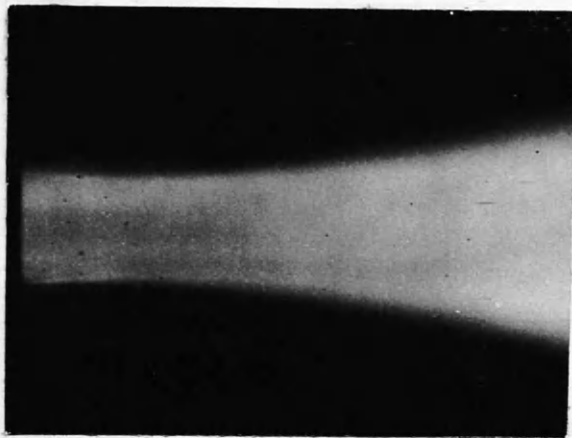
20

FIG. 7 Cont'd.

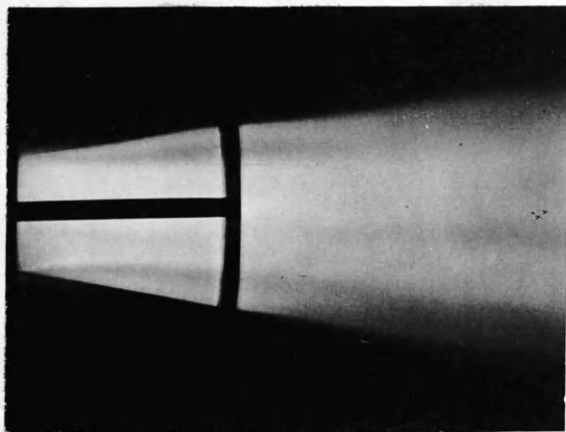
FLAME APPEARANCE IN FLAME SPREADING SYSTEMS

Approach Mach No. 0.28

Pilot fuel/air ratio 0.062 by weight:
Secondary fuel/air ratio 0.057 by weight.



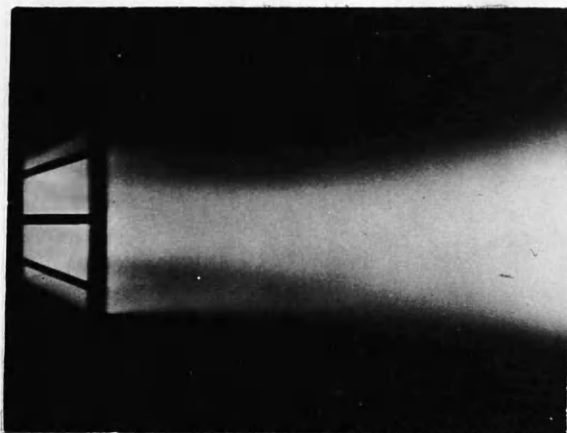
21



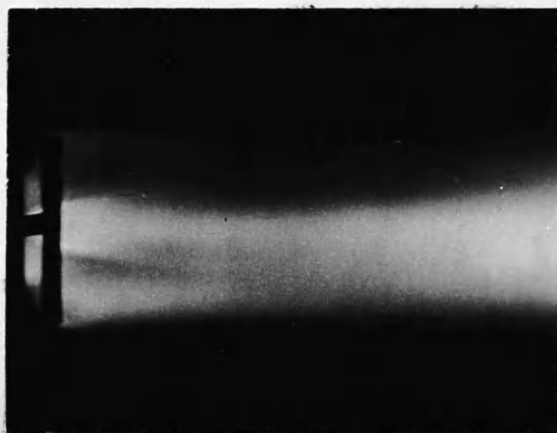
22



23



24



25

to 0.05 by weight.

The ratio of secondary fuel flow to secondary air flow was varied from zero to 0.07 by weight.

To provide a record of some of the flame observations, direct photographs were taken of flames obtained (a) with no spreader attached to the pilot (Photographs Nos. 1, 6, 11, 16, 21) and (b) with each of the following spreader systems attached to the pilot:-

Four fingers, $\frac{1}{2}$ in. wide at inclination of 10° .
(Photographs Nos. 2, 7, 12, 17, 22).

Four fingers, $\frac{1}{2}$ in. wide at inclination of 31° .
(Photographs Nos. 3, 8, 13, 18, 23).

Eight fingers, $\frac{1}{4}$ in. wide at inclination of 31° .
(Photographs Nos. 4, 9, 14, 19, 24)

and Four fingers, $\frac{1}{2}$ in. wide at inclination of 60° .
(Photographs Nos. 5, 10, 15, 20, 25).

Photographs were taken at Mach Numbers upstream of the pilot of 0.12 and 0.28. At the approach Mach Number of 0.12 flames were photographed at secondary fuel/air ratios of 0 and 0.028 by weight, and at the approach Mach Number of 0.28 at secondary fuel/air ratios of 0, 0.028 and 0.057 by weight. The photographs, numbered 1 to 25, are given in Fig. 7. Special blue sensitive plate, type LN, was used for all the flame photographs. Photographs Nos. 1 to 4 and 6 to 25 inclusive were taken with an exposure time of $\frac{1}{2}$ second at f22. Photograph No. 5, which is slightly overexposed, was taken with an exposure time of $\frac{1}{2}$ second at f16.

Since successive photographs of one flame may appear to be slightly different due to variations in the processes involved in developing, printing, etc., caution is required in comparing the flame photographs shown in Fig. 7.

However the following observations may be made from these photographs and from the visual studies described above.

(a) With all the spreaders tested, when secondary fuel was supplied flame gases were present in the wakes at the tips of the fingers. In other words, flame had "spread" to the tips of the fingers (see Photographs 7, 8, 9, 10 etc.) Visual observations are in agreement with this conclusion.

However with many spreader arrangements, particularly with those having finger inclinations of 30 degrees or more, and with those using the thinner fingers, there was little indication that the flames in the wakes of the fingers were initiating general combustion of the secondary fuel-air mixture as it passed the fingers. For example with $\frac{1}{2}$ inch wide fingers at an inclination of 60° , at an approach Mach Number of 0.28 and a secondary fuel/air ratio of 0.057, while there is seen to be some flame in the wake of the finger at the top of the spreader (Photograph No. 25), there is little sign of general combustion of the secondary mixture until well downstream of the finger. Under the same flow conditions but with the fingers inclined at 10° (Photograph No. 22) it

appears that the flame gases present in the wakes of the fingers are effective in starting progressive combustion of the secondary fuel-air mixture.

These observations do not necessarily mean that no benefit was gained from the spreader with the finger inclination of 60° , since the turbulence due to the fingers may have had a beneficial effect on the rate of combustion of the secondary mixture when this combustion began about 10 inches downstream of the spreader. On the other hand this turbulence might tend to cause quenching. A quenching effect, which is described in paragraph 3.44 of Chapter 3, was encountered in the Tailpipe Apparatus when spreaders having fingers of steep inclination were used.

This question of whether flame spreading by physical objects such as fingers which act effectively as flame holders is better than flame spreading resulting from general turbulence is discussed in Chapter 6. Experiments are suggested which should answer this question.

(b) Photographs Nos. 1 to 4 (at Mach Number 0.12) and 11 to 15 (at Mach Number 0.28) show the effect of the spreader systems on the pilot flame when no secondary fuel is supplied. The shortening of the pilot flame with increasing finger inclination may be due to some of the burning pilot gases being dispersed by being drawn into the wakes of the fingers. The shortening may also be due to increased mixing

of the secondary air with the pilot flame as it emerges from the downstream end of the pilot.

Whether the shortening of the pilot flame by attaching spreaders is accompanied by incomplete combustion of the pilot fuel might be determined by sampling and analysing the gases downstream from the pilot.

In addition to the observations of the flames described above, some tests were made without lighting the pilot fuel-air mixture. The unlit fuel mixed with the pilot air and formed a spray which was easily recognisable, and, in the absence of secondary fuel, this acted as a tracer for the pilot gas. With each of the spreaders tested some of this pilot fuel spray was seen to travel along the wakes of the fingers to the end furthest from the pilot, thus suggesting a flow or mass transfer of pilot gas along the wake of the spreader fingers. This indication was confirmed by sampling tests which are discussed in paragraph 2.22 below.

In all the experiments described above the flame spreader was attached to the pilot so that the roots of the flame spreader fingers were level with the downstream end of the pilot. In addition one test was made in which the spreader having three 1 inch wide fingers at 18° inclination was attached to the pilot so that the roots of the finger were $7/16$ inch upstream of the downstream end of the pilot. With this arrangement, observations of unlit pilot fuel again indicated that pilot gases flowed out along the wakes of the

fingers. Also when the pilot flame was lit, and secondary fuel supplied, flame gases were seen along the wakes of the fingers. These observations indicate that the performance of the spreader had not been appreciably altered by moving the spreader this small distance of $7/16$ inch upstream, and that the length of the recirculation zone behind the 1 inch wide fingers is greater than $7/16$ inch. Longwell (1955) has since studied the recirculation zone behind flame holding gutters of widths 1 inch and $2\frac{1}{4}$ inch and has found the zone to be four to five baffle dimensions in length.

2.22 Gas Sampling.

Samples were taken from points in the wake of a finger of each of the two following spreader arrangements:-

- (a) spreader having four fingers, $\frac{1}{2}$ inch wide, at an inclination of 18°
- and (b) spreader having eight fingers, $\frac{1}{4}$ inch wide, at an inclination of 31° .

It had also been intended to take samples using the spreader having four fingers $\frac{1}{2}$ inch wide at 31° inclination, as this would have provided information on the influence of finger inclination and finger width on the composition of the gases present in the wake. Unfortunately the experiments had to be curtailed to allow some tests to be carried out on the Tailpipe Apparatus before the author's return to Glasgow

University for the winter session.

Sampling and Analysis.

The sampling probe consisted of a 1 mm. outside diameter hypodermic tube surrounded by a small water jacket. The samples were drawn into 1 litre Haldane bottles and were later analysed by a gravimetric method (Lloyd, 1948). In the gravimetric train used, the sample was first passed through a condenser maintained at a temperature of roughly -80°C . by solid carbon dioxide and acetone. Any condensible fuel present in the sample was removed at this stage. After leaving the condenser, the sample passed through two U-tubes, the first containing "Anhydrone" (magnesium perchlorate) to absorb water vapour, and the second containing "carbosorb" (caustic soda on asbestos) to collect carbon dioxide. The increase in weight of the "carbosorb" U-tube over the period in which the sample was passed through the train gave the concentration of carbon dioxide. After leaving these U-tubes the sample entered a tube furnace which was packed with cupric oxide on silica chips and maintained at a temperature of 330°C . Oxidation of any hydrogen and carbon monoxide present in the sample took place in the furnace, the quantities of these gases being obtained from the increase in the weights of two further U-tubes containing respectively anhydrone and carbosorb which were placed at the furnace exit.

TABLE 1.

RESULTS OF SAMPLING TESTS

Conditions under which samples were taken.

Sample No.	M	f/a _p	f/a _s	Spreader System	Finger Length in.	Distance x in.
1	0.29	0.062	0	(a)	3 $\frac{1}{8}$	2 $\frac{3}{4}$
2	0.29	0.062	0	(a)	3 $\frac{1}{8}$	1 $\frac{7}{8}$
3	0.28	0.062	0.028	(a)	3 $\frac{1}{8}$	2 $\frac{3}{4}$
4	0.28	0.063	0.028	(a)	3 $\frac{1}{8}$	1 $\frac{7}{8}$
5	0.28	0.062	0	(b)	1 $\frac{7}{8}$	1 $\frac{1}{2}$
6	0.28	0.062	0.028	(b)	1 $\frac{7}{8}$	1 $\frac{1}{2}$

Where M is the Mach Number upstream of the pilot

f/a_p is the fuel/air ratio by weight of the pilot stream,

f/a_s is the fuel/air ratio by weight of the secondary stream,

x is the distance from the finger root, along the finger, to the point of sampling.

Spreader system (a) refers to spreader having four fingers, $\frac{1}{2}$ " wide, at an inclination of 18 degrees,

Spreader system (b) refers to spreader having eight fingers $\frac{1}{4}$ " wide, at an inclination of 31 degrees.

ANALYSES OF SAMPLES.

Sample No.	% by weight		
	CO ₂	CO	H ₂
1	7.8	0.0	0.01
2	4.7	0.9	0.03
3	13.7	3.0	0.06
4	5.2	2.0	0.03
5	1.1	0.5	0.03
6	1.5	0.6	0.03

Results.

The conditions under which the samples were taken, and the analyses by weight are given in Table 1.

From the analyses of the samples taken when no secondary fuel was supplied (Samples Nos. 1, 2 and 5) it is evident that appreciable quantities of pilot gases are present in the wakes of the fingers. With the $\frac{1}{2}$ inch wide finger at 18° inclination the concentration of carbon dioxide close to the end furthest from the pilot is roughly one third of the concentration of carbon dioxide present in uniform, completely burned, pilot gases.

Comparison of Samples Nos. 1 and 2 indicates that the concentration of carbon dioxide is much higher at the end of the finger furthest from the pilot than it is at the intermediate point at which Sample No. 2 was taken. Combustion of the carbon monoxide present at the intermediate point can only account for a part of this increase in carbon dioxide concentration along the finger. This suggests either that the flow pattern behind the finger is very complex, some pilot gases reaching the tip of the finger without passing through the zone from which Sample No. 2 was drawn, or that the method of sampling was inaccurate. For example the sampling tube ($3/16$ inch o.d.) may have presented too large a blockage in the wake of the finger and so have caused a change in the flow distribution.

Fig. 8 TAILPIPE APPARATUS

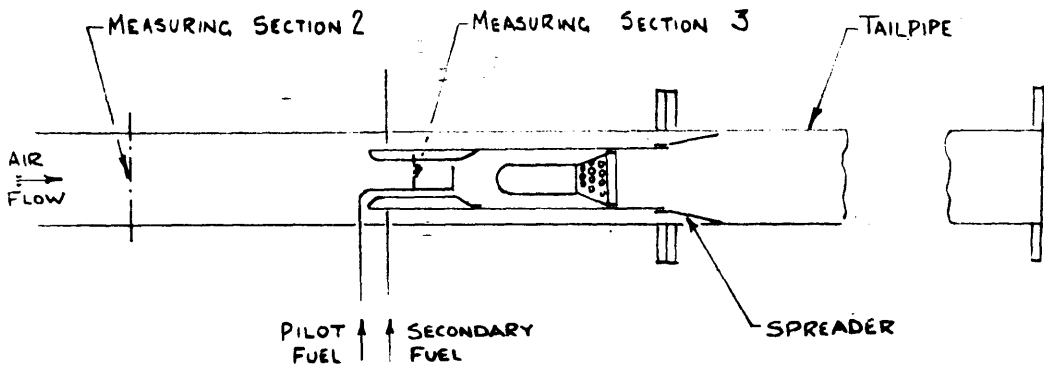
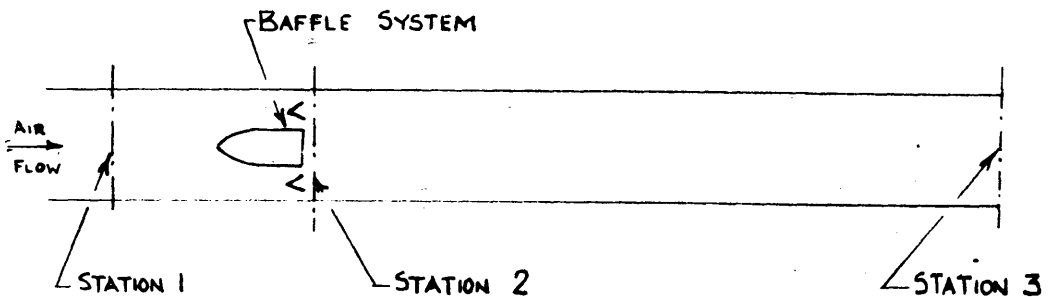


Fig. 9 IDEAL RAMJET COMBUSTION SYSTEM



In spite of the uncertainties resulting from the method of sampling the results given below provide some quantitative information on the flow of pilot gases behind the flame spreading fingers.

2.3 Tailpipe Apparatus.

The experiments with this apparatus were intended to provide data on the influence of flame spreaders on the overall combustion efficiency of the ramjet.

The apparatus consisted of a 3 inch diameter pilot carried within a 5 inch diameter duct, the duct being continued as a parallel-sided tailpipe beyond the downstream end of the pilot (see Fig. 8). This arrangement is equivalent to the Open Jet Apparatus used in the previous experiments but with the outer duct (7.2 inch diameter) removed and with a tailpipe attached to the 5 inch diameter duct. The pilot and the fuel injection systems from the Open Jet Apparatus were used again ⁱⁿ ~~the~~ the Tailpipe Apparatus.

Traversing total head tubes at Measuring Sections 2 and 3 (Fig. 8), with associated static pressure wall tapings, metered the flows of total air and pilot air respectively. The pilot and secondary fuel flows were again measured by rotameters.

2.31 Method of Calculation of Combustion Efficiency.

The derivations of the relationships introduced in this paragraph are given in Appendix I.

The method of calculation of the combustion efficiency is

based on a comparison with the following idealised combustion system, a sketch of which is given in Fig. 9. Between Stations 1 and 2 the air suffers a pressure drop due to the baffle system. Immediately after Station 2 fuel is injected at right angles to the direction of flow (i.e. the momentum of the fuel may be neglected). Combustion then takes place and is completed by the time the gases reach the tailpipe exit (Station 3), at which stage the flow is considered to be choked. It is assumed that downstream from Station 2 there is no pressure drop due to friction between the gases and the duct walls. One dimensional flow is assumed.

From the Mach Number upstream of the baffle system, M_1 , and from an assumed value of the Baffle Loss Coefficient, the Mach Number at Station 2, M_2 , is calculated using the expression :-

$$\lambda \frac{\gamma}{2} M_1^2 = 1 - \frac{M_1}{M_2} \left[\frac{1 + \frac{1}{2} (\gamma - 1) M_1^2}{1 + \frac{1}{2} (\gamma - 1) M_2^2} \right]^{\frac{1}{2}} \quad \dots \text{Eqn. 2.1}$$

where γ is the ratio of the specific heat at constant pressure to the specific heat at constant volume, and where λ is the Baffle Loss Coefficient, which is defined as the drop in static pressure past the baffle system per unit inlet velocity head.

The Air Specific Impulse S_a , defined as the gross thrust per unit air mass flow rate, is then obtained from the Mach Number at Station 2 by the equation :-

Fig. 10 THEORETICAL FUEL/AIR RATIO AS A FUNCTION OF AIR SPECIFIC IMPULSE
(From Morley, 1953)

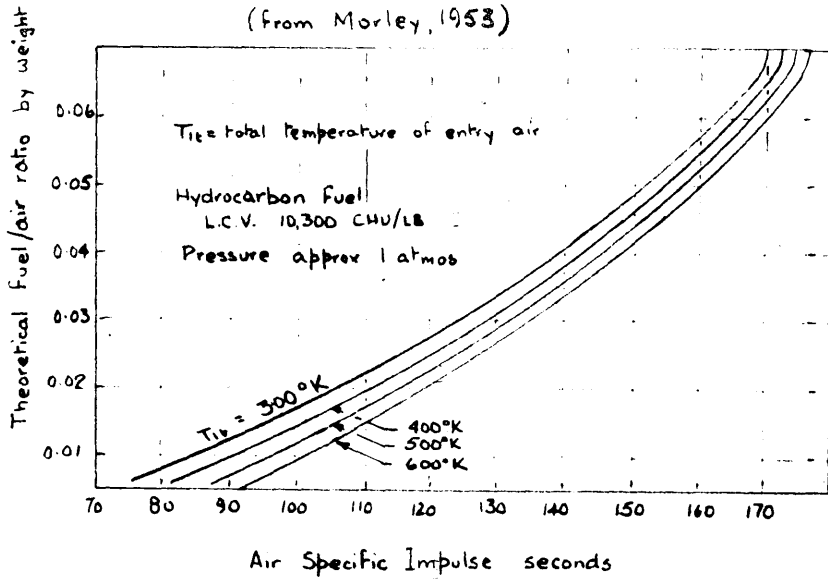
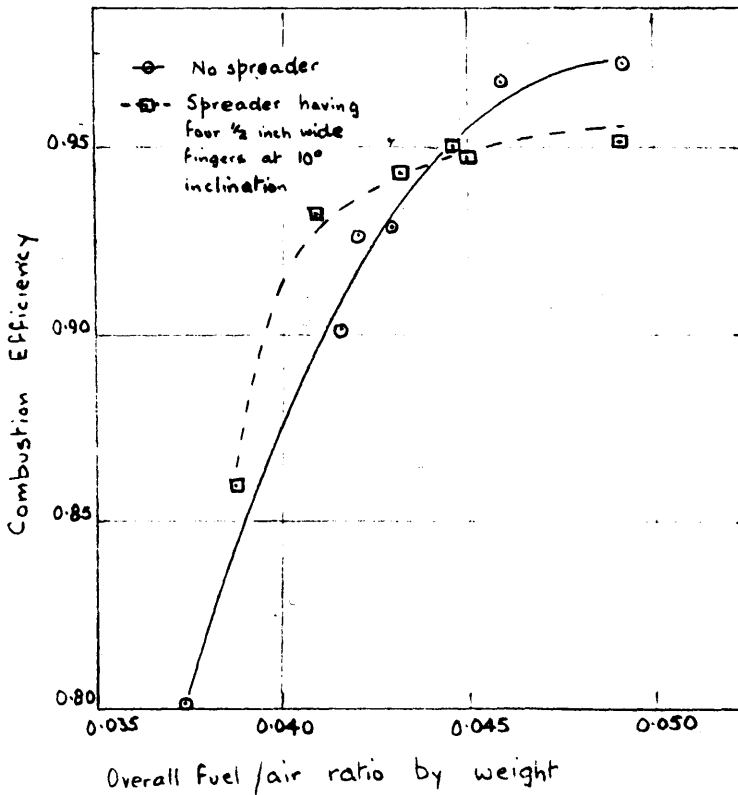


Fig. 11 INFLUENCE OF SPREADER ON COMBUSTION EFFICIENCY



$$S_a = \frac{\left(\frac{RT_{1t}}{\gamma g} \right)^{\frac{1}{2}} (1 + \gamma M_2^2)}{M_2 (1 + \frac{1}{2} (\gamma - 1) M_2^2)^{\frac{1}{2}}} \dots\dots\dots \text{Eqn. 2.2}$$

where R is the Gas Constant for air, T_{1t} is the total head temperature at Station 1, and g is the acceleration due to gravity.

The theoretical fuel/air ratio which, with complete combustion, would have given this value of Air Specific Impulse is then obtained from the relationships shown in Fig. 10. The ratio of this theoretical fuel/air ratio to the actual fuel/air ratio is taken to be the combustion efficiency.

The relationship shown in Fig. 10 between Air Specific Impulse and Theoretical Fuel/Air Ratio was obtained by Beeton (1949) and has been published by Morley (1953, p.198). A fuel of lower Calorific Value 10,300 C.H.U./lb. and composition by weight, carbon 85%, hydrogen 15%, was taken as the basis of Beeton's calculations. These properties are representative of the fuel (Ramjet Kerosine) used in the experiments described both in this Chapter and in the following Chapter. The manner in which the relationship indicated in Fig. 10 is obtained is outlined in Appendix I.

2.32 Experimental method and discussion of results.

Combustion Efficiency.

All measurements were made using a tailpipe of length 6 feet.

Initial experiments were carried out without

any spreader attached to the pilot. Since the method of calculation of combustion efficiency employed in this series of experiments requires a value of the Baffle Loss Coefficient and since this Coefficient cannot be measured satisfactorily from pressure measurements alone while combustion is taking place, a number of pressure readings were first taken for flow without combustion. From the values of "cold" Baffle Loss Coefficient obtained in this way the "hot" Baffle Loss Coefficient was estimated to be about 3.0 for the system without any spreader attached to the pilot.

After the readings giving the "cold" Baffle Loss Coefficient had been noted, the burner was lit and pressure and velocity head observations were taken over a range of overall fuel/air ratios for conditions giving choked flow at the tailpipe exit. Before each set of readings the pilot fuel flow was adjusted to give a stoichiometric pilot fuel-air mixture.

The values of combustion efficiency obtained from these readings for the system in which no spreader was used are plotted in Fig. 11.

A similar series of readings was taken when the spreader, having four $\frac{1}{2}$ inch wide fingers at 10° inclination, was attached to the downstream end of the pilot. In this case a "hot" Baffle Loss Coefficient of 3.5 was used in calculating the combustion efficiency, the values of which are also plotted in Fig. 11.

In comparing the combustion efficiency values obtained in these experiments with different spreader arrangements it must be remembered that an error in the assumed value of the Baffle Loss Coefficient causes an error in the values obtained for the combustion efficiency. It is thought that the error in the Baffle Loss Coefficient values used in the above calculations is less than 0.5, the resulting error in the values of combustion efficiency being less than 4% for a typical reading.

From Fig. 11 it is seen that the combustion efficiency values obtained both with and without the spreader are very high when compared with values normally met in a ramjet (Morley, 1953, p.198). Also it is seen that no significant advantage is gained by using the spreader, possibly because the combustion efficiency is already high without any spreader.

These experiments revealed the shortcomings of this method of studying the influence of spreader geometry on combustion efficiency. These shortcomings are

(a) that the combustion efficiency values depend on a value of the Baffle Loss Coefficient which can only be estimated, and

(b) that with a tailpipe of 6 feet length the combustion efficiency without a spreader is too high, in the range of fuel/air ratios tested, for any appreciable advantage resulting from the use of flame spreaders to be shown.

With a shorter tailpipe the combustion efficiency without a spreader will be lower, and under these conditions a noticeable gain may be achieved by using a flame spreader.

Stability of the Combustion System.

The performance of the system using the spreader having eight $\frac{1}{2}$ inch wide fingers at 18° inclination was also studied. With this arrangement, when secondary fuel was introduced the pilot flame was extinguished almost immediately. The richest overall fuel/air ratio at which the burner remained alight was roughly 0.025 by weight. This extinction was probably due to quenching by severe mixing and perturbations. Quenching of the pilot flame as a result of severe mixing has also been encountered, in a similar apparatus, by Fenn (1955). Olsen and Gayhart (1955) in studies of flame kernels propagating in a flowing gas stream have also found that the flame can be quenched by excessive turbulence.

While the precise mechanism of the quenching described above may still be in doubt, Berl, Rice and Rosen (1955) have shown theoretically, for one of the models that they have envisaged to represent combustion in turbulent streams, that extinction can take place in the event of excessively rapid mixing. In the model considered, laminar flame propagation from a source takes place until a given fraction of the total volume has been burned. The mixture is then made homogeneous

and the chemical reaction proceeds according to the classical reaction rate theory. It is shown that the time required for complete combustion becomes excessive, in other words the flame is virtually quenched, if the mixing to a homogeneous state takes place before roughly one quarter of the initial mixture has been burned by the laminar flame propagation.

It has also been shown by Spalding (1953) and by Lewis and von Elbe (1951), p.360, that a pocket of flame gas will be extinguished if it is less than a critical size.

It is relevant to note that the extinction observed in the Tailpipe Apparatus, which is described above, was not encountered in the Open Jet Apparatus. For simple flame holders, the attachment of a long tailpipe has also been found to cause a decrease in the stability limits (Barrere and Mestre, 1954).

2.4 Conclusions.

The main deductions of the preliminary experiments on flame spreading described in this Chapter are:-

(a) Mass transfer, or flow, of pilot gases takes place along the wakes of the flame spreading fingers.

(b) Flame gases present in the wake of a finger do not always start progressive combustion of the neighbouring fuel-air mixture.

(c) With a tailpipe of length 6 feet the combustion efficiency for the system without any flame spreader is too high for a significant gain to be observed when using a flame spreader.

(d) The pilot flame in the enclosed burner can be extinguished by the use of a spreader which causes too severe mixing.

The results, described in paragraph 2.3 above, which were obtained with the Tailpipe Apparatus, were used as a guide to the design of a systematic series of experiments to determine the influence of spreader geometry on combustion. These experiments, which were carried out on a second visit to the National Gas Turbine Establishment, Pyestock, are described in Chapter 3.

Deductions (a) and (b) above indicate that two of the most important processes in the spreading of a flame by the use of fingers are the flow along the wake of the finger and the initiation of combustion by flame sources.

CHAPTER 3.

MEASUREMENTS OF COMBUSTION EFFICIENCY IN RAMJETS
USING FLAME SPREADERS.

- 3.1 Introduction.
- 3.2 Apparatus.
- 3.3 Experimental.
- 3.4 Influence of Spreader geometry on combustion efficiency.
 - 3.41 Agreement with results of first series of experiments.
 - 3.42 Tailpipe Length.
 - 3.43 Number of fingers and width of fingers.
 - 3.44 Finger Inclination.
 - 3.45 Position of spreader.
 - 3.46 Shape of spreader.
- 3.5 Baffle Loss Coefficients.
- 3.6 Stability Limits.
- 3.7 Conclusions.

CHAPTER 3.3.1 Introduction.

The experiments described in Chapter 2, using the Tailpipe Apparatus, provided little data on the influence of flame spreader geometry on combustion efficiency. However, these experiments revealed the shortcomings of the method which had been employed, and the experience gained was used in planning a second series of experiments described below, which was carried out on a second visit to the National Gas Turbine Establishment, Pyestock, during the Summer of 1953.

3.2 Apparatus.Combustion system.

The combustion system was identical to the one used in the Tailpipe Apparatus, as described in the preceding Chapter, except that two shorter tailpipes, of lengths 4ft. 6 in., and 3 ft., were used in some of the tests, in place of the 6 foot long tailpipe. A sketch of the system has been given in Fig. 8. The flow of air through the pilot was measured at Measuring Section 3 by a traversing total head tube with associated static pressure wall tappings. A pitot-static tube mounted centrally in the duct at Measuring Section 2 metered the flow of "total" air (pilot air plus secondary air). This pitot-static tube was calibrated by a British Standard Orifice plate. For the calibration, several lengths of 12 inch diameter duct, in which the orifice plate was mounted, were

TABIE 2.

SPREADER ARRANGEMENTS AND TAILPIPES USED
IN COMBUSTION EFFICIENCY MEASUREMENTS.

	Tailpipe Length ft.	Spreader		
		Width of fingers. in.	No. of fingers	Inclination of fingers
a	6	No spreader		
b	6	$\frac{1}{2}$	Four	10°
c	6	$\frac{1}{4}$	Eight	10°
d	4.5	No spreader		
e	4.5	$\frac{1}{2}$	Four	10°
f	4.5	$\frac{1}{4}$	Eight	10°
g	3	No spreader		
h	3	$\frac{1}{2}$	Four	10°
i	3	$\frac{1}{2}$	Eight	10°
j	3	$\frac{1}{2}$	Four	30° /
k	3	$\frac{1}{4}$	Four	10°
l	3	$\frac{1}{4}$	Eight	10°
m	3	$\frac{1}{8}$	Eight	10°
n	3	$\frac{1}{8}$	Eight	30°
o	3	$\frac{1}{2}$	Four	10°
		With roots of finger $\frac{3}{8}$ inch upstream from end of pilot		
p	3	Four 60° included angle Vee's, $\frac{1}{2}$ inch wide at 30° inclination		

/ modified pilot.

attached to the tailpipe outlet.

Ramjet kerosine was again used as the fuel. At the air inlet temperatures used in these experiments of 130°C . very little of the fuel had vapourised when the mixture entered the combustion zone.

Thrust Meter.

In the combustion efficiency experiments described in the preceding Chapter the efficiency could only be calculated by assuming a "hot" Baffle Loss Coefficient. This weakness in the experimental method was eliminated in the tests described in this Chapter by the use of a Meter which measured the thrust resulting from the momentum of the hot gases leaving the tailpipe exit.

3.3 Experimental.

Geometric variables.

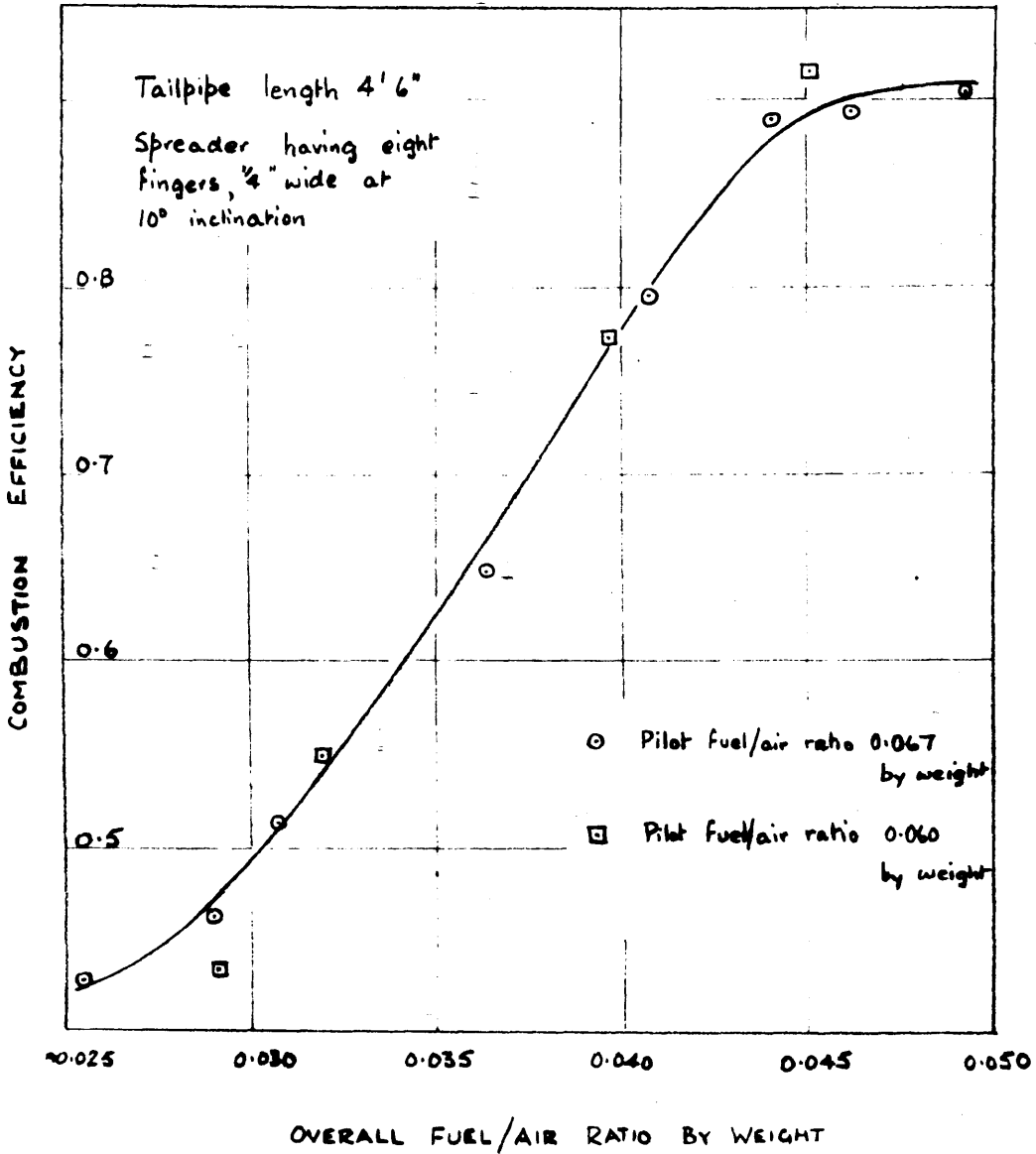
For each of the three tailpipe lengths, the various flame spreader systems with which combustion efficiency measurements were taken are given in Table 2.

An attempt was also made to obtain combustion efficiency measurements using a spreader having three 1 inch wide fingers at 10° inclination. However, quenching, similar to that described in Chapter 2, was encountered and prevented the burner being brought to choked tailpipe exit conditions.

Pilot fuel/air ratio.

Each set of readings on which the combustion efficiency calculations are based was taken for conditions giving choked

FIG. 12 INFLUENCE OF PILOT FUEL/AIR RATIO ON COMBUSTION EFFICIENCY



flow at the tailpipe exit. Before each set of readings was taken the pilot fuel flow was adjusted to give a stoichiometric pilot fuel/air ratio (0.067 by weight). That a slight error in setting the pilot fuel flow causes negligible difference to the resulting value of combustion efficiency is demonstrated by the results of one test in which the thrust measurements were taken for pilot fuel/air ratios of both 0.067 and 0.060 by weight. The results of the two sets of experiments, which are plotted in Fig. 12, are in very good agreement.

Wilkerson and Fenn (1953) found that large variations in pilot heat input caused appreciable changes in the overall combustion efficiency, as discussed in Chapter 1, paragraph 1.34. However the range of variation of pilot heat input which was possible in the experiments described here was so small by comparison that no significant changes in efficiency were observed.

Overall fuel/air ratio.

Measurements were taken for overall fuel/air ratio by weight ranging from about 0.025 up to the rich extinction limit, which usually occurred at a fuel/air ratio (overall) of about 0.05.

Calculation of Combustion Efficiency.

The Thrust Meter measures the nett thrust. From this value the gross thrust is obtained by adding to it the product of the atmospheric pressure and the exit area of the

tailpipe. The Air Specific Impulse is then determined by dividing the gross thrust by the air mass flow rate. Having obtained the Air Specific Impulse in this way, the combustion efficiency is calculated as indicated in paragraph 2.31 of Chapter 2. The combustion efficiency is again taken to be the ratio of the theoretical fuel/air ratio which, with complete combustion, would have given the measured value of Air Specific Impulse, to the actual fuel/air ratio.

The value of the Baffle Loss Coefficient for burning conditions may be obtained by using Equations 2.2 and 2.1 given in Chapter 2. From Equation 2.2 the Mach Number after the baffle system, M_2 , is determined, and substitution in Equation 2.1 then gives the Baffle Loss Coefficient.

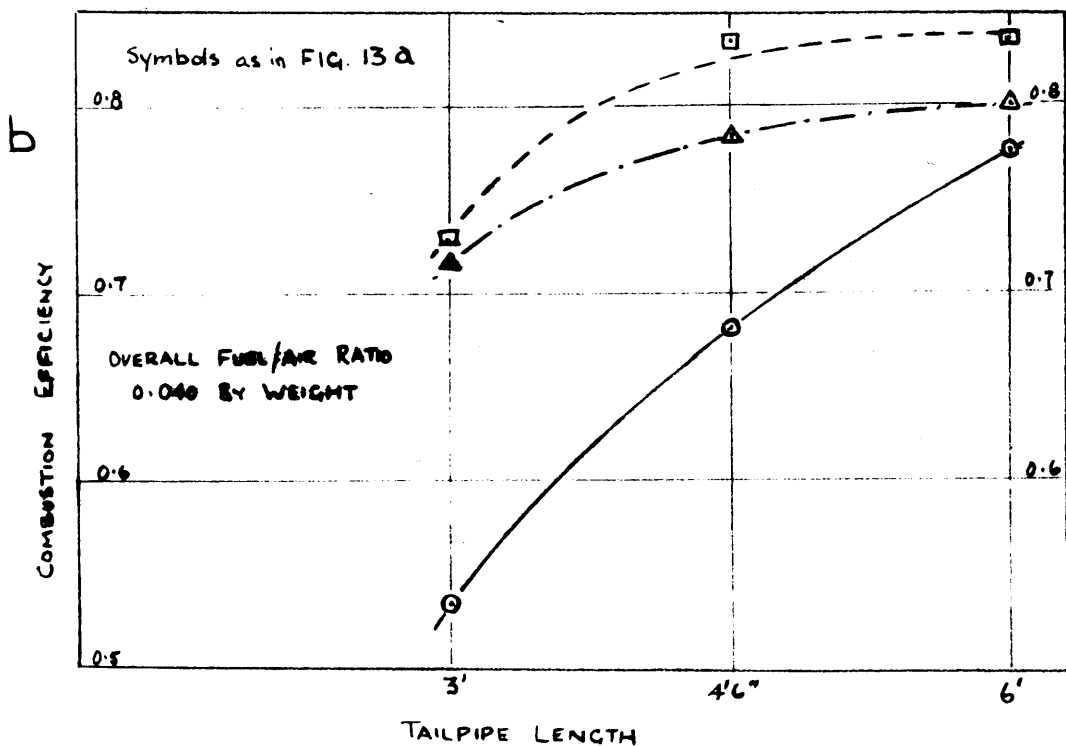
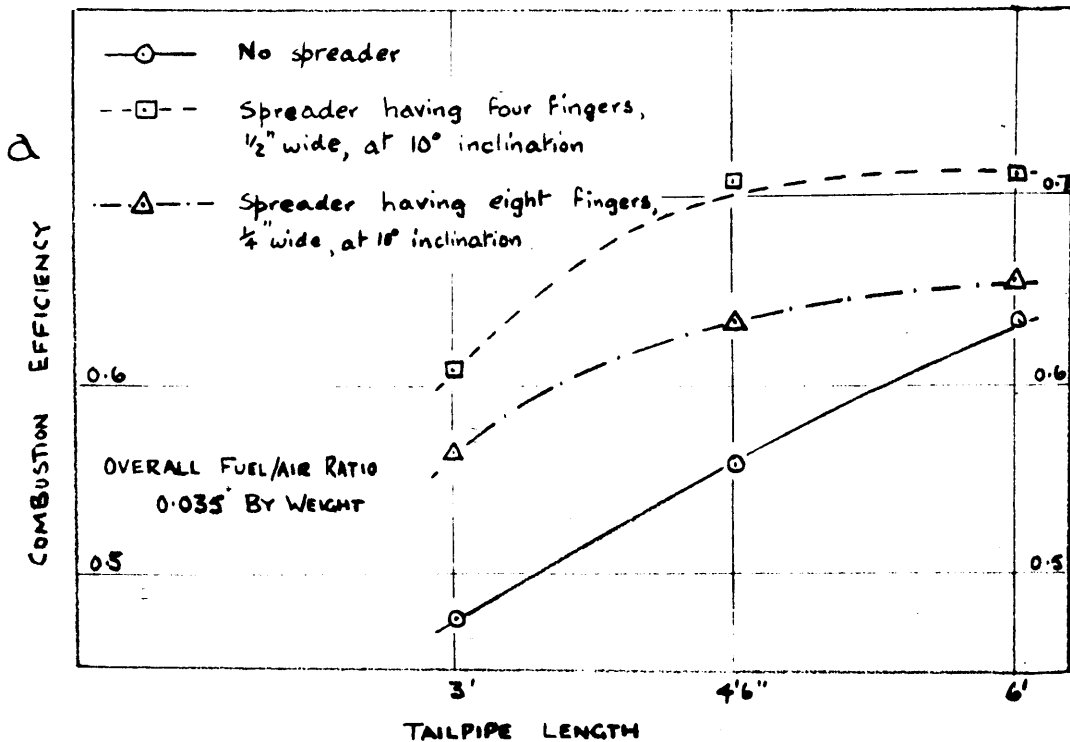
3.4 Influence of Spreader Geometry on Combustion Efficiency.

The results of a typical set of combustion efficiency measurements are given in Fig. 12. It is seen that the efficiency varies markedly with the overall fuel/air ratio. To aid the comparison of the efficiencies obtained with the various combustion systems, values of combustion efficiency corresponding to overall fuel/air ratios by weight of 0.035, 0.040 and 0.045 were interpolated, where possible, for each of the spreader and tailpipe arrangements.

3.41 Agreement with results of first series of experiments.

Some of the experimental conditions of the first series of experiments were repeated in this second series of

FIG. 13 INFLUENCE OF TAILPIPE LENGTH ON COMBUSTION EFFICIENCY



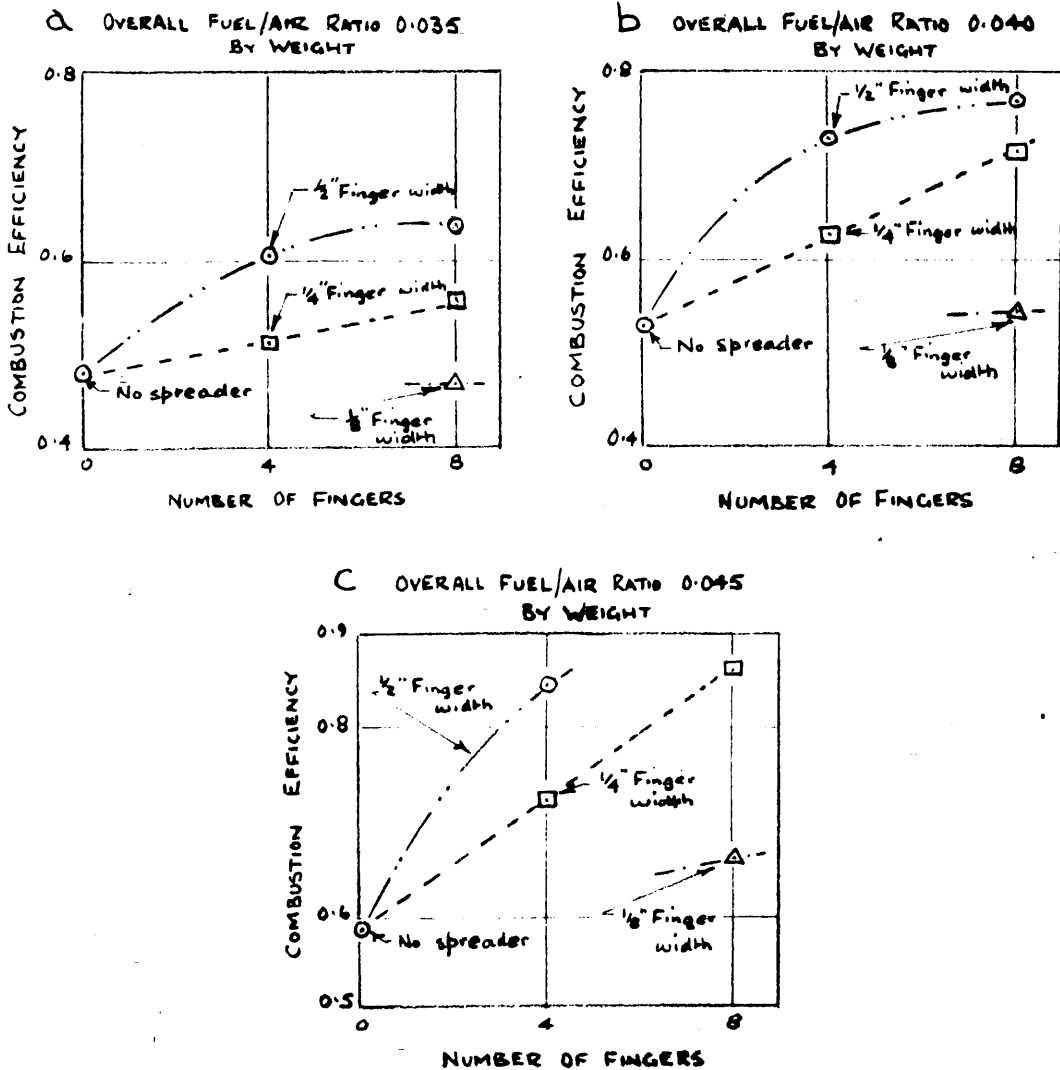
experiments. It was found that the efficiency values obtained in the first series of experiments were slightly higher than the corresponding figures determined from the thrust measurements in the experiments now being described. This difference is principally due to the values of the "hot" Baffle Loss Coefficient that were assumed in the first series of experiments having been slightly in error. The measurements taken in the second series of experiments enabled the combustion efficiency to be determined independently of the Baffle Loss Coefficient, and also enabled the "hot" Baffle Loss Coefficient to be obtained directly. Thus the "hot" Baffle Loss Coefficient for the system without any spreader and using the 6 foot long tailpipe was found, in the second series of experiments, to be 3.4, compared with the value of 3.0 which had been assumed in obtaining the efficiency results of the first series of experiments. A similar small error was found in the value of the "hot" Baffle Loss Coefficient assumed in the first series of experiments for the system using the spreader having four $\frac{1}{2}$ inch fingers at 10° inclination.

3.42 Tailpipe Length.

The results showing the influence of tailpipe length on combustion efficiency for three different spreader arrangements are presented in Figs. 13a and b, using the interpolated efficiency values corresponding to overall fuel/air

FIG. 14 INFLUENCE OF NUMBER OF FINGERS AND WIDTH OF FINGERS ON COMBUSTION EFFICIENCY

TAILPIPE LENGTH 3'
FINGER INCLINATION 10°



ratio by weight of 0.035 and 0.040. These results show that, while a reduction in tailpipe length causes a decrease in the combustion efficiency, this drop in performance can be remedied, within limits, by the attachment of suitable flame spreaders. The combustion system using the 3 foot long tailpipe and the spreader having four $\frac{1}{2}$ inch wide fingers at 10° inclination gives efficiencies similar to those obtained using a tailpipe of length about 5 feet but without any flame spreader. The gains achieved by flame spreaders when long tailpipes are used are much less than those obtained with a short tailpipe, particularly for overall fuel/air ratios richer than 0.04 by weight. In fact with the 6 foot long tailpipe, attaching flame spreaders produces virtually no change in the efficiency of combustion for overall fuel/air ratios by weight in the range 0.04 to 0.05. This observation is in agreement with the results, described in Chapter 2, of the first series of combustion efficiency experiments.

3.43 Number of fingers and width of fingers.

The influences of the number and width of the fingers on the combustion efficiency are shown in Fig. 14a, b and c. The tailpipe of length 3 feet was used in obtaining these data since it is with the shorter tailpipes that the largest gains result from the use of spreaders. All the results shown in Fig. 14 are for fingers having an inclination of 10° to the direction of flow.

Number of Fingers.

It is seen that, within the limits studied in these experiments, increasing the number of fingers improves the performance as measured by the combustion efficiency. With the $\frac{1}{4}$ inch wide fingers the increase in efficiency is roughly proportional to the number of fingers. This linear relationship does not apply however to the fingers of $\frac{1}{2}$ inch width, for with them, the advantage gained in increasing the number of fingers from four to eight is much less than that gained by introducing the first four fingers. This result suggests that, with the $\frac{1}{2}$ inch wide fingers, an optimum distribution of the pilot gases which feed the spreader fingers is being approached.

Width of fingers.

For the range of conditions studied the combustion efficiency performance is seen to improve with an increase in the width of the fingers. The $\frac{1}{8}$ inch wide fingers, which were the thinnest fingers tested, have little effect when the overall fuel/air ratio is less than 0.04 by weight.

Equal blockage.

- The performance of the $\frac{1}{2}$ inch wide fingers in the weaker mixtures is so much superior to that of the $\frac{1}{4}$ inch wide fingers that, for systems of equal blockage, the spreader using the wider fingers gives the better combustion efficiency performance over most of the studied range of fuel/air ratios.

A similar result, only more marked, is found on comparing the equal blockage spreaders using $\frac{1}{4}$ -inch and $\frac{1}{8}$ inch wide fingers.

At fuel/air ratios richer than those studied here a spreader using thin fingers may prove to be superior to a spreader of equal blockage employing thicker fingers. To extend the experiments to this range a tailpipe of length less than 3 feet would be necessary since, with the 3 foot long tailpipe, the combustion efficiency using the spreader having four $\frac{1}{2}$ inch wide fingers at 10° inclination is roughly 90% (fuel/air ratio 0.05 by weight). Also a burner having a higher rich extinction limit than the one used in the above experiments would be required. The reduction in tailpipe length may result in a small improvement in the stability limits (Barrere and Mestre, 1954), but it is not thought that this would be adequate.

The above results indicate that increasing either the number of fingers or the width of the fingers results in an increase in the combustion efficiency. While there is a maximum geometric limit to the number and width of fingers that can be used in any one system it is probable that before this limit is reached the combustion system will be extinguished by quenching of the pilot gases, as discussed in paragraph 2.32 of Chapter 2. This limit due to quenching of the pilot is also influenced by the inclination of the fingers, possibly to a greater extent than it is influenced by the width

FIG. 15 INFLUENCE OF FINGER INCLINATION ON COMBUSTION EFFICIENCY

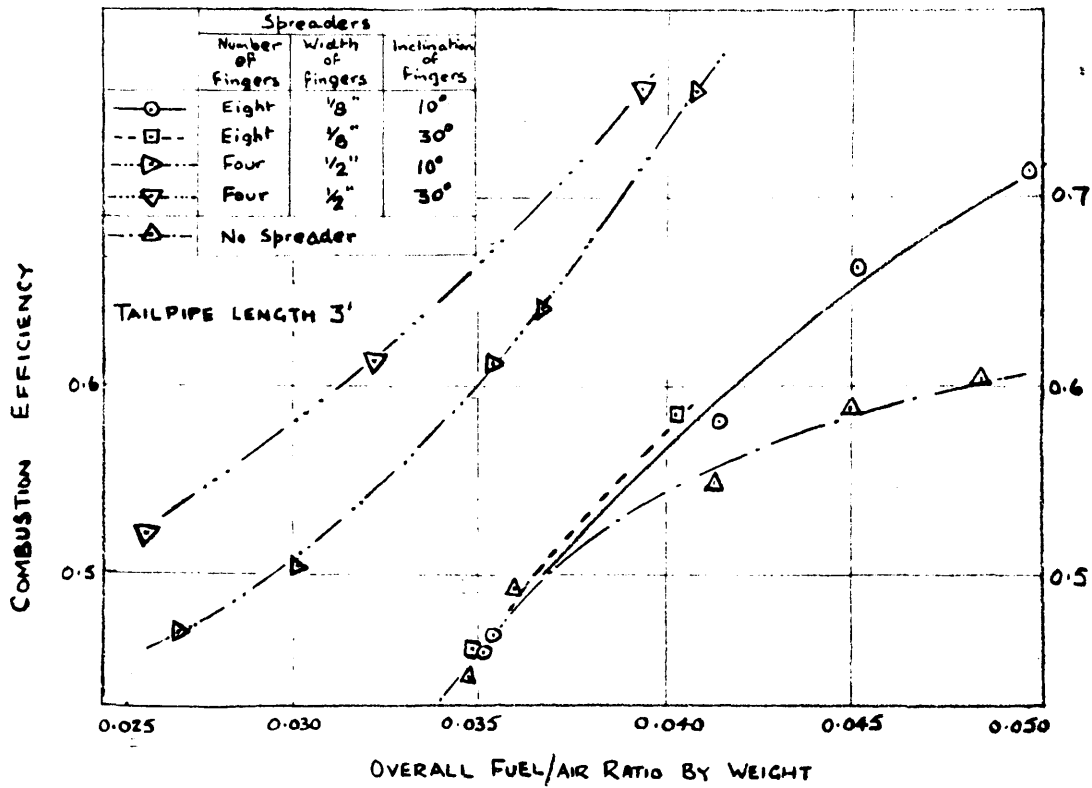
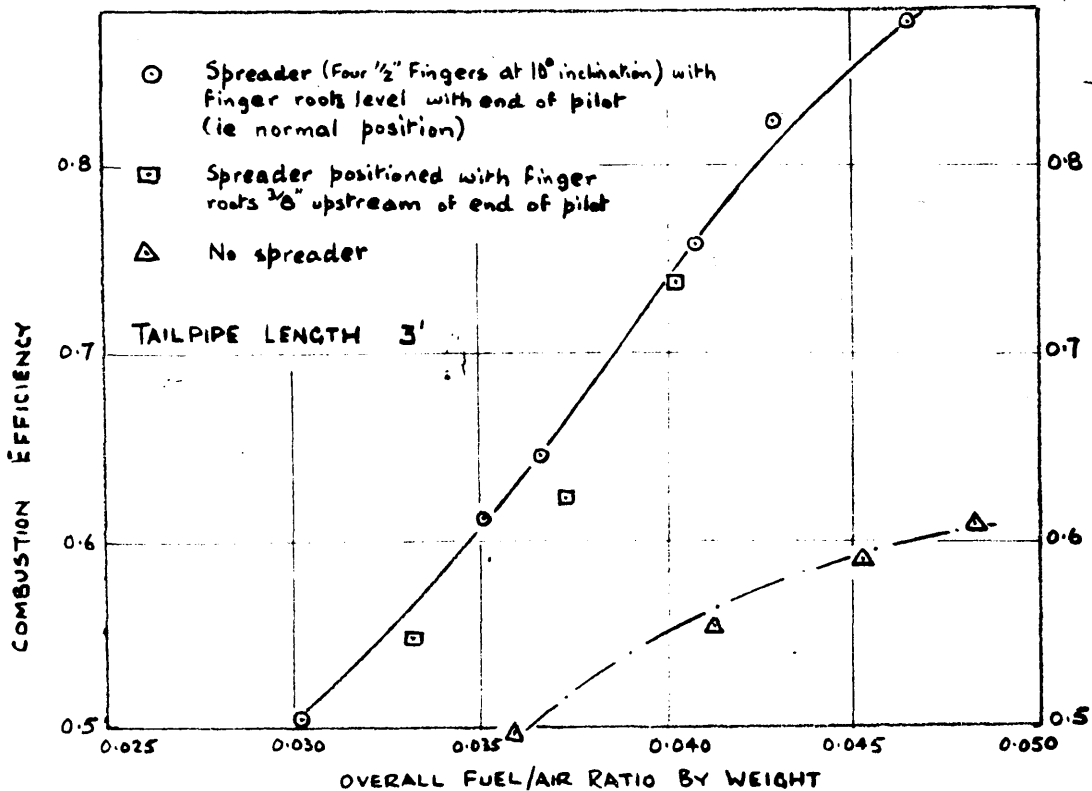


FIG 16 INFLUENCE OF SPREADER POSITION ON COMBUSTION EFFICIENCY



and number of fingers (c.f. paragraph 3.44 below).

3.44 Inclination of fingers.

The results of experiments to determine the influence of finger inclination on combustion efficiency are shown in Fig. 15. Finger widths of $\frac{1}{8}$ inch and $\frac{1}{2}$ inch were used. With the $\frac{1}{8}$ inch wide fingers at 30° inclination little difficulty was experienced in bringing the burner to choked tailpipe exit conditions, and in obtaining the combustion efficiency measurements. However, when the spreader having four fingers $\frac{1}{2}$ inch wide at 30° inclination was used, quenching of the pilot was encountered. To improve the stability of the system the distance from the pilot colander baffle to the downstream end of the pilot was increased from 3.5 inches to 6.5 inches. With this modified system the results shown in Fig. 15 for the $\frac{1}{2}$ inch wide fingers at 30° inclination were obtained. It is thought that this alteration in the pilot design made only a small difference, if any, to the combustion efficiency measurements. However no combustion efficiency readings were taken using other spreaders with this modified pilot system.

With the $\frac{1}{8}$ inch wide fingers the effect of the inclination of the fingers on the combustion efficiency performance is not clearly revealed. All that can be said is that, within the range of mixture strengths in which a comparison may be made, the spreader in which the fingers are at an inclination of 10° produces little improvement in the

combustion efficiency compared with the system using no spreader. On increasing the inclination of the fingers to 30° the performance is only slightly, if at all, improved.

A similar increase from 10° to 30° in the inclination of the $\frac{1}{2}$ inch wide fingers leads to a small improvement in the combustion efficiency values. The gain is of the same magnitude as the gain achieved by increasing the number of fingers from four to eight and keeping the finger inclination 10° .

3.45 Position of spreader.

In the experiments described in Chapter 2 using the Open Jet Apparatus a test is reported in which a spreader was placed with the roots of its fingers $7/16$ inch upstream from pilot outlet. That test indicated that the mass transfer of pilot gases still took place into, and along, the wakes of the fingers. A similar experiment was carried out in the series of combustion efficiency measurements described in this Chapter. The spreader tested in this way had four $\frac{1}{2}$ inch wide fingers at an inclination of 10° . The combustion efficiency measurements obtained with this arrangement are shown in Fig. 16, alongside the efficiency values obtained with the spreader in its normal position. It is seen that the efficiency results of the two sets of readings are in fairly good agreement, confirming that the operation of this spreader, as a means of improving the combustion efficiency, is not appreciably altered by introducing the pilot gases at a

FIG. 17 INFLUENCE OF SPREADER SHAPE ON COMBUSTION EFFICIENCY

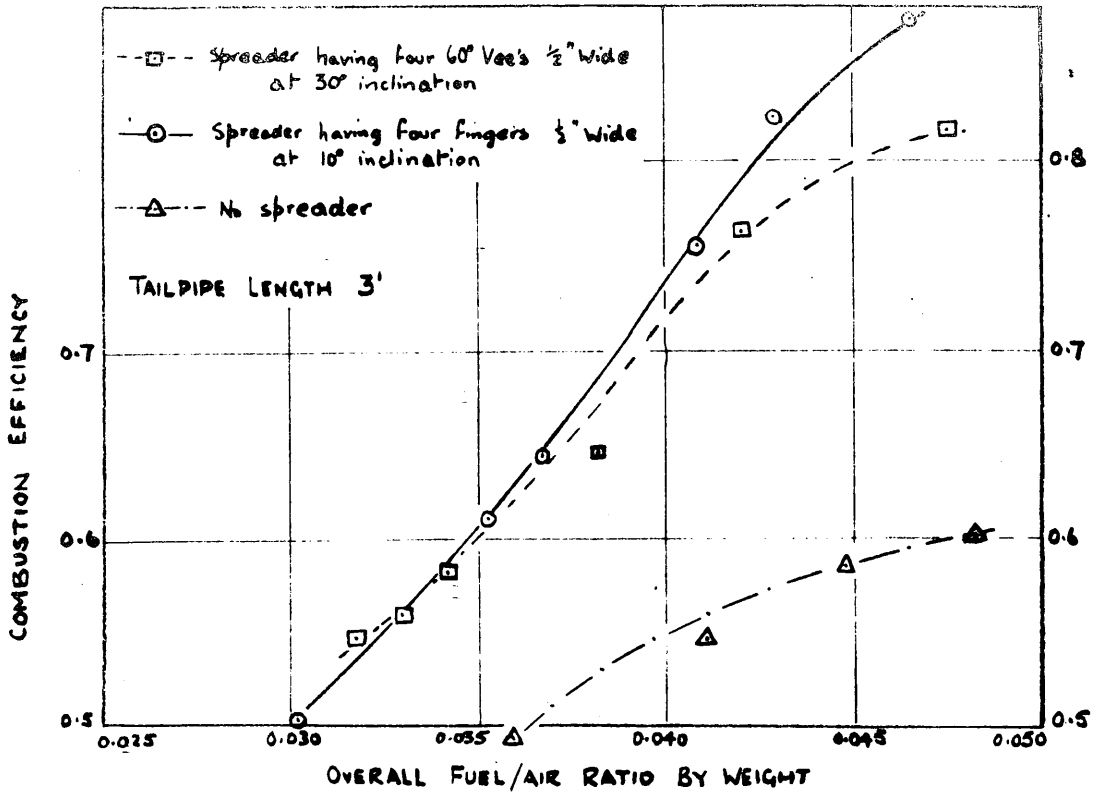
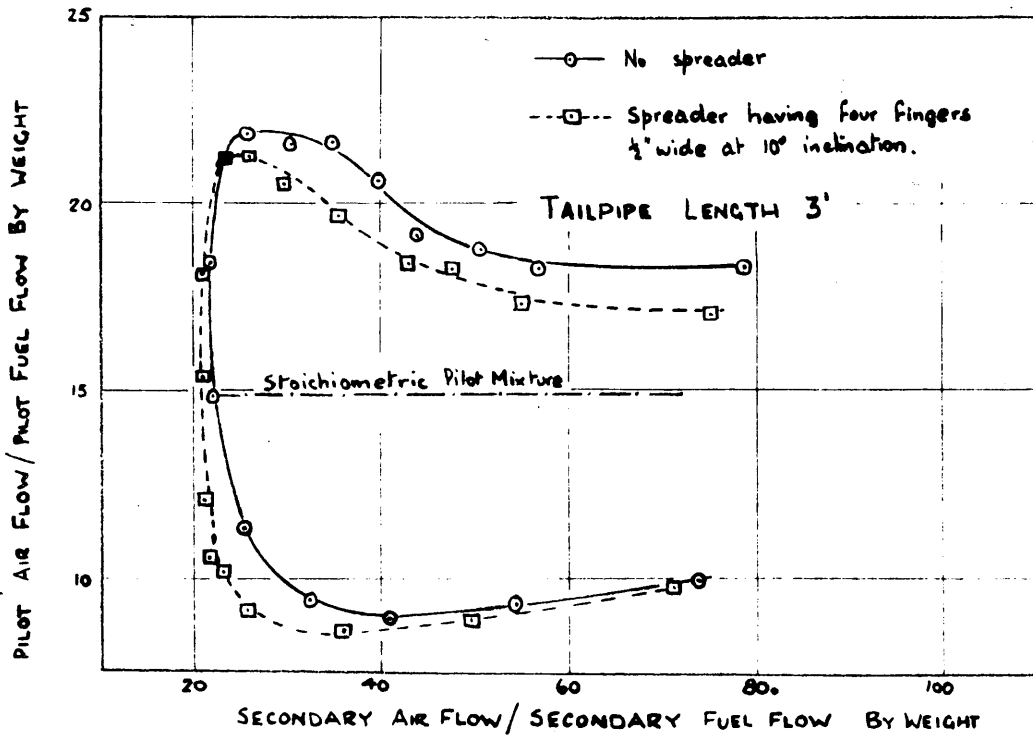


FIG. 18 OVERALL STABILITY LIMITS



short distance downstream from the root of the finger, instead of at the root of the finger. Longwell's measurements (1955) of the length of the recirculation zone behind a gutter provide an explanation of the above result.

3.46 Spreader shape.

One test was made using a spreader consisting of four 60° included angle Vee gutters, instead of flat fingers. The vees, open at the downstream end, were $\frac{1}{2}$ inch wide and were inclined at 30° to the axis of the burner. The results are presented in Fig. 17. It is seen that the efficiency values, over most of the fuel/air ratio range, are not as high as those obtained with the spreader having four flat fingers, $\frac{1}{2}$ inch wide, at an inclination of 10° to the axis of the burner.

3.5 Baffle Loss Coefficients.

Baffle Loss Coefficients under burning conditions were obtained from the thrust readings and the pressure and velocity head readings. The values of the "hot" Baffle Loss Coefficient lay between 3.0 and 4.0, depending on the spreader system and the length of tailpipe used. This influence of tailpipe length indicates that not all the pressure drop due to friction and eddying takes place at the baffle system, as is assumed in the ideal combustion system considered in Appendix I. This observation does not influence the values of combustion efficiency quoted in this Chapter since these values were obtained directly from the thrust

measurements, and no assumption regarding the Baffle Loss Coefficient was required in the calculation.

The values of "hot" Baffle Loss Coefficient were found to be almost independent of the approach Mach Number as it varied from 0.18 to 0.3.

3.6 Stability Tests.

Supplementary to the combustion efficiency measurements described above, the overall stability limits under choked tailpipe exit conditions were obtained (a) with no spreader and (b) with the spreader having four $\frac{1}{2}$ inch wide fingers at an inclination of 10° . A tailpipe of length 3 feet was used for these tests. The results are plotted in Fig. 18. The attachment of this spreader results in only a slight decrease in stability. However the experience gained while taking the combustion efficiency readings with the other spreader arrangements suggests that an increase in the width, number or inclination of the fingers will eventually bring about an appreciable reduction in the stability limits.

3.7 Conclusions.

The experiments described in this Chapter show that, for combustion systems using a simple pilot concentric with the main duct, if the combustion efficiency is low (say less than 70%), the efficiency may be improved by attaching flame spreaders to the downstream end of the pilot. Increasing the width, number or inclination of the fingers which constitute

TABLE 3.

COMBUSTION EFFICIENCIES IN A 1.875 inch
DIAMETER RAMJET.

From Mullen, Fenn and Garmon (1951)

Stoichiometric mixture

Vapourised n - heptane - air

Tailpipe length in.	Combustion Efficiency	
	with cone pilot	with cone pilot plus four radial gutters
14	30%	73%
18	70%	about 95%

the spreader improves the combustion efficiency performance.

However if these increases are carried beyond a certain limit, quenching of the pilot takes place. This limit due to quenching of the pilot may be altered by changing the pilot design. With the system studied (3 inch diameter pilot, 5 inch diameter duct) a good compromise between combustion efficiency and stability was provided by the spreader having four $\frac{1}{2}$ inch wide fingers at an inclination of 10° to the direction of flow. Such spreaders lose much of their effect when the overall fuel/air ratio becomes less than, say, 0.03 by weight.

In this group of experiments the overall fuel/air ratio by weight was limited to less than 0.05, owing to the low rich extinction limit of the burner system used. While it is expected that spreaders consisting of flat fingers will prove equally effective in rich mixtures, a few confirmatory experiments conducted in rich mixtures would be valuable.

Agreement with literature.

Mullen, Fenn and Garmon (1951) have measured the combustion efficiency in a 1.875 inch inside diameter ramjet. An independent oxygen-hydrogen pilot was used, the pilot gases entering the combustion chamber from the open base (0.75 inch diameter) of a 30° included angle cone. The main stream was carburetted with vapourised n-heptane. Efficiency results

are quoted in Table 3 for two tailpipe lengths using (a) the simple pilot and (b) a pilot embodying four radial gutters, $\frac{1}{4}$ inch wide, which traverse the annular space between the cone base and the duct walls. The results, which are similar to the results described in this Chapter, confirm that striking gains in combustion efficiency can be achieved by the use of these gutters, especially when the efficiency of the simple system is low, owing to a short tailpipe being used.

CHAPTER 4.

DEVELOPMENT OF APPARATUS FOR SMALL SCALE FLAME SPREADING EXPERIMENTS.

- 4.1 Introduction.
- 4.2 Air and fuel supplies.
 - 4.21 Air supply.
 - 4.22 Fuel supply.
 - 4.23 Flow measurement.
 - Flow transition in capillary meters.
 - Influence of temperature and pressure on capillary meter calibrations.
- 4.3 Burner design.
 - 4.31 Preliminary experiments using an oblique stabiliser.
 - 4.32 Preliminary experiments using a normal stabiliser with a pilot flame.
 - 4.33 Preliminary experiments using an oblique stabiliser with a pilot flame.
 - 4.34 Influence of preliminary experiments on the burner design.
- 4.4 Experimental techniques.
 - 4.41 Ionisation Probe.
 - 4.42 Calibration of Ionisation Probe in laminar flames.
 - Design of calibration burner.
 - Calibration experiments.
 - Position of schlieren image relative to the direct visual image.
 - 4.43 Ionisation Probe measurements in turbulent flames.
 - 4.44 Gas Analysis.
- 4.5 Summary.

CHAPTER 4.4.1 Introduction.

One of the conclusions of the experiments described in Chapter 2 is that while flame gases are generally present in the wakes of the fingers, they do not always initiate general combustion of the secondary fuel-air mixture, as it passes the finger. In the apparatus used in these preliminary flame spreading experiments there was no direct control of the flow of piloting gases along the wakes of the fingers. It was decided that this problem of the initiation of combustion by a source should be studied in small scale experiments at Glasgow University. The apparatus to be used should enable the piloting energy to be supplied directly to the position at which the combustion of the main fuel-air stream is to be initiated. The development of the apparatus for use in these experiments is described in this Chapter.

Unfortunately the experiments using this apparatus have not yet been carried out as the author has been called up for National Service. A plan of the suggested small scale experiments is given in Chapter 6.

4.2. Air and Fuel Supplies.

As mentioned in Chapter 1, flow and pressure fluctuations tend to take place when confined flames burn in high velocity streams (Longwell, 1955; and others). These fluctuations can cause inconsistencies in the combustion

characteristics of the system. For example Barrere and Mestre (1954) observed that an increase in tailpipe length caused a reduction in the stability limits of gutter type flame holders.

To limit the influence of these fluctuations on the results of the small scale experiments, the planning of which is described here, it was decided that the flow velocity at inlet to the combustion chamber should not exceed 60 ft/sec.

4.21 Air Supply.

Three Keith Blackman Blowers were connected in series to provide the air supply. These blowers give an air flow velocity of up to 80 ft/sec. through a test section of cross-sectional dimensions 2 x 1 inch, the delivery pressure from the blowers at this flow velocity being 80 cm. water. At this flow, and with a ratio of unburned gas density to burned gas density of eight, it is estimated that the pressure drop due to heat release within the chamber is 52 cm. water. The balance in pressure of 28 cm. water is available for metering, friction, etc.

4.22 Fuel Supply.

The fuel chosen for these small scale experiments was "Stenched Butane", butane being the heaviest of the paraffin hydrocarbons which are gaseous at room temperatures and pressures. The butane was supplied in cylinders by Imperial Chemical Industries, Billingham. An analysis, supplied

TABLE 4.

ANALYSIS OF A TYPICAL SAMPLE OF "STENCHED
BUTANE^m.

Constituent	% by volume
Pentanes	0.1
Normal-butane	16.1
Iso-butane	33.5
Propylene	2.5
Ethane	0.2
Butadiene	15.2
Butenes	32.4
	100.0

by the manufacturers, of one delivery of butane is given in Table 4. It is understood that the composition may vary considerably from one delivery of butane to another.

4.23 Flow measurement.

The air supplied by the three Keith Blackman blowers is measured by a British Standard Orifice Plate, fitted with D and D/2 taps.

In certain experiments, which are described below, small air flows were used (less than 1200 ml/sec., ^{i.e.} /2.5 cu.ft./min.). These air flows were provided by small pumps, and the flow rates were measured by capillary meters. Capillary meters were also used to measure butane flows.

A capillary meter (Benton, 1919; Ergun, 1953) consists of one or more lengths of small bore capillary tube through which the gas flows, the pressure drop across the capillary tube being indicated by a manometer. The volume flow rate through a capillary tube is related approximately to the differential head by the expressions -

For laminar flow through the capillary tube -

$$h = 1.88 \frac{\rho V^2}{gd^4} + 41 \frac{\eta l V}{gd^4} \dots\dots\dots \text{Eqn. 4.1}$$

and for turbulent flow through the capillary tube -

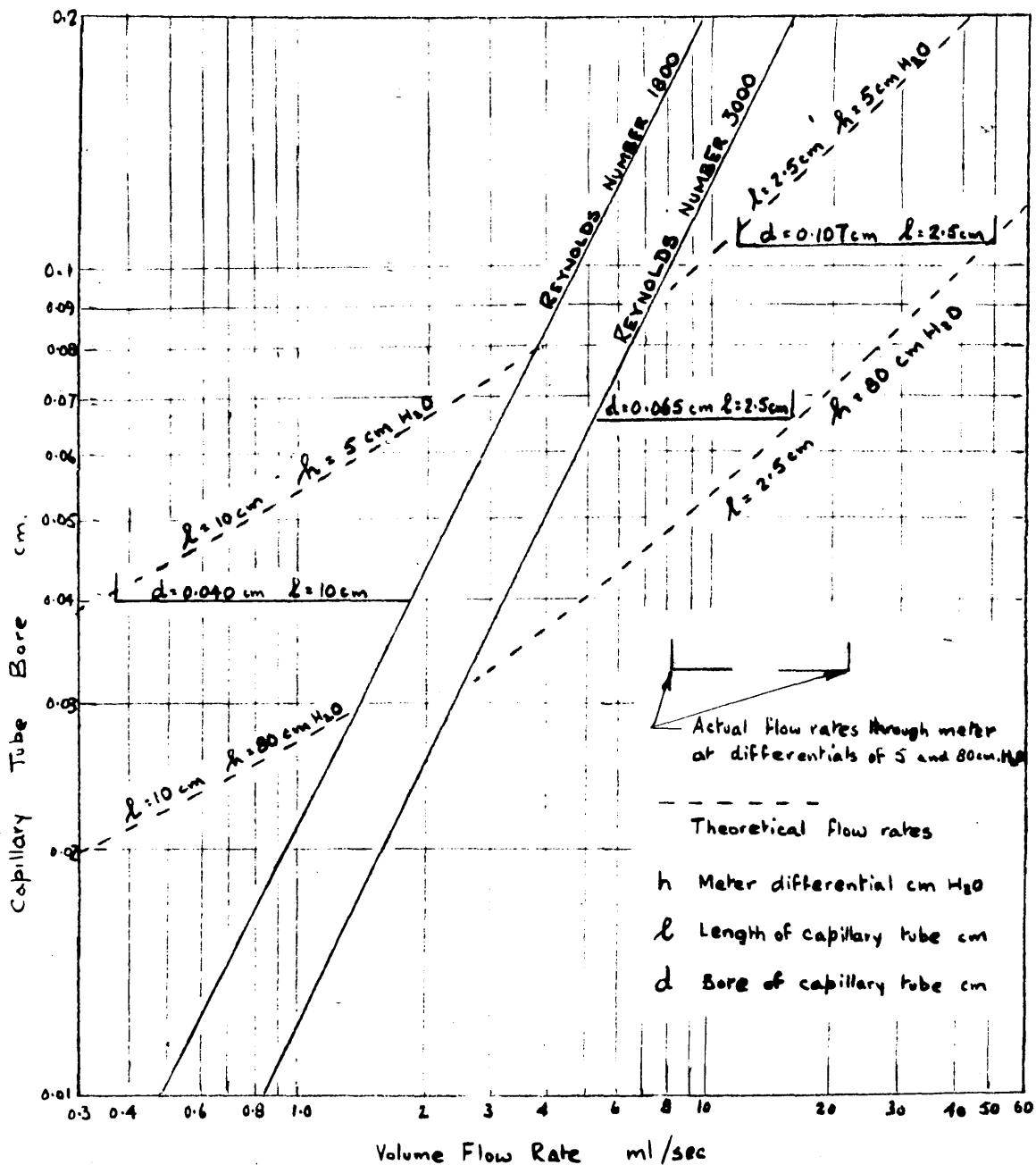
$$h = 1.14 \frac{\rho V^2}{gd^4} + \frac{\rho l V^2}{gd^5} \left[0.0058 + 0.50 \left(\frac{1}{N_{Re}} \right)^{0.35} \right] \dots\dots \text{Eqn. 4.2}$$

where h is the pressure drop across the meter, ρ is the density of the fluid, V is the volume flow rate, g is the acceleration

FIG. 19 VOLUME FLOW RATE THROUGH A CAPILLARY METER

Single Capillary Tube

Butane at 20°C, 76 cm Hg



due to gravity, d is the bore of the capillary tube, γ is the absolute viscosity, l is the length of the capillary tube and N_{Re} is the Reynolds Number of the flow through the capillary tube.

Owing to the irregularity of the shapes of the entries to the capillary tubes, and owing to the difficulty of obtaining an accurate measurement of the tube bore, the flow rates calculated from the above expressions are liable to be in error by about 10%. Thus these expressions are only useful at present as a means of selecting the meters necessary to cover a given range of flow rates. For this purpose, graphs have been prepared from the expressions indicating the influence of tube bore on the volume flow rate of both air and butane. A portion of the graph for butane at 20°C, 76 cm. Hg. is given in Fig. 19.

Once a meter has been selected and prepared, and before it is used, it is calibrated against a standard - either a Soap Bubble Meter, a Wet Gas Meter, or a Dry Gas Meter. Some notes on the calibration of Capillary meters by these standard meters are given in Appendix III. The ranges of the observed calibrations of several meters are shown in Fig. 19, where they may be compared with the predicted ranges.

Flow transition in capillary meters.

Part of the pressure drop across a capillary meter is due to wall friction. For flows where the Reynolds Number (based on the tube bore) is less than 2000 or greater than

3000, the laws relating the friction pressure drop to the flow rate are well established. In the intermediate range of Reynolds Number the friction pressure drop may not be consistent at one flow rate, depending on whether the flow had previously been increased from the laminar region, or decreased from the fully turbulent region. To avoid this uncertainty, capillary meters were never used within this transitional range of Reynolds Number. Referring to Fig. 19, the butane flow rate between 1.8 ml/sec. (0.040 cm. bore, 10 cm. tube length) and 5.2 ml/sec. (0.065 cm. bore, 2.5 cm. tube length) was covered by using a capillary meter having four capillary tubes in parallel, each tube being 0.040 cm. bore and 10 cm. long. This meter covered the range from 1.4 to 7.2 ml/sec. without the Reynolds Number exceeding 1800.

Influence of temperature and pressure on capillary meter calibrations.

It is seen from Equations 4.1 and 4.2 that the volume flow rate at any one meter differential is a function of the density and the absolute viscosity of the fluid. The density is a function of both the fluid temperature and pressure, and the absolute viscosity is a function of the temperature, so that a calibration of volume flow rate against meter differential which is taken at one fluid pressure and temperature is, in general, valid only at these conditions. From day to day it is found that the temperature and pressure vary at the

capillary meter. However Equations 4.1 and 4.2 may be used to estimate the amount by which the calibration will change due to these temperature and pressure variations.

For example, for a long capillary tube in which the flow is laminar the major portion of the meter differential is due to viscous drag, so that the volume flow rate is roughly inversely proportional to the absolute viscosity (Equation 4.1). Thus the volume flow rate at any one head is, to a fair approximation, independent of the pressure and inversely proportional to the absolute temperature. A typical range of temperatures encountered in one series of experiments was from 14°C. to 22°C. Thus a volume flow rate calibration for this meter taken at the lower temperature would be in error by about 3% if used when the fluid temperature is 22°C.

For a short capillary meter in which the flow is turbulent (Equation 4.2) the pressure drop due to accelerating the fluid into the meter constitutes the major portion of the meter differential. This leads to the approximation that the flow rate at any one differential is inversely proportional to the square root of the fluid density, i.e. is directly proportional to the square root of the temperature and is inversely proportional to the square root of the pressure. The barometric pressure may vary from about 74 to 78 cm. mercury over a series of experiments so that here again an error of up

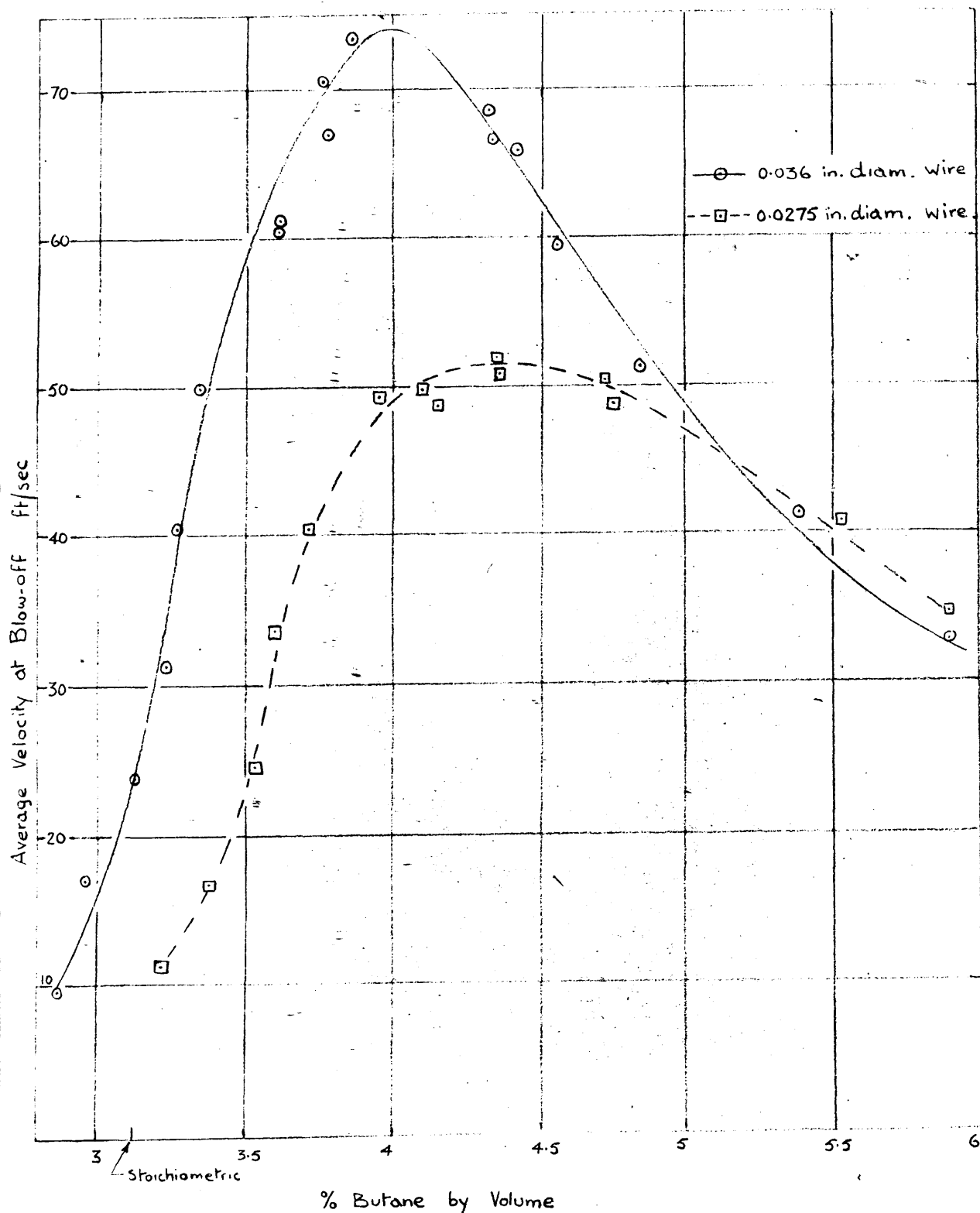
to about 3 or 4% may result from the use, over the entire range of temperatures and pressures, of a calibration taken at one set of conditions.

For many purposes these errors, resulting from the use of a single calibration for all temperatures and pressures, may be tolerated. However, for more accurate work the original calibration may be corrected by using the approximate relationships indicated above. Alternatively the capillary meter may be recalibrated against the standard meter for each set of fluid conditions. The first method is considerably quicker, especially when only a few flow readings have been taken but it is advisable to check the calibration periodically against a standard to ensure that the capillary tube has not become fouled by dirt.

4.3 Burner design.

The experiments, the design of which is described in this Chapter, are intended to investigate the influence of heat, or energy, supply to a source on the initiation of general combustion from that source. It is advantageous to have a source on which the flame is not self-anchored, i.e. the flow velocity should exceed the blow-off velocity for zero source energy input. It had been decided that the flow velocity should not exceed 60 ft/sec., in order to minimise flow and pressure fluctuations, as discussed in paragraph 4.2 above. Thus a source is required of dimensions such

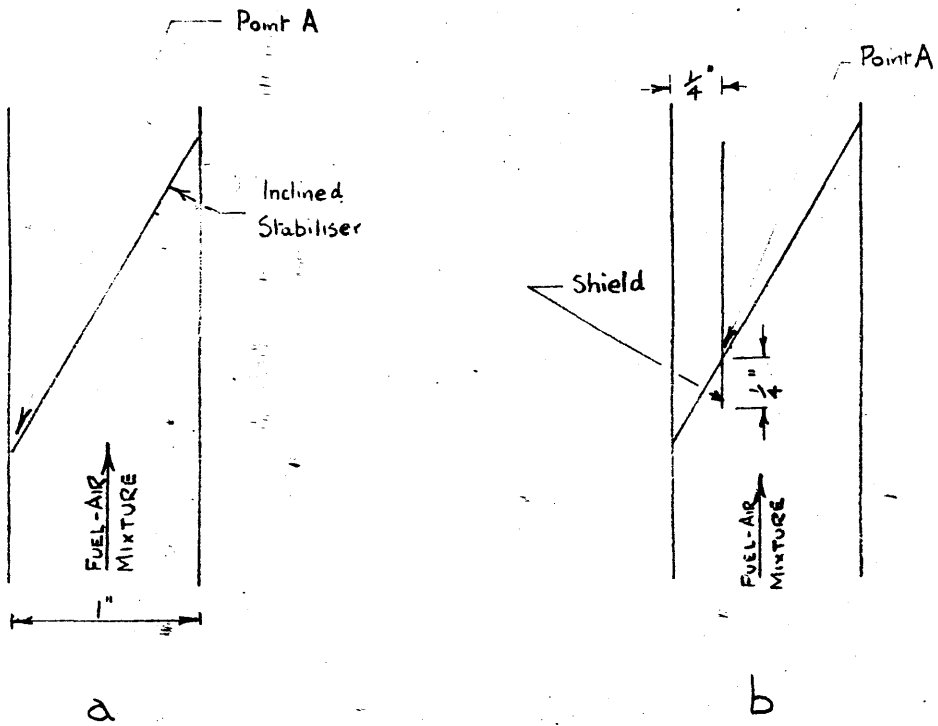
FIG. 20 BLOW-OFF FROM WIRE STABILISERS



that the peak of the blow-off velocity versus fuel concentration curve is less than 60 ft/sec. Estimates based on Scurlock (1948) indicated that the dimension of the source should be less than 0.04 inch. Since this result is based on considerable extrapolation, a series of blow-off experiments was carried out, using as stabilisers wires of diameter 0.036 and 0.0275 inch placed normally across a 1 x 1 inch test section. The test section was unenclosed beyond the stabiliser. The results of these experiments are given in Fig. 20. Flames were also lit on a wire of diameter 0.020 inch at flow velocities ranging from 11 to 40 ft/sec., and over a range of butane concentrations, but on no occasion did the flame remain alight for more than about 15 sec. after the piloting flame was removed.

It is noted that the peaks of the stability curves shown in Fig. 20 lie considerably on the rich side of the stoichiometric fuel concentration. This phenomenon has been discussed by Williams and Shipman (1953) and Zukoski and Marble (1955) who attribute it to the importance of diffusion in the mechanism of anchoring of flames behind small baffles (Reynolds Number less than 10^4). Oxygen has a higher diffusivity than the fuel, butane, and so diffuses more rapidly from the fresh mixture into the anchoring zone. As a result the fuel concentration within the anchoring zone is less than the concentration in the approach stream.

FIG. 21 APPARATUS FOR TESTING INCLINED WIRE STABILISER



From the blow-off experiments described above it is seen that the dimension of the source should not exceed 0.03 inch. Originally it had been intended to supply the source with flame gases. However, in view of the mechanical difficulties involved in supplying the energy in this form to the source, it was decided that the source should be an electrically heated wire.

Several preliminary experiments were carried out using unheated wires placed obliquely across the main stream. These experiments, which aided the design of the burner, are described below. The wires are referred to below as "stabilisers".

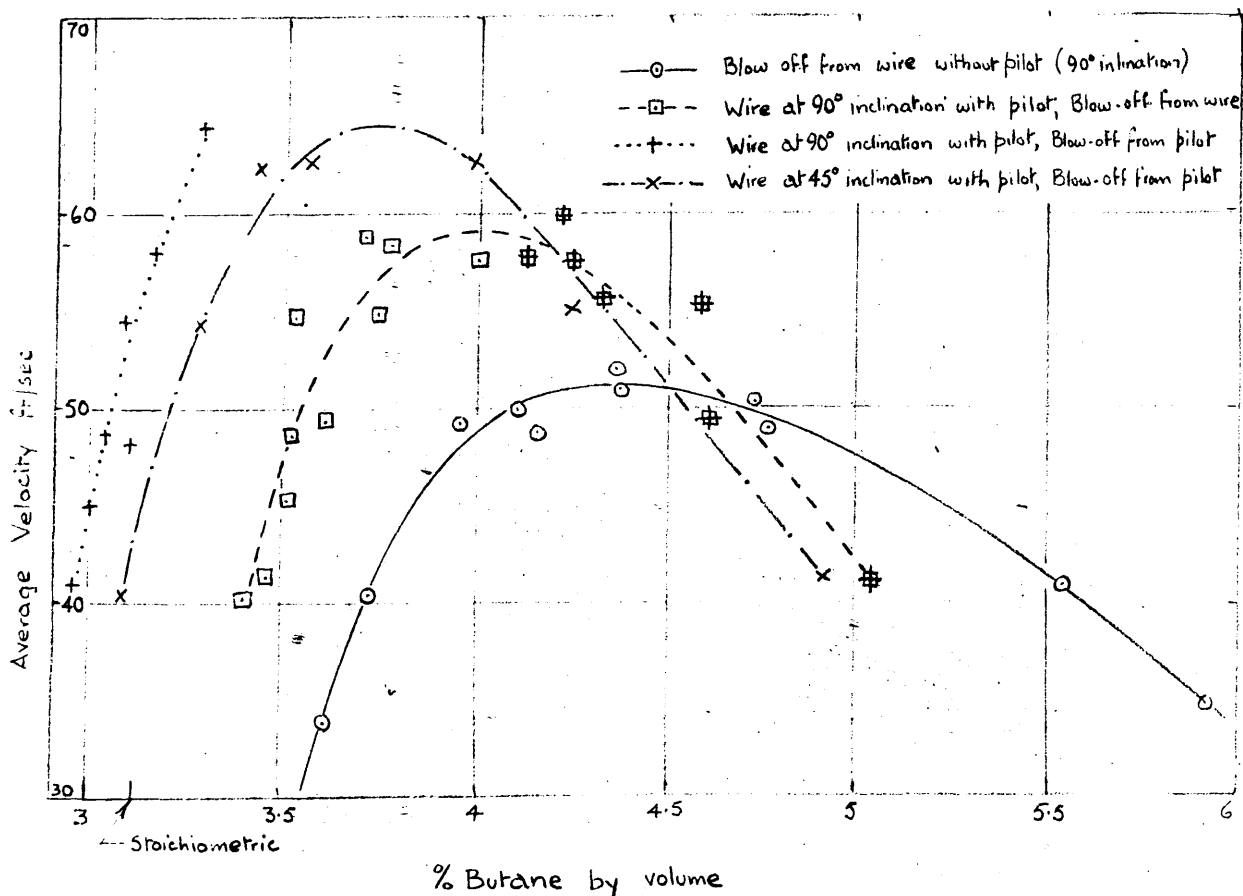
4.31 Preliminary experiments using an oblique stabiliser.

A wire stabiliser, of diameter 0.036 inch, was placed across the 1 x 1 inch test section at an inclination of 30° to the direction of flow (Fig. 21a). At a flow velocity of 10 ft/sec. it was found that a flame was stable over only a narrow range of fuel/air ratios. Beyond this range a flame, which was initially present from end to end of the wire, was seen to recede gradually from the point A, until extinction occurred. When a shield was introduced, as shown in Fig. 21b it was observed that a flame was never stable, and extinction took place much more rapidly.

This experiment shows the influence of the flow velocity at the point A on the stability of a flame which is self anchored in the wake of an oblique stabiliser. The experiment

FIG 22 BLOW-OFF FROM WIRE STABILISERS WITH FLAME PILOT

WIRE DIAMETER 0.0275 IN.



also indicates that the performance of such an inclined stabiliser will be very much altered by the presence of a steady pilot flame at the upstream end of the stabiliser, as flame failure in the above tests was due to failure of the flame to anchor at the point A.

As a pilot flame system, placed at the roots of the fingers, is used in the practical application of flame spreading fingers, some experiments were carried out on stabilisers provided with flame pilots.

4.32 Preliminary experiments using a normal stabiliser with a pilot flame.

A wire of diameter 0.0275 inch was used as the stabiliser in this experiment. The pilot flame which was employed was the flame anchored on a double loop bent in the stabiliser wire, the test portion of the stabiliser wire leaving from the downstream face of the loop. The stability limits were observed for this system. At the rich extinction limit the flame lifted simultaneously from the test stabiliser and from the pilot loop, at flow conditions roughly corresponding to the rich blow-off limits of the simple 0.0275 inch diameter wire. However at the weak limit, the flame lifted first from the stabiliser test wire, followed by blow-off from the pilot loop. For practical purposes this lifting of the flame, which had been anchored on the stabiliser test wire, took place abruptly, and at flow velocities and fuel concentrations slightly beyond the weak stability limits

of the wire without a pilot. The results of this experiment are plotted in Fig. 22.

4.33 Preliminary experiments using an oblique stabiliser with a pilot flame.

A wire of diameter 0.0275 inch was again used as the test stabiliser, the wire being inclined at 45° to the direction of flow. The flame anchored on a loop in the wire was again used as the pilot flame. In this case, provided that a flame remained anchored on the pilot, there was always visible evidence of a flame behind the stabiliser. The stability limits of the pilot are plotted in Fig. 22. On the weak side, these limits lie considerably beyond the stability limits of the normal stabiliser, even when it was provided with a pilot.

These experiments were hampered by the small stability range of the pilot, and they show the importance of an independent flame pilot system.

An interesting, and possibly important, phenomenon was observed when the "Ionisation Probe" was used to study the flame propagating from the inclined test wire. The Ionisation Probe is discussed later in paragraph 4.41, but in the tests here it was used only to indicate the presence of a flame between the probe wire and the stabiliser test wire, or pilot loop. The output from the probe was connected to an Oscilloscope to allow observation of the manner in which the probe signal varied with time. A flow velocity of

40 ft/sec. was used for these tests. As the weak limit was approached, with the probe wire placed in the flame propagating from the test stabiliser, the oscilloscope indicated that for an appreciable fraction of the total time there was no flame present between the probe wire and the stabiliser wire. Under the same conditions the probe wire was placed in the flame emanating from the pilot loop itself, and no periods of flame absence were observed. Hence the instantaneous gaps in the flame behind the test stabiliser appear to be due to a failure in the process of flame spreading along the wake of the wire.

No corresponding failure in the flame spreading mechanism was observed at the rich extinction limit.

4.34 Influence of preliminary experiments on the burner design.

The experiments described above have shown that a source dimension of 0.03 inch, or less, must be used in order that a flame will not be self-anchored at flow velocities of 60 ft/sec. This result has led to the proposed use of electrical energy instead of flame gases as a means of supplying energy to the source.

It has also been shown in the preliminary experiments that the performance of a stabiliser which is placed obliquely across the main stream will be considerably influenced by the presence of a steady pilot flame at the upstream end of the wire.

A burner has been designed and constructed, using the experience gained in these preliminary experiments. It has a test section of cross-sectional dimensions 2 x 1 inch. The stabiliser wire, which may be electrically heated, is placed either normally across the stream, or at an inclination of 30° to the stream, the wire traversing the 2 inch dimension of the cross-section. A small pilot flame, in which an independent supply of premixed air and butane is burned, surrounds the upstream end of the stabiliser wire.

The preliminary experiments have also influenced the design of the Ionisation Probe, one of the instruments to be used with the burner described above. Circuits have been added to the amplifier which will give a quantitative measure of the fraction of the total time that the Probe signal is less than a predetermined value. This instrument should be able to supply useful information on the apparent failure in the flame spreading mechanism which was observed in the preliminary experiments using an inclined stabiliser provided with a pilot flame. The details of this circuit, and of the Ionisation Probe, are given below in paragraphs 4.41, 4.42 and 4.43.

4.4 Experimental techniques.

Two experimental techniques have been developed to study the propagation of a flame from the source. These are the Ionisation Probe, and gas sampling and analysis using an Infra Red Gas Analyser.

FIG 23 PRELIMINARY IONISATION PROBE CIRCUIT

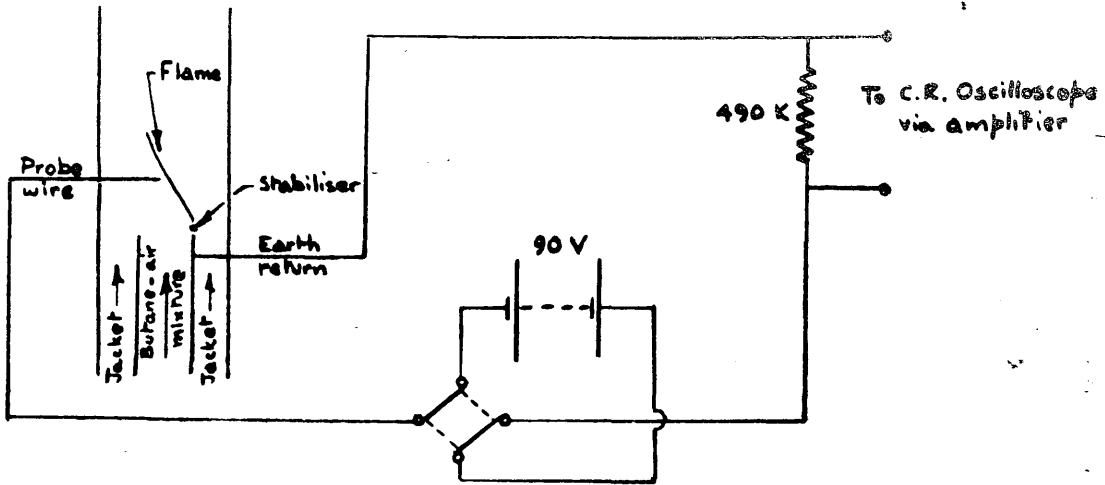
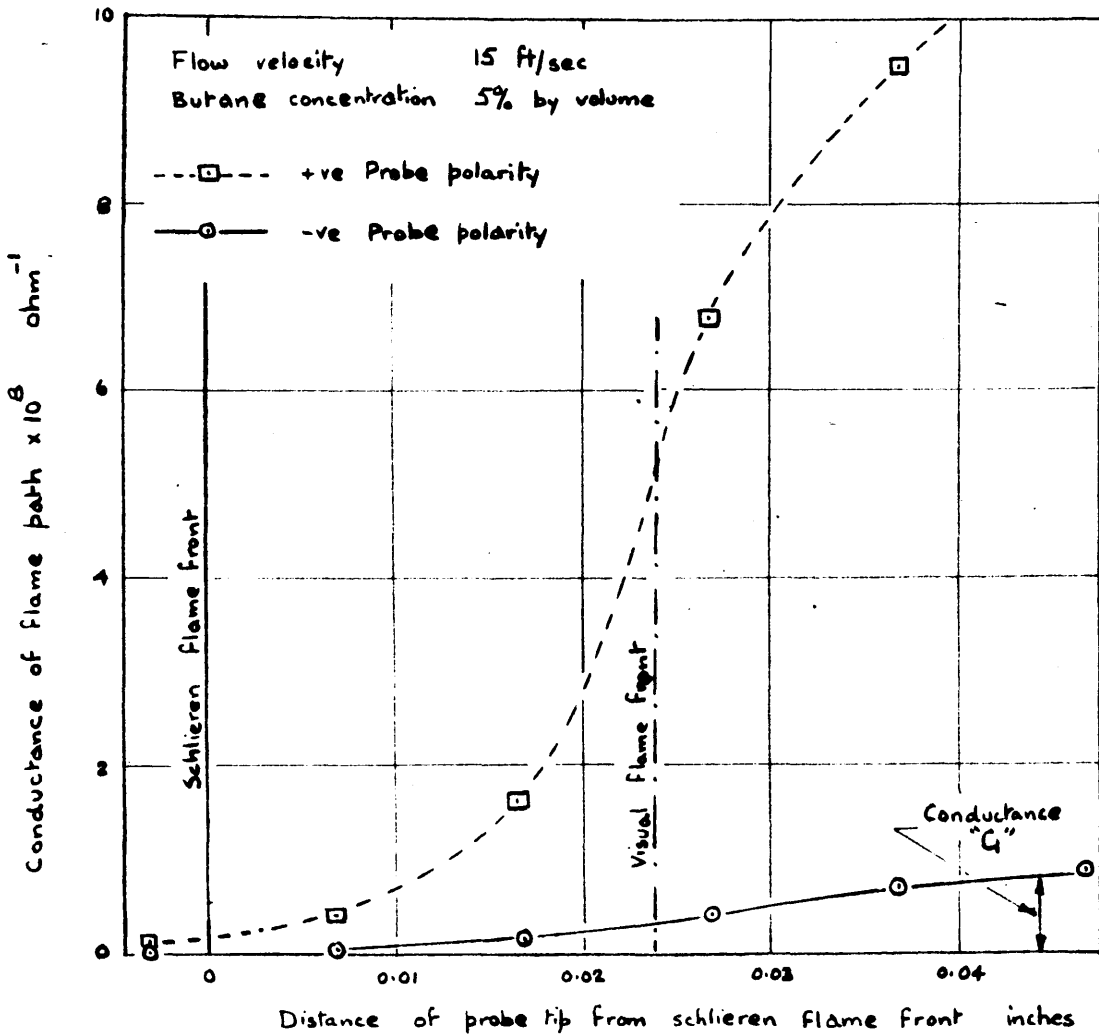


FIG 24 INFLUENCE OF PROBE POLARITY ON SIGNAL



4.41 Ionisation Probe.

The Ionisation Probe is intended to be a means of locating a flame front.

The operation of the Probe depends on the presence within the flame front of ions, or charged particles (Thomson and Thomson, 1928, p.399). Karlovitz, Denniston, Knapschaefer and Wells (1953) show that the ion concentration rises rapidly from zero as the unburned gases enter the flame zone. As the gases leave the flame zone the ion concentration drops again to a fairly constant value. If two probe wires at different potentials are introduced into the flame zone, the ions act as carriers, and a small current flows. The voltage distribution between the two electrodes in such a system has been studied by Wilson (1931), who found that the major portion of the voltage drop between the electrodes takes place close to the negative electrode. This result suggests that, when the electrodes are only partially immersed in the flame, the amount of current flowing depends principally on the flame conditions around the negative electrode.

To test this conclusion, some preliminary experiments were carried out using the apparatus and simple circuit outlined in Fig. 23. In these experiments a probe which could be moved through the flame front was used as one of the electrodes, the burner, at earth potential, acting as the second electrode. The results are shown in Fig. 24 of two

traverses made using opposite polarities of the moving probe.

In a second experiment, a wire similar to the traversing probe wire was immersed in the flame in a fixed position. When this wire was used in place of the burner as the second electrode the results obtained with a negative potential on the traversing probe were unchanged from those shown in Fig. 24. With a positive potential on the traversing electrode the maximum signal only reached the maximum value that had been obtained when the traversing probe had a negative potential (Conductance "G", shown in Fig. 24.)

It was observed in these experiments that, for practical purposes, the signal was independent of the distance between the traversing probe wire and the second electrode.

These results confirm that the current flowing between the probes depends principally on the flame conditions close to the negative probe. Thus if the traversing probe is given a negative potential, the signal indicated will be a function of the flame position relative to the position of the tip of the traversing probe wire, provided that the second electrode, which can be the burner itself, makes a reasonable connection with the flame.

An Ionisation Probe, in which the traversing probe has a negative potential, has been developed by Karlovitz, Denniston, Knapschaefer and Wells (1953). Care is taken to cool

FIG. 25 SKETCH OF IONISATION PROBE

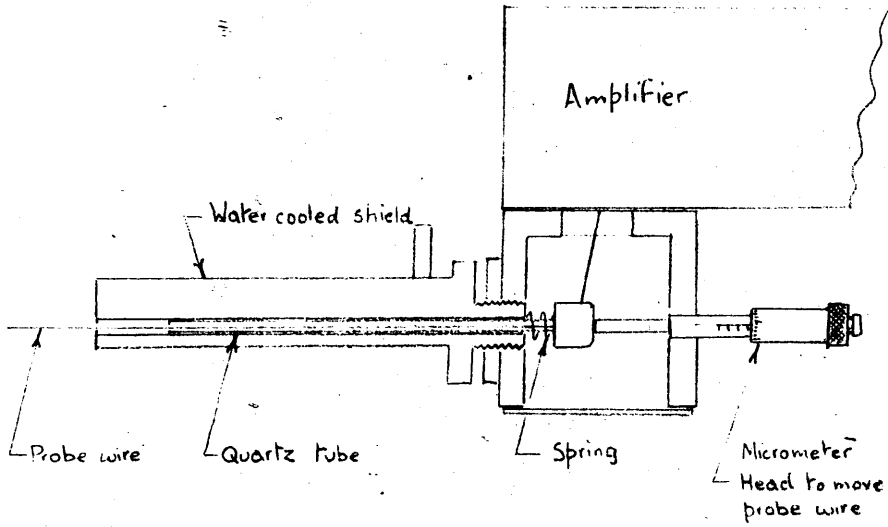
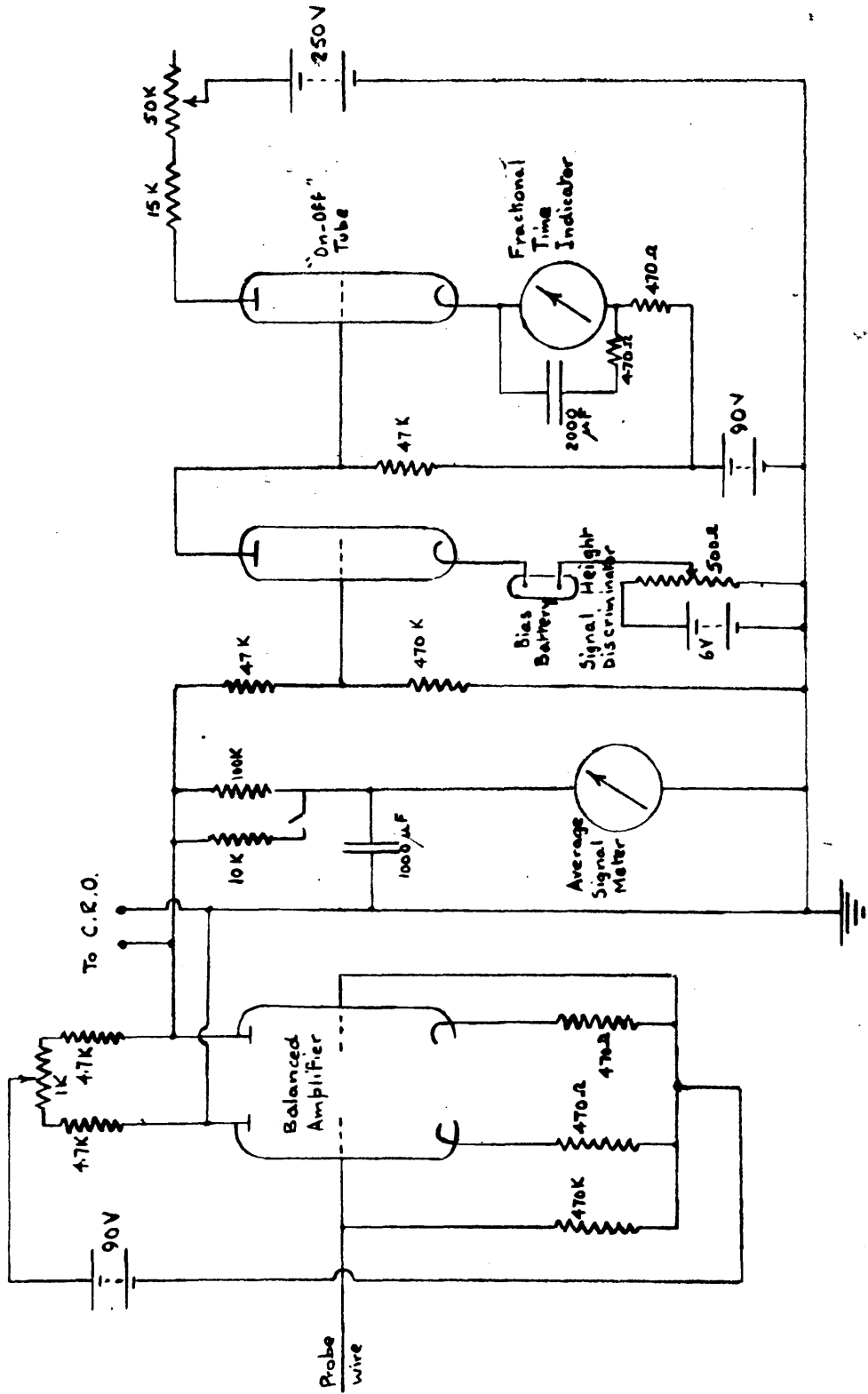


FIG. 26 ELECTRONIC CIRCUITS - IONISATION PROBE

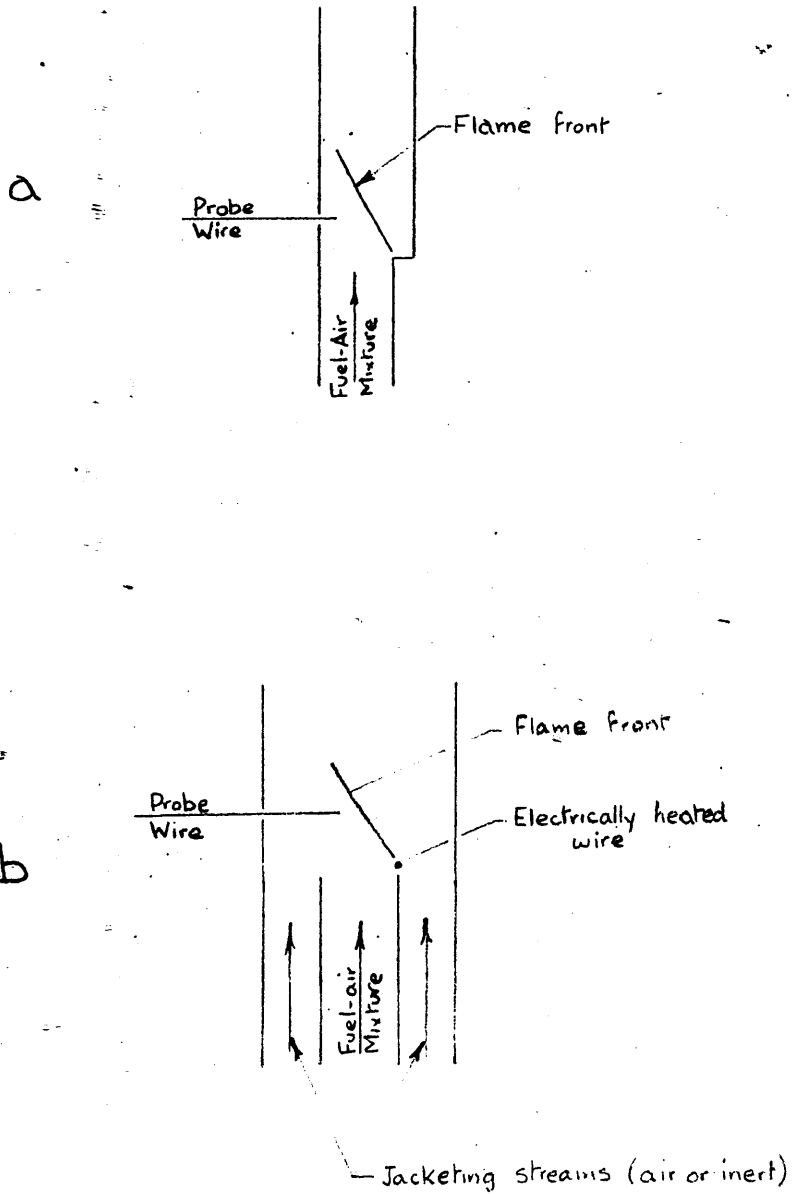


the insulation around the traversing probe, otherwise the insulation may become heated and provide a path between the probe and earth, leading to erroneous results. Drawings of this probe, and the associated electronic circuits were generously given to the author by Dr. Karlovitz, and from these drawings a similar probe was assembled. A sketch of the probe is given in Fig. 25. The circuits are shown in Fig. 26. The assembly of the electronic circuits was carried out at the National Gas Turbine Establishment, Pyestock, and the author wishes to thank those members of the staff who were responsibly for this work.

The average signal meter, shown in Fig. 26 measures the time average conductance of the path between the negative probe and the earth return. The signal height discriminator, and the fractional time indicator are included for the analysis of the fluctuating signals which are encountered in measurements of turbulent flames. These circuits are discussed later in paragraph 4.43.

As stated above, the Ionisation Probe is intended to be a means of rapidly locating a flame front. In the preliminary tests it was observed that the signal obtained when the probe was fully immersed in the flame varied considerably with the fuel concentration. Thus it was apparent that, before the probe could be used as a means of defining the position of a flame front, it had to be calibrated, over a range of fuel concentrations, in flames

FIG. 27 LAMINAR BURNERS FOR THE CALIBRATION OF IONISATION PROBE



whose position could be defined by some other means.

4.42 Calibration of the Ionisation Probe in laminar flames.

Since the position of a laminar flame may be defined by schlieren or visual observation more easily than the position of a turbulent flame, it was decided that the calibration should be carried out using a flat laminar flame. When the Ionisation Probe is used as an experimental technique in the flame spreading experiments the probe will approach the flame front from the unburned gas side, and so it appeared advisable for the probe to be calibrated in a burner in which the probe traverses towards the flame from the cold gas side. Bearing in mind these two requirements, two designs of calibrating burners were considered. Sketches of these twodesigns are given in Fig. 27a and b. A two-dimensional burner of the type shown in Fig. 27b was chosen, because with this burner any quenching effects of the walls on the flame will be reduced.

In the type of burner chosen the flow velocity must exceed the velocity at which a flame lifts from the mouth of the rectangular channel. When the literature was examined for information on flame stabilisation on rectangular burners it was found that the correlating formula obtained by Grumer, Harris and Schultz (1953) predicted anomolous results for the dimensions likely to be met in the Ionisation Probe Calibration Burner. To investigate this

apparent inconsistency in the literature, a series of experiments was carried out on flame blow-off from rectangular burners. These experiments are described in Chapter 5 of this Thesis.

Design of Calibration Burner.

Using the results of the blow-off experiments which are described in Chapter 5, cross-sectional dimensions of $\frac{1}{8}$ x 1 inch were chosen for the inner rectangular channel of the calibration burner.

When the flame is surrounded by an inert gas, such as carbon dioxide, the critical boundary gradient for blow-off passes through a maximum when the butane concentration by volume is about 3.6% (Lewis and von Elbe, 1951, p.287; Wohl, 1953) so that the maximum critical gradient should not exceed 5000 sec.^{-1} (from Fig. 34). This gradient corresponds to an average flow velocity in the $\frac{1}{8}$ x 1 inch channel of roughly 8 ft/sec. The Reynolds Number at this flow rate is 920. These figures apply to the case where the surrounding inert atmosphere is stationary. In the calibration burner the surrounding atmosphere flows at a velocity usually equal to the average velocity of the butane-air mixture, so that one would expect the maximum blow-off velocity to be less than 8 ft/sec., thus giving more than a twofold range of flow velocities within the laminar range.

In the experiments described below it was found that the

FIG. 28. APPARATUS USED IN THE CALIBRATION OF THE IONISATION PROBE.

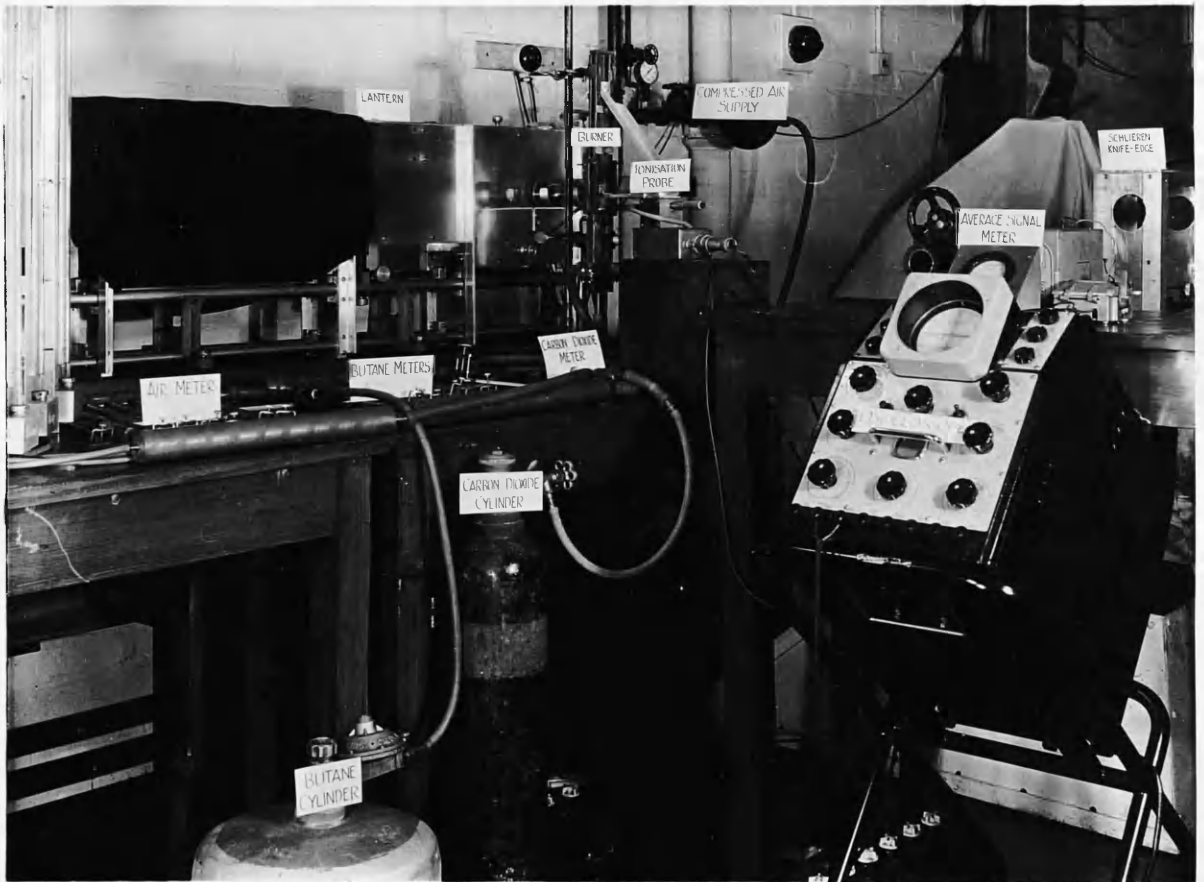


FIG. 29. TYPICAL SCHLIEREN IMAGE OF A LAMINAR FLAME,
SHOWING TIP OF IONISATION PROBE.

Flow velocity 15 ft/sec.
Butane concentration 3.5% by volume.



FIG. 30. COMPARISON OF DIRECT AND SCHLIEREN IMAGES OF
A LAMINAR FLAME.

Interrupted schlieren image superimposed on direct
visual image.

Flow Velocity 15 ft/sec. Butane concentration 3.5%
by volume.



TABLE 5.

CALIBRATION OF IONISATION PROBE IN LAMINAR FLAMES -
RANGES OF CONDITIONS.

Flow Velocity ft/sec.	Butane Conc. %	Probe Height inches.
7	2.5 - 6	0.13
15	2.6 - 6	0.13
	3.5	0.07 - 0.32

maximum blow-off velocity in an equal velocity carbon dioxide atmosphere was less than 7 ft/sec.

Calibration experiments.

The Ionisation Probe was calibrated by traversing the probe through the flame and noting the average signal meter reading for various positions of the probe tip relative to the region of maximum schlieren deflection in the flame. A photograph of the Ionisation Probe, the calibration burner, and the lantern and knife edge of the schlieren system, as they were used in the calibration experiments is given in Fig. 28. Not included in the photograph are the two 12 inch diameter mirrors and the screen on-to which the schlieren image of the flame was projected. The parallel light test section, in which the laminar burner was placed, was formed between these two mirrors.

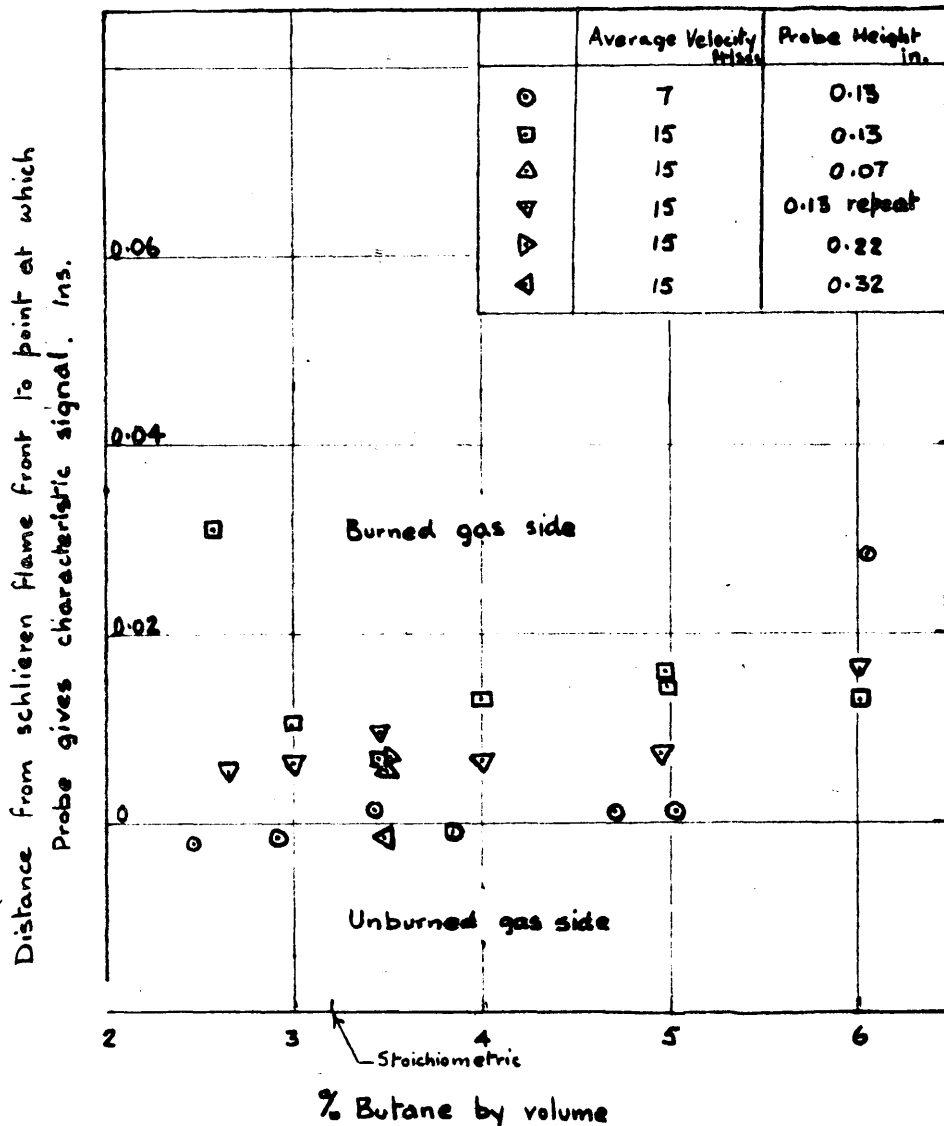
A typical flame schlieren image, as it was projected on to the screen, is shown in Fig. 29. When the probe wire was moved through the flame front the shadow of the probe wire crossed the schlieren image of the flame. This can be seen taking place in the photograph. The position of the probe when the tip appeared at the centre of the image was taken as the reference position for the traverse.

The ranges of flow velocities, fuel concentrations and probe heights within which traverses were made are given in Table 5 (the probe height is taken as the distance between the centre line of the stabiliser wire and the centre line of

FIG. 31 CALIBRATION OF IONISATION PROBES IN LAMINAR FLAMES

Comparison of schlieren flame front with flame position indicated by ionisation Probe

Characteristic signal 5 scale divisions
 Corresponding conductance $6 \times 10^{-10} \text{ ohm}^{-1}$



the probe wire). The traverses gave results similar to those shown in Fig. 24.

The probe signal, which was measured by the average signal meter, was also fed into a cathode ray oscilloscope. The oscilloscope traces showed that the signal was quite steady, a result one would expect.

It was found that the results of the traverses were virtually independent both of the heating current flowing within the stabiliser wire, and of the velocity of the jacketing carbon dioxide stream.

As a first attempt at correlating the results of the traverses, a characteristic signal value was selected, and the distance from the schlieren image to the point on the traverse where this signal was given, was plotted for each of the traverses. It was found that when a low value of characteristic signal, 5 divisions (corresponding to a flame conductance of $6 \times 10^{-10} \text{ ohm}^{-1}$) was chosen, a good correlation was obtained, the "characteristic point" for each of the traverses except two being within 0.02 inch of the schlieren flame front. This correlation is shown in Fig. 31. The two traverses which give least satisfactory agreement with the correlation were made in flames burning in mixtures in which the fuel concentration was at its maximum and minimum values. It is seen that the influence on the results of velocity, and of probe height, is small. In view of the limitations of the apparatus this correlation seems to be as

satisfactory as can be obtained.

These experiments show that, by choosing a signal meter reading of 5 divisions (corresponding to a flame conductance of $6 \times 10^{-10} \text{ ohm}^{-1}$), the Ionisation Probe can locate a laminar flame front to within 0.02 inch of the position of the schlieren image. The method is applicable to butane concentrations ranging from 2.8 to 5.5% by volume.

The diameter of the probe wire used in these experiments was 0.028 inch. A wire of this diameter does have a slight effect on the shape of the laminar flame, although the influence on the results described above is not thought to be appreciable. Since these experiments were carried out, tests have been reported (Summerfield, Reiter, Kebely and Mascolo, 1955) in which a probe of diameter 0.0055 inch was used. While the results obtained by Summerfield and his associates were similar in nature to those described above, it might be useful to repeat some of the above traverses using a smaller diameter probe wire.

Position of the schlieren image relative to the direct visual image.

Since the definition of the "position of flame front" in terms of the schlieren image is to some extent arbitrary it is interesting to compare the positions of the schlieren and direct visual images. The results of a typical test are shown in Fig. 30. In this photograph an interrupted schlieren image is superimposed on a direct visual image of

the same flame. It is seen that the schlieren image lies to the right (the unburned gas side) of the visual image of the flame front by about 0.02 inch (after correcting for magnification factor of 2.1). This observation is quantitatively in fair agreement with the results^{given}/by Broeze (1949) and others.

4.43 Ionisation Probe measurements in turbulent flames.

When the Ionisation Probe is used in turbulent flames the oscilloscope shows that the signal is not steady but fluctuates considerably. Typical traces of these fluctuating signals have been published by Summerfield, Reiter, Kebely and Mascolo (1955). Summerfield and his colleagues argue that, since these traces show a large number of intermediate values of signals, rather than only high and low values, the probe observations support their conception of a turbulent flame as a zone of distributed reaction, as opposed to Karlovitz's model (1954) of wrinkled laminar flame fronts. While the wrinkled laminar flame front model is probably of only limited application, the author feels that this model is not necessarily disproved in Summerfield's experiments. The traverses through laminar flames which are described in paragraph 4.42 show that the probe has to move a distance of roughly 0.05 inch before the maximum signal is reached. Also it is possible, according to Karlovitz's model for the laminar flame front at the traversing point to be

instantaneously inclined towards the probe wire, rather than normal to it. Thus, if a turbulent flame consists of fluctuating laminar flame sheets, it is quite possible for the Ionisation Probe to indicate intermediate values of signal.

To aid the analysis of fluctuating signals, two additional instruments have been incorporated in the circuits of the Ionisation Probe which were described in paragraphs 4.41 and 4.42 above. These are the Signal Height Discriminator and the Fractional Time Indicator. These two instruments are used in conjunction, the Fractional Time Indicator measuring the fraction of the total time that the signal is less than the value set on the Signal Height Discriminator. These instruments should prove particularly valuable in investigating the type of flame spreading failure encountered in flames propagating in weak mixtures from behind inclined stabilisers (c.f. paragraph 4.33).

4.44 Gas Analysis.

The second experimental technique which has been developed for use in the flame spreading experiments is gas analysis.

Analyses giving local, or overall combustion efficiencies would be very useful, but, using methods such as the Gravimetric Train (Lloyd, 1948), or the Haldane Apparatus, the time required to analyse each sample would be considerable. To provide a rapid means of analysing samples an Infra Red Gas Analyser was purchased.

In this instrument there are two optical paths, each having an infra red light source at one end, and a detection cell containing the gas to be analysed at the other. The two detection cells are separated by a diaphragm. The test cell, through which the sample to be analysed is passed, is placed in one of the optical paths. If the constituent, whose concentration is to be measured, is present in the sample as it passes through the test cell, this gas absorbs some of the radiation which has a wavelength within the characteristic absorption band of the gas. Thus less radiation remains to be absorbed by the detection cell at the end of the optical path containing the test cell. This causes a reduction in the heating effect within this cell, and, to maintain the pressure balance between the two detection cells, the diaphragm moves. This movement alters the capacity of a condenser, allowing the movement to be magnified electronically to give a deflection on a scale.

The instrument can measure the concentration of either carbon dioxide, carbon monoxide, or methane. Two detecting condensers are used - one containing carbon dioxide for the carbon dioxide analysis, and the other containing a mixed filling of carbon monoxide and methane. To analyse for methane the second condenser is used, and carbon monoxide is passed through a filter cell placed in the same optical path as the test cell. When analysing for carbon monoxide the same condenser is used, but methane is passed through

the filter cell. For each of the three gases which can be analysed, three concentration ranges are available, full scale deflection being given by either 3%, or 14% or 100% by volume of the test gas.

With this instrument, analyses for one particular constituent, for example carbon dioxide, should be obtained fairly rapidly, the only delay being the time required to flush the test cell. However, if it is wished to change from measuring one constituent to measuring another, some time must be allowed to elapse before readings are recommenced.

4.5 Summary.

Suitable air and fuel supplies have been provided for use in small scale flame spreading experiments.

Methods of measuring air and fuel flow rates have been investigated. For measuring the main air flow rate, a British Standard Orifice is used. Capillary meters are used for measuring fuel flow rates and for measuring the rate of flow of auxiliary air.

A burner has been constructed in which the source is electrically heated. This burner incorporates an independent flame pilot.

An Ionisation Probe has been calibrated in laminar flames for use in locating flame fronts. Instruments have

been added to the circuits to aid the analysis of measurements taken in turbulent and in "intermittent" flames.

A quick method of analysing for carbon dioxide, or carbon monoxide, or methane, has been provided.

CHAPTER 5.

FLAME BLOW-OFF FROM RECTANGULAR BURNERS.

- 5.1 Introduction.
 - 5.11 Prediction of blow-off.
 - 5.12 An Anomaly.
- 5.2 Experimental.
 - 5.21 Apparatus
 - 5.22 Flame lifting
 - 5.23 Flash-back.
 - 5.24 Pressure gradient.
- 5.3 Correlation of blow-off results.
 - 5.31 Local boundary velocity gradients.
 - 5.32 Blow-off from an infinite slit in turbulent flow.
 - 5.33 Average velocity gradient.
- 5.4 Correlation of friction coefficients.
- 5.5 Conclusions.

CHAPTER 5.5.1 Introduction.

In the design of the burner which was used in the calibration of the Ionisation Probe, described in the preceding Chapter, information was required on the blow-off of laminar pre-mixed flames from rectangular burners. Formulae published in the literature predicted anomolous results when they were applied to the range of dimensions likely to be met in the calibrating burner. To correct this discrepancy in the literature, and to provide the necessary design information, a series of flame blow-off experiments was carried out.

These preliminary calculations based on the published formulae, and the experiments which were carried out to clarify the literature are described in this Chapter.

5.11 Prediction of blow-off.

It has been shown for circular burners of different diameters that the stability limits can be correlated by the boundary velocity gradient calculated for flow without combustion (Lewis and von Elbe, 1943, and others; c.f. paragraph 1.31 of Chapter 1 of this thesis). Grumer, Harris and Schultz (1953) have investigated blow-off and flash-back in non-circular ports, and they conclude that neither the boundary velocity gradient at the centre of one side, nor that at a corner, as calculated for flow in the absence of a

TABIE 6

BLOW-OFF VELOCITIES PREDICTED BY METHOD OF
GRUMER AND CO-WORKERS (1953)

Rectangular burner of cross-sectional width 0.125 in.
 2% Butane mixture. Critical "g" from circular burner
 data 400 sec.⁻¹ (Wohl, 1953)

Burner cross-sectional length. in.	0.063	0.125	0.25	0.50	1.0	2.0
Average velocity at blow-off. ft/sec.	0.17	0.42	0.58	0.50	0.31	0.16

flame, can be used to correlate the stability limits of non-circular burners. It is thought by Grumer and his associates that this is due to flame thrust causing a redistribution of the velocity regime compared with that observed in flow when no flame is present. However, they claim that, in the laminar range, the stability limits of non-circular channels are correlated with circular channel stability limits by using the appropriate relationship for the friction coefficient, λ , in the equation -

$$g = \frac{\lambda V N_{Re}}{2 \pi d^3} \quad \dots\dots\dots \text{Eqn. 5.1}$$

For square channels

$$\lambda = \frac{75.5}{N_{Re}^{1.11}} \quad \dots\dots\dots \text{Eqn. 5.2}$$

and for rectangular channels

$$\lambda = \frac{161}{N_{Re}^{1.27}} \quad \dots\dots\dots \text{Eqn. 5.3}$$

where g is the boundary velocity gradient for comparison with circular burner stability data, V is the volume flow rate, N_{Re} is the Reynolds Number = $\rho \bar{u} d / \mu$, and d is the equivalent hydraulic diameter = $4 \times \text{area} / \text{perimeter}$.

5.12 An anomaly.

Equations 5.1 and 5.2 above were used to predict the velocities at which flames will "blow-off" from rectangular burners of cross-sectional width 0.125 inch and cross-sectional lengths varying from 0.063 to 2 inch. The results of these calculations for a 2% butane in air mixture are given in Table 6.

The calculations show that the method proposed by Grumer, Harris and Schultz predicts that, for this cross-sectional width, as the cross-sectional length increases beyond about 0.5 inch and tends to infinity, the average velocity at blow-off decreases and tends to zero, a results which one would not expect. For a burner of finite cross-sectional width and infinite cross sectional length, i.e. neglecting end effects, one would expect the average velocity at blow-off in laminar flow to be given by -

$$\bar{u} = \frac{1}{3} b g \quad \dots\dots\dots\text{Eqn. 5.4}$$

where b is the half cross-sectional width, and \bar{u} is the average velocity. For a burner of cross-sectional width 0.125 inch this expression gives an average velocity at blow-off of 0.7 ft/sec.

Thus the literature appears to be misleading on this subject. In view of this discrepancy a series of experiments has been carried out on the blow-off of butane-air flames from rectangular ports.

In the experiments on which the relationships of Grumer, Harris and Schultz are based (equations 5.1 to 5.3 above), the minimum value of the ratio of channel cross-sectional width to cross-sectional length was 0.28. It should be noted that the anomolous behaviour indicated above occurs at values of this ratio which are less than 0.25.

5.2 Experimental

5.21 Apparatus.

Blow-off limits were obtained for burners of the following cross-sectional dimensions:- 0.07 x 0.13 inch, 0.13 x 0.13 inch, 0.25 x 0.13 inch, 0.51 x 0.13 inch, 1.0 x 0.12 inch and 2.0 x 0.13 inch. The burners were not water-jacketed, but it is thought that the blow-off limits would not have been appreciably altered by water-jacketing, as it was observed from several tests that a blow-off limit taken immediately after a flame was lighted on a cold burner was in agreement, within experimental error, with the limit taken after the flame had been alight on the burner for some time.

In each burner the approach length was greater than the Transition Length for a cylindrical channel of similar equivalent hydraulic diameter, and in which the flow Reynolds Number is 2000. The Transition Length, X , is given by (Prandtl, Tietjens, 1934, p.22) -

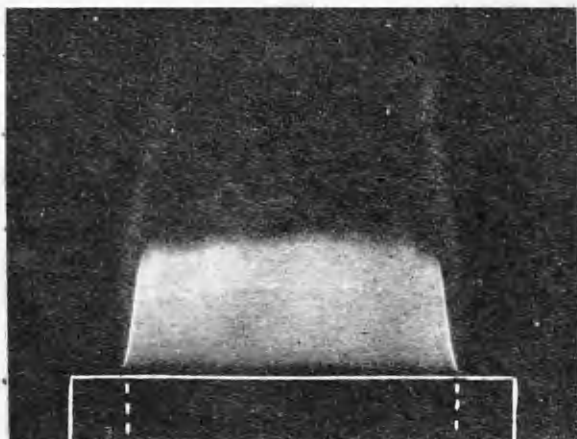
$$X = 0.065 d N_{Re} \dots\dots\dots \text{Eqn 5.5}$$

The Transition Length is the length of channel required to change an initially flat velocity profile into one in which the velocity at the centre of the channel is within 1% of the central velocity in Poiseuille flow.

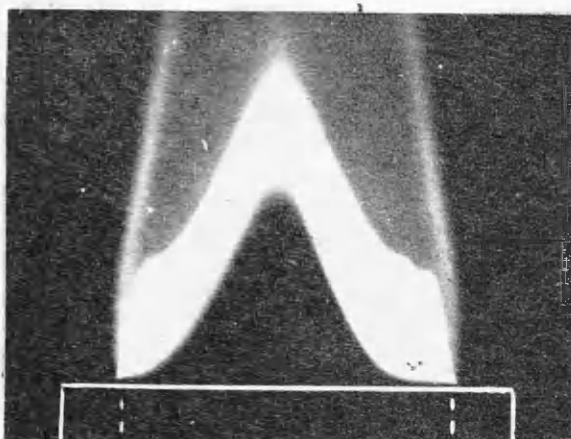
Equation 5.5 has been experimentally confirmed only for flow in cylindrical channels.

FIG. 32. FLAME BLOW-OFF PHOTOGRAPHS

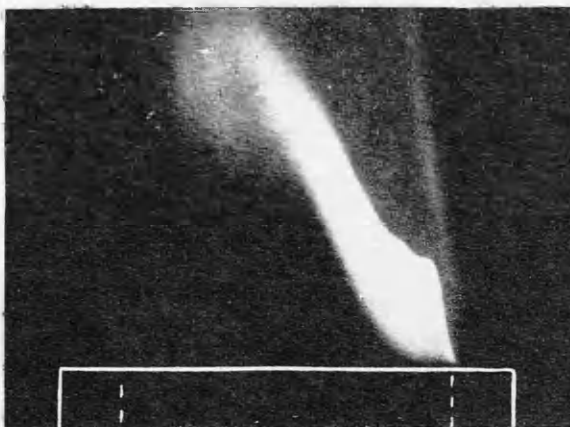
2.00 x 0.125 in. Rectangular Burner.



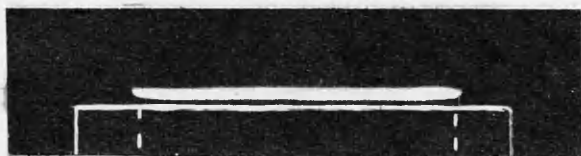
a. Flow Velocity 9.6 ft/sec.
Butane Conc. 3.96%



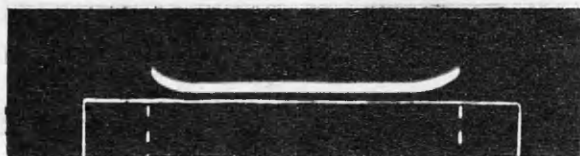
b. Flow Velocity 9.6 ft/sec.
Butane conc. 3.78%



c. Flow Velocity 9.6 ft/sec.
Butane conc. 3.64%
Final Blow-off at Butane conc. 3.23%



d. Flow Velocity 0.9 ft/sec.
Butane conc. 2.33%



e. Flow Velocity 0.9 ft/sec.
Butane conc. 2.23%

Final Blow-off at Butane conc. 2.16%

The butane and air flows were measured by capillary meters, within an estimated accuracy of 3%.

5.22 Flame lifting.

The flames did not always lift simultaneously from all parts of the burner port, as can be seen from Fig. 32 which shows flames anchored above the 2.0 x 0.13 inch burner. (The photographs were taken in a direction normal to the long side of the burner port). At the flow velocity of 9.6 ft/sec. the flame lifts first from the centre of the long sides of the burner port (Fig. 32a, b and c), and at the flow velocity of 0.9 ft/sec. incipient flame lift occurs at the corners of the port (Fig. 32d and e). The existence of these two forms of blow-off may be due to the influence of flame thrust on the flow distribution. In Poiseuille flow in the rectangular channel of the burner the wall velocity gradients are lowest at the corners (Smith, Edwards and Brinkley, 1952). However, when a flame is anchored above the burner, the flame pressure will cause a spreading of the flow lines which will increase the velocity gradients at the corners. It is estimated (Wohl, Kapp and Gazley, 1949) that this spreading of the flow lines is proportional to the term $(S_u/\bar{u})^2$, where S_u is the laminar burning velocity. At the conditions corresponding to the flames shown in Fig. 32a, b and c this term has the value 0.02, and at the conditions corresponding to the flames shown in Fig. 32d and e the term has the value 0.73.

The greater tendency for flow redistribution at the lower velocity may be the cause of the incipient flame lift from the corners of the burner port shown in Fig. 32d and e.

The type of blow-off shown in Fig. 32a, b and c was only observed with the three largest burners (viz., those having dimensions 0.51 x 0.13 inch, 1.0 x 0.12 inch and 2.0 x 0.13 inch), and that shown in Fig. 32d and e was only observed with the 2.0 x 0.13 inch burner. On all other occasions the flame lifted from all parts of the burner port at the same flow condition.

5.23 Flash-back.

Several flash-back limits were taken with the larger burners. As these burners were not water-jacketed however, the results may be of doubtful value, since locally hot walls probably have a greater influence on flash-back than on blow-off.

5.24 Pressure gradient.

In addition to the blow-off and flash-back observations, the pressure gradient along each of the burner channels was measured over a range of flows.

5.3 Correlation of blow-off results.

5.31 Local boundary velocity gradients.

As stated in the Introduction (paragraph 5.11), the wall velocity gradient has been used successfully to correlate blow-off limits for circular burners. The

applicability of this correlation to rectangular burners has been examined with reference to the lifting of a flame from the centre of the long side of the burner port, using the results of the experiments described in paragraph 5.2 above. In calculating the wall velocity gradients corresponding to the flows at which the flame lifted (and in predicting from the critical gradients the velocities at which the flames will lift) it was assumed that Poiseuille flow occurs at the burner port, and that the velocity profile is unaltered by the presence of a flame. With these assumptions the velocity u at a point having co-ordinates (x, y) relative to an origin on the axis, is given by the following expression which is derived in Appendix IV -

$$u = -\frac{1}{2\eta} \frac{dp}{dz} \left[(b^2 - y^2) + \frac{32b^2}{\pi^3} x \sum_{n=0}^{\infty} \frac{(-1)^{n+1} \cosh \frac{(2n+1)\pi x}{2b} \cos \frac{(2n+1)\pi y}{2b}}{(2n+1)^3 \cosh \frac{(2n+1)\pi a}{2b}} \right] \dots \text{Eqn. 5.6}$$

where dp/dz is the pressure gradient in the direction of flow, η is the absolute viscosity, a is the half cross-sectional length and b is the half cross-sectional width.

The average velocity \bar{u} is obtained by integrating the above expression over the cross-sectional area -

FIG. 33

BLOW-OFF FROM RECTANGULAR BURNERS

Average velocity at blow-off from burners of port width 1/8 inch.

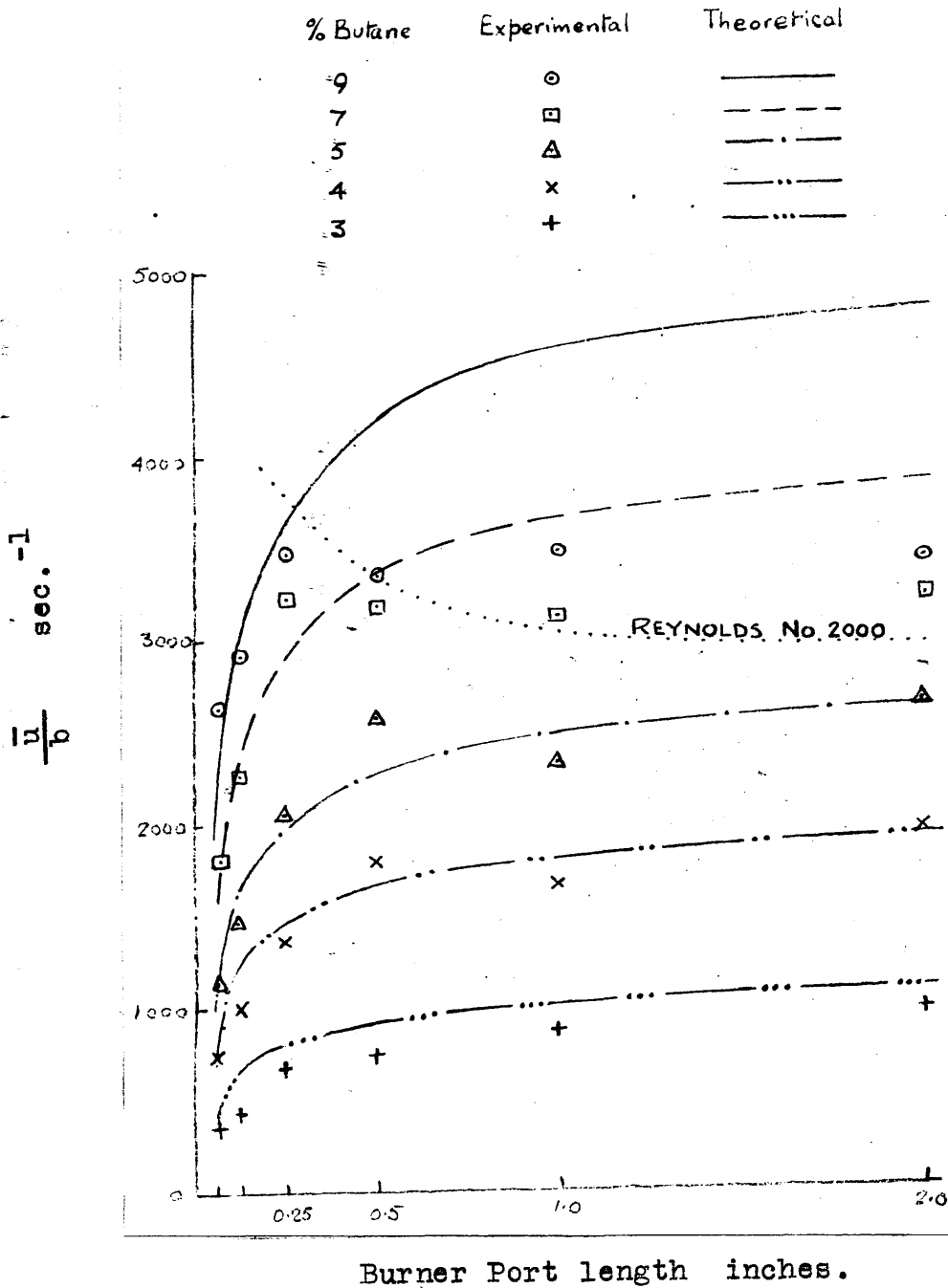


TABLE 7.

VALUES OF FUNCTIONS P AND Q

b/a	0	0.1	0.2	0.3	0.4	0.5
P	3.00	3.20	3.43	3.67	3.88	4.07
Q	0.0104	0.0118	0.0131	0.0143	0.0153	0.0161

b/a	0.6	0.7	0.8	0.9	1.0
P	4.23	4.38	4.52	4.66	4.80
Q	0.0167	0.0171	0.0174	0.0175	0.0176

$$\bar{u} = \frac{1}{ab} \int_{x=0}^x=a \int_{y=0}^y=b u \, dx \, dy \quad \dots\dots\dots \text{Eqn. 5.7}$$

The wall velocity gradient at the centre of the long side, ξ_c , is given by -

$$\xi_c = - \left(\frac{\partial u}{\partial y} \right)_{x=0, y=b} \quad \dots\dots\dots \text{Eqn. 5.8}$$

Substituting equation 5.6 in equations 5.7 and 5.8 and combining gives -

$$\xi_c = P \frac{\bar{u}}{b} \quad \dots\dots\dots \text{Eqn. 5.9}$$

where

$$P = \frac{3 \left[1 - \frac{8}{\pi^2} \sum_{n=0}^{\infty} (2n+1)^{-2} \text{Sech} \frac{(2n+1)\pi a}{2b} \right]}{1 - \frac{192}{\pi^5} \frac{b}{a} \sum_{n=0}^{\infty} (2n+1)^{-5} \text{Tanh} \frac{(2n+1)\pi a}{2b}} \quad \dots\dots\dots \text{Eqn. 5.10}$$

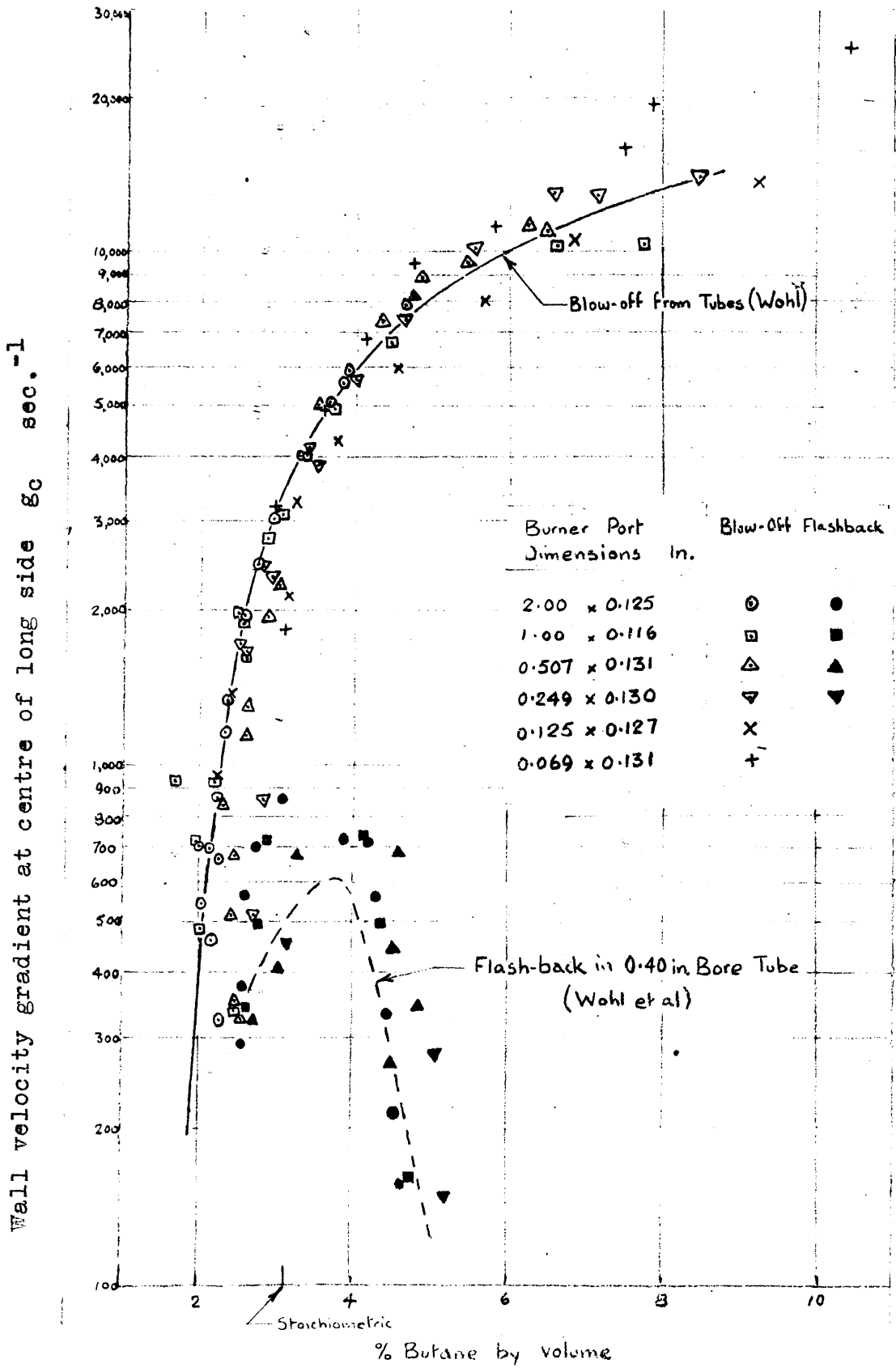
The series used in equation 5.10 have been summed by Smith, Edwards and Brinkley (1952) for various values of the ratio b/a . From their results the function P has been calculated and is given in Table 7.

Test of hypothesis.

The critical velocity gradients obtained from blow-off tests on circular burners for butane concentrations of 3, 4, 5, 7 and 9% were taken from Fig. 16 of Wohl (1953), and substituted in equation 5.9. In this way, values of the group \bar{u}/b were obtained for various values of the ratio b/a . The group \bar{u}/b was then plotted against the burner port/length for a burner port width of 0.125 inch, giving the lines indicated

FIG. 34. STABILITY LIMITS OF RECTANGULAR BURNERS

Wall velocity gradient at centre of long side for flame lifting or flashing back at centre of long side.



as "Theoretical", in Fig. 33. The experimental points at the corresponding butane concentrations shown in this Fig. were obtained by interpolating the experimental observations, lift from the centre of the long side being taken as the flame stability criterion, since this is the point at which the wall velocity gradient is calculated. A line corresponding to a Reynolds Number of 2000 is drawn in the Figure. It is seen that there is good agreement between the blow-off velocities predicted by this hypothesis and the experimental results where the Reynolds Number is less than 2000 but at higher Reynolds Numbers agreement ceases to exist. This limitation on the application of equation 5.9 is to be expected, because the relationships from which it is derived are applicable only to laminar flow. In channels of rectangular cross-section, as in circular channels, laminar flow breaks down at a Reynolds Number of about 2000 (McAdams, 1942, p.124).

In view of the success, shown in Fig. 33 of the application of the wall velocity gradient correlation to blow-off from rectangular burners the boundary velocity gradient has been calculated using equation 5.9, for all the observations of flame lifting from the centre of the long side for which the Reynolds Number was less than 2000. The resulting values of the gradient, g_c , are plotted in Fig. 34.

The solid curve drawn in Fig. 34 represents the correlation obtained by Wohl (1953) for blow-off from circular burners. There is again seen to be good agreement between the blow-off limits of the various rectangular burners and the blow-off correlation for circular burners, indicating that the wall velocity gradient correlation of flame lifting may be extended to rectangular burners, at least within the range tested.

The flash-back limits which were obtained are also plotted in Fig. 34, where they are compared with the flash-back limits obtained in a 0.4 inch bore tube by Wohl, Kapp and Gazley (1949). That the rectangular burners were not water-jacketed may be the reason for the wall velocity gradients at flash-back generally being higher in the rectangular burners than in the circular burner.

5.32 Blow-off from an infinite slit in turbulent flow.

In circular burners in which the flow is turbulent the wall velocity gradients at blow-off have been calculated by several groups of workers using values of the friction coefficient relevant to turbulent flow (Wohl, Kapp and Gazley, [1949]; Bollinger and Williams, 1947). Their results are in agreement with the correlation obtained from the stability limits taken in laminar flow. Treating the 2.0 x 0.13 inch burner as a rectangular burner of infinite cross-sectional length and 0.13 inch cross-sectional width enabled the average

FIG 35 VELOCITIES AT BLOW-OFF FROM 2.00 x 0.125 IN. BURNER

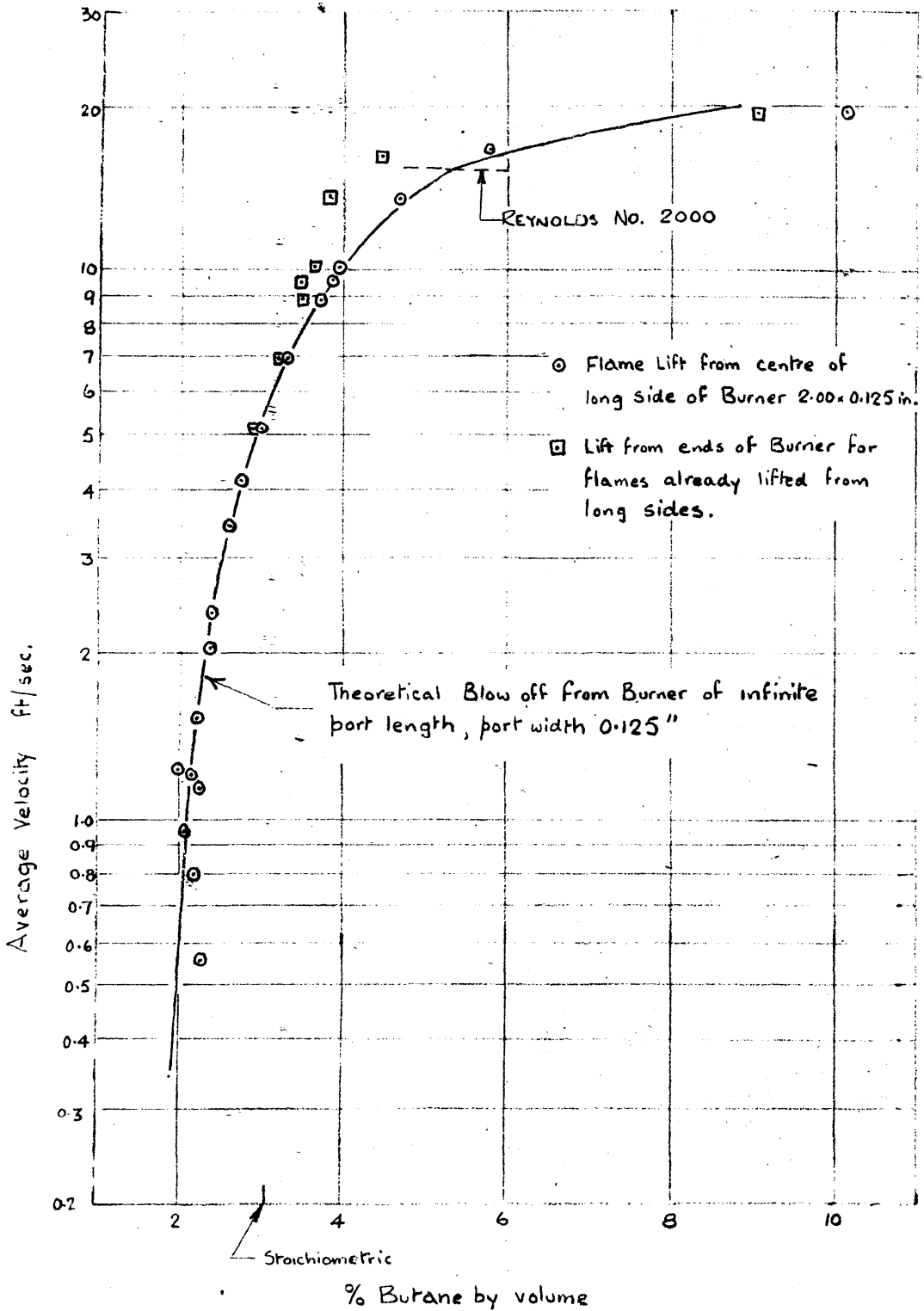
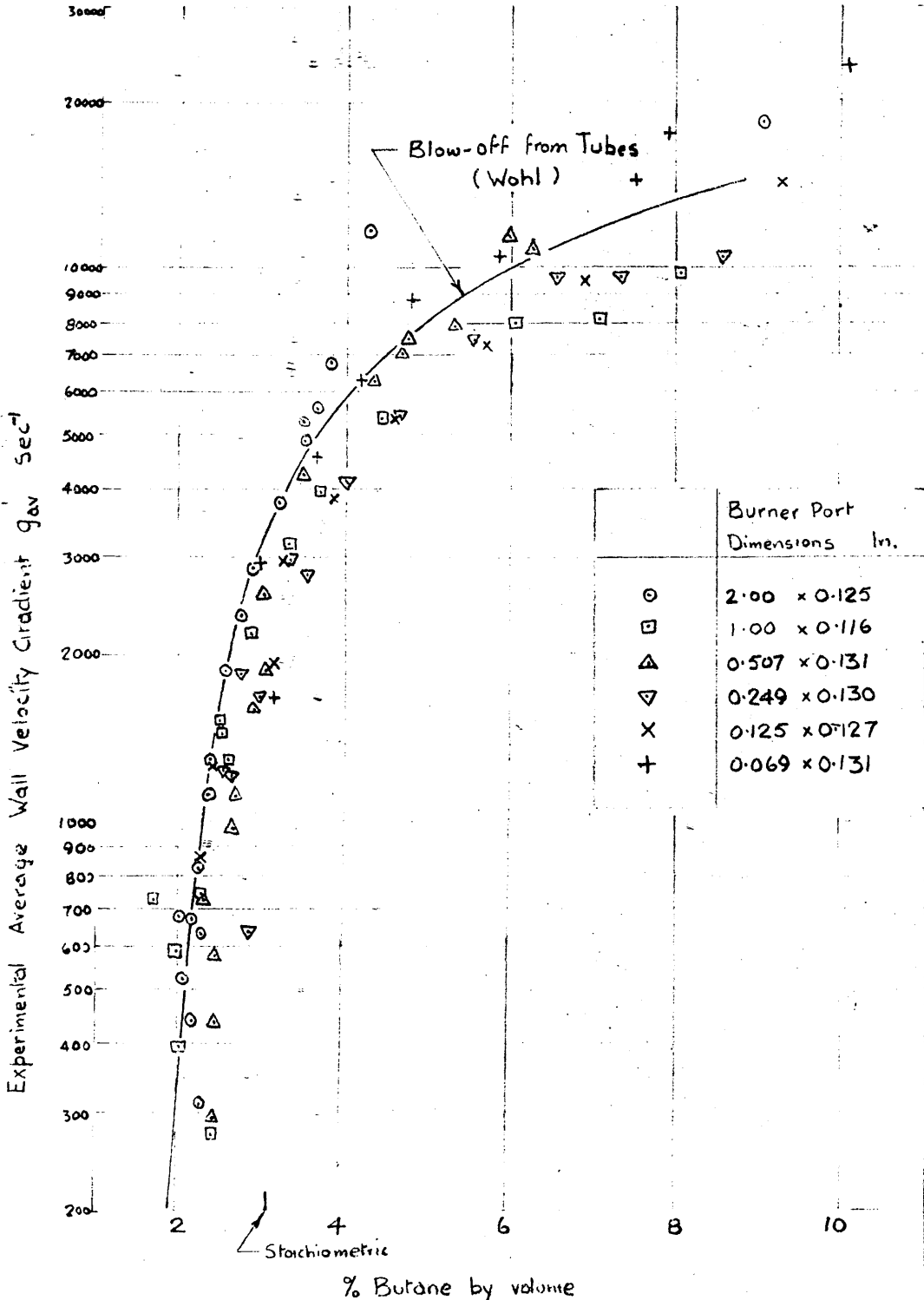


FIG. 36.

BLOW-OFF FROM RECTANGULAR BURNERS

Experimental average wall velocity gradient for final flame lift.



blow-off velocities in both the laminar and turbulent ranges to be predicted from the critical velocity gradients published by Wohl (1953). This theoretical blow-off limit is plotted in Fig. 35 where it is compared with the experimental results. The few experimental limits taken in the turbulent region are in fair agreement ^{with} the theoretical curve. The agreement between the observed velocities, within the laminar range, for flame lifting from the centre of the long side and the theoretical velocities is excellent, as is to be expected from the correlation already shown in Fig. 34.

5.33 Average velocity gradient.

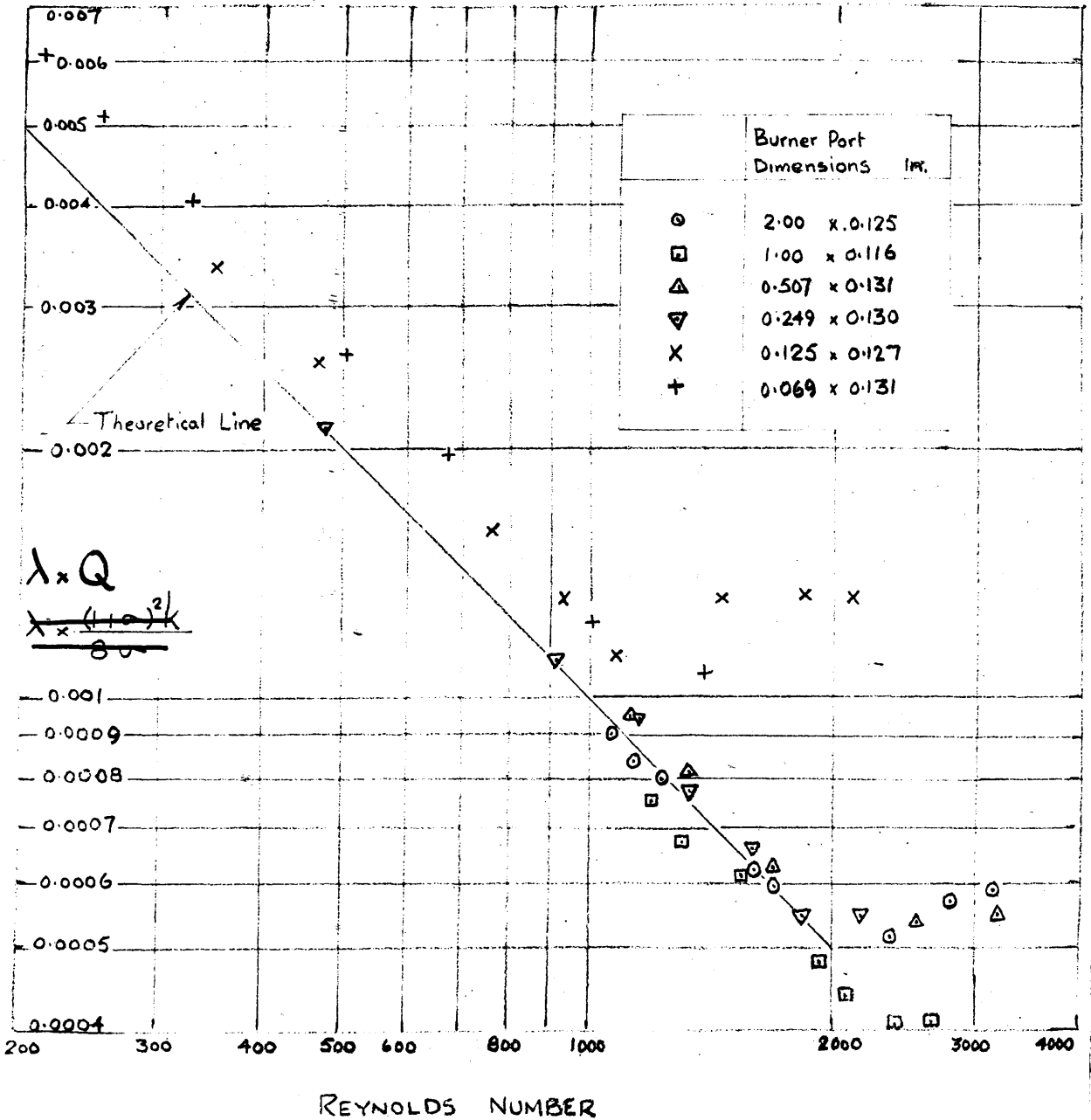
The blow-off limits of the rectangular burners have also been correlated in Fig. 36 by the average wall velocity gradient. The average wall velocity gradient g_{av} , was obtained from the pressure gradient measurements using the equation -

$$g_{av} = - \frac{1}{\eta} \cdot \frac{dp}{dz} \cdot \frac{\text{area}}{\text{perimeter}} \quad \dots\dots\dots \text{Eqn. 5.11}$$

where dp/dz is the pressure gradient in the direction of flow.

In the correlation shown in Fig. 36 the blow-off limit is taken to be the condition at which the flame finally lifts from the burner port. The blow-off limit for circular burners which was obtained by Wohl (1953) is again drawn, as a solid line, for comparison. The correlation is less satisfactory than the one obtained by using Equation 5.9 to

FIG. 37 FRICTION COEFFICIENT λ IN RECTANGULAR CHANNELS



calculate the theoretical boundary velocity gradient. However, this method of obtaining the average wall velocity gradient from the pressure drop along the channel is applicable to turbulent, as well as to laminar, flows.

5.4 Correlation of Friction Coefficients.

The Friction Coefficient, λ , as used here, is given by the expression -

$$\frac{dp}{dz} = - \lambda \frac{\rho \bar{u}^2}{2d} \dots\dots\dots \text{Eqn. 5.12}$$

where ρ is the density of the fluid.

In steady laminar flow in a channel of rectangular cross-section the average velocity, \bar{u} , is given by equation 5.7

Substituting equation 5.7 in equation 5.12 leads to

$$Q \lambda = \frac{1}{N_{Re}} \dots\dots\dots \text{Eqn. 5.13}$$

where

$$Q = \frac{(a+b)^2}{96a^2} \left[1 - \frac{192}{\pi^5} \frac{b}{a} \sum_{n=0}^{\infty} (2n+1)^{-5} \text{Tanh} \frac{(2n+1)\pi a}{2b} \right] \dots\dots \text{Eqn. 5.14}$$

Using the arithmetic summations published by Smith, Edwards and Brinkley (1952), values of the function Q have been calculated for various values of the ratio b/a . The results are given in Table 7.

Values of the friction coefficients for the rectangular channels were calculated from the pressure gradient readings, using Equation 5.12. These values, multiplied by the appropriate values of the function Q , are plotted in

Fig. 37. From this graph it is seen that the laminar flow linear relationship between the Friction Coefficient and the Reynolds Number breaks down, in the four larger channels, at a Reynolds Number of roughly 2000. However, in the two smaller channels the transition from laminar flow appears to begin at a Reynolds Number nearer to 1000. For the laminar range points there is considerable scatter about the theoretical line, although for the individual burners the differences between the experimental points and the theoretical values are consistent. It is probable that these consistent discrepancies are at least partly due to inaccuracies in estimating the mean dimensions of the channel cross-sections. For example, an error of 0.004 inch in the measurement of the cross-sectional dimensions of the 0.13 x 0.13 inch burner (i.e. 3%) can cause a consistent error of 16% in the value of the term $q \lambda$ calculated from the experimental readings.

Lines drawn through the laminar range experimental points for the various burners have gradients of 45° , confirming that the friction coefficient for each channel is inversely proportional to the Reynolds Number, as indicated in Equation 5.13. This is in disagreement with the conclusions of Grumer, Harris and Schultz (1953) who calculated the friction coefficient from flame stability results, using equation 5.1, and found it to be inversely proportional to a power of the Reynolds Number, as shown in Equations 5.2 and 5.3.

5.5 Conclusions.

The experiments described above indicate that, for the burners tested -

1. When the Reynolds Number is less than 2000, the limits for flame lifting from the centre of the long side of the burner port can be correlated by the wall velocity gradient calculated at that point, it being assumed in calculating the velocity gradient that the flame causes no redistribution of the flow from the Poiseuille velocity profile.
2. The final flame lift limits can be roughly correlated by the average wall velocity gradient obtained from the measured pressure gradient. This correlation can be applied to systems in which the flow Reynolds Number exceeds 2000.
3. The friction coefficient for the flow in the burner channels is inversely proportional to the Reynolds Number, provided that the flow is laminar. The constants of proportionality are in fair agreement with those predicted by the laminar flow equations.

That the blow-off limits may be directly correlated by the theoretical wall velocity gradient is in disagreement with the conclusions of Grumer, Harris and Schultz (1953). This disagreement may be due to the use by Grumer and his colleagues of burners of larger dimensions than those used in

the experiments described here. In the larger burners the flow velocities at which the Reynolds Number is equal to 2000 are lower, and at the lower velocities the influence of flame thrust on the flow distribution is probably more important (Wohl, Kapp and Gazley, 1949). One would expect Conclusion 1 above to be valid only when the flow redistribution due to flame thrust is not significant. It should also be noted that the conclusions of Grumer and his associates were based largely on flash-back limits, whereas the conclusions above are drawn only from flame blow-off observations.

The application of the results of these flame blow-off experiments to the design of the laminar burner used in the calibration of the Ionisation Probe has been discussed in paragraph 4.42 of Chapter 4.

CHAPTER 6.

CONCLUSIONS AND SUGGESTIONS FOR FURTHER RESEARCH.

- 6.1 Results of the researches.
- 6.2 Suggested experiments using the small scale apparatus.
- 6.3 Other studies suggested by this work.
 - 6.31 Flame spreading.
 - 6.32 Flame blow-off from rectangular burners.

CHAPTER 6.6.1 Results of the researches.

The large scale experiments, described in Chapters 2 and 3, showed that finger type flame spreaders can produce considerable improvement in the combustion efficiency performance of a high velocity combustion system. Quantitative data, which should be useful to engine designers, have been obtained on the influence of some geometric variables, viz., number, width and inclination of fingers and tailpipe length, on the combustion efficiency of a typical ramjet system. The experiments indicated that two important processes involved in the operation of a finger type flame spreader are (a) the flow of pilot gases along the wake of the finger, and (b) the initiation of progressive combustion in a gas stream by a source.

A small scale apparatus (Chapter 4) has been constructed to study process (b) - the ignition process. Preliminary experiments were undertaken to permit a rational design of this apparatus. These experiments also revealed an interesting form of "intermittent" flame (paragraph 4.33). An outline of suggested experiments using the small scale apparatus is given in paragraph 6.2 below.

Two techniques have been developed for flame location and efficiency measurements in the small scale experiments. These are the Ionisation Probe and Gas Analysis. The

Ionisation Probe has been shown to provide an accurate means of locating a laminar flame front. Additional circuits have been coupled to the probe output which should be helpful in the study of the intermittent flame mentioned above, and in locating turbulent flames.

A subsidiary research into the conditions governing flame anchoring on rectangular burners (Chapter 5) has developed into a very fruitful project in its own right. Flame blow-off limits for rectangular burners have been successfully correlated with those for circular burners.

The leading results of this thesis have been published; copies of the relevant papers are bound in this volume.

6.2 Suggested experiments using the small scale apparatus.

It will be recalled that the small scale apparatus has a test section having a rectangular cross-section of dimensions 2 x 1 inch. A wire stabiliser is placed across the test section at an inclination of either 90° or 30° to the direction of flow of the main stream. This stabiliser wire may be electrically heated. A pilot flame, supplied with fuel and air flows separate from the main stream, surrounds the upstream end of the stabiliser wire.

Two series of experiments are suggested using this apparatus, the first being "stability tests" and the second "propagation tests".

Stability Tests.

In these tests the stability limits of flames anchored behind the stabiliser wire are to be observed. The variables to be studied are flow velocity, pilot heat input, electrical input to the stabiliser wire, stabiliser wire diameter and stabiliser inclination.

Should "intermittent" flames (c.f. paragraph 4.33) be observed, the Fractional Time Indicator attached to the Ionisation Probe might prove useful in indicating a stability limit. The stability limit might be considered to be the condition when the Time Indicator shows the flame to be absent from the stabiliser for 50% of the total time.

The stability results might be correlated by groups similar to those used by Spalding (1954) and Spalding and Tall (1954).

Propagation Tests.

The propagation of the flame behind the stabiliser may be measured by making Ionisation Probe traverses and gas sampling traverses through the flame at one or more planes downstream from the stabiliser. The variables to be studied are the fuel concentration, flow velocity, pilot heat input, electrical heat input to the stabiliser wire, stabiliser wire diameter and stabiliser inclination.

These experiments should provide information on the performance of a line source as a means of starting general

progressive combustion. It should be noted that the conditions affecting combustion in this low velocity system (60 ft/sec.) may be different from those existing in a combustion chamber in which the flow is choked at the chamber outlet. In the high velocity chamber the mixing processes become increasingly important, and the concept of ^{continuous} a/turbulent flame front may no longer be valid.

6.3 Other studies suggested by this work.

6.31 Flame spreading.

Since mixing has a considerable influence on the combustion rate (Berl, Rice and Rosen, 1955), future work might fruitfully be directed towards achieving the controlled mixing necessary to give the optimum heat release rates.

It has been shown that finger type flame spreaders may improve the combustion efficiency of a system. It would be useful to know if these finger type spreaders achieve their effect simply by creating general turbulence, as was the case with the orifices used by Wilkerson and Fenn (1953). An answer to this question might be given by a comparison of the combustion efficiency measurements taken with a finger type flame spreader, and with an orifice giving similar values of the pilot heat mixing factor K (c.f. paragraph 1.46).

Since extreme rates of mixing can cause instability of the pilot, it is essential that a piloting system be

developed which will be effective even when rapid mixing is taking place within the chamber. The effect of heat losses from the stabilising zone (Spalding and Tall, 1954), and the ways in which they may be avoided, are important.

6.32 Flame blow-off from rectangular burners.

The range of application of the wall velocity gradient correlation of flame lifting from rectangular burners might be extended by measuring the blow-off limits of butane-air flames above burners of cross-sectional widths of more than $1/4$ inch. In these larger burners the flow will generally be turbulent. It may not be possible to calculate the wall velocity gradient at the centre of the long side from the dimensions and the average flow velocity at the blow-off limit. However, an average wall velocity gradient may be determined from the friction coefficient and, if the hypothesis remains valid, a rough correlation should be obtained. The hypothesis may be tested more accurately by observing the limits for burners whose cross-sectional length is at least ten times as great as the cross-sectional width. For these burners the wall velocity gradient at the centre of the long side may be calculated quite accurately by considering the burner to be an infinite slit.

At the high blow-off velocities which will be observed in these larger burners, the influence of flame thrust on the flow distribution should be negligible.

APPENDIX I.ONE DIMENSIONAL FLOW IN A RAMJET COMBUSTION CHAMBER.

In Chapters 2 and 3 experiments are described in which pressure readings or thrust measurements were used to calculate the efficiency of combustion in a ramjet. The relationships which were used in these calculations were obtained by Beeton (1949). An outline of the derivation of these relationships is given below.

Flow is considered through an idealised combustion system, a sketch of which has been given in Fig. 9. It is assumed that the working fluid passes through the following stages. Between Stations 1 and 2 the air suffers a pressure drop due to the baffle system. Immediately after Section 2 fuel is injected in a direction perpendicular to the air stream (i.e. the momentum of the fuel is not considered). Combustion then takes place and is completed by the time the gases reach the exit (Station 3), at which point the flow is considered to be choking. The cross-sectional areas at Stations 1, 2 and 3 are equal, the chamber walls being parallel. It is assumed that downstream from station 2 there is no pressure drop due to friction with the duct walls.

Air Specific Impulse.

The Air Specific Impulse, S_a , is defined by the gross thrust per unit mass flow rate of air through the combustion chamber.

$$S_a = \frac{P_3 A + \frac{u_3}{g} m_3}{m_2} \quad \dots\dots\dots \text{Eqn. I.1}$$

where P_3 is the static pressure (absolute), u_3 is the gas velocity, m_3 is the mass flow rate of gas, all at Station 3, and m_2 is the mass flow rate at Station 2. (m_2 is the mass flow rate of air, m_3 includes the fuel flow rate), g is the acceleration due to gravity, and A is the cross-sectional area.

Applying the equation of Conservation of Momentum between Stations 2 and 3 gives -

$$\frac{P_3 A + \frac{u_3}{g} m_3}{m_2} = \frac{P_2 A}{m_2} + \frac{u_2}{g} \quad \dots\dots \text{Eqn. I.2}$$

where P_2 and u_2 are the static pressure (absolute), and gas velocity respectively at Station 2.

Applying the Continuity Equation to Station 2 gives

$$m_2 = \frac{P_2}{RT_2} A u_2 \quad \dots\dots\dots \text{Eqn. I.3}$$

where R is the Gas Constant for air and T_2 is the static temperature at Station 2.

Combining Equations I.1, I.2 and I.3 gives -

$$\begin{aligned} S_a &= \frac{RT_2}{u_2} \left(1 + \frac{u_2^2}{gRT_2} \right) \\ &= \frac{1 + \gamma M_2^2}{M_2} \left(\frac{RT_2}{g} \right)^{\frac{1}{2}} \quad \dots\dots \text{Eqn. I.4} \end{aligned}$$

where M_2 is the Mach Number at Station 2 and γ is the ratio of the specific heat of air at constant pressure to the specific heat at constant volume.

Also

$$\frac{T_{2t}}{T_2} = 1 + \frac{\gamma - 1}{2} M_2^2 = \frac{T_{1t}}{T_2} \quad \dots\dots\dots \text{Eqn. I.5}$$

where T_{1t} and T_{2t} are the total temperatures at Stations 1 and 2 respectively.

Substituting Equation I.5 in Equation I.4 gives -

$$S_a = \frac{1 + \gamma M_2^2}{M_2} \left(\frac{\frac{R T_{1t}}{\gamma g}}{1 + \frac{\gamma - 1}{2} M_2^2} \right)^{\frac{1}{2}} \quad \dots\dots\dots \text{Eqn. I.6}$$

This expression relates the Air Specific Impulse to the Mach Number immediately downstream from the baffle system.

Baffle Loss Coefficient.

The Baffle Loss Coefficient λ is defined as the pressure loss past the baffle system per unit inlet velocity head -

$$P_1 - P_2 = \lambda \frac{\rho_1 u_1^2}{2g} \quad \dots\dots\dots \text{Eqn. I.7}$$

where P_1 , ρ_1 and u_1 are the static pressure (absolute), air density and air velocity respectively at Station 1.

Since the flow areas at Stations 1 and 2 are equal -

$$\rho_1 u_1 = \rho_2 u_2 \quad \dots\dots\dots \text{Eqn. I.8}$$

Expressing Equation I.8 in terms of the Mach Numbers and Static pressures gives -

$$\frac{P_2}{P_1} = \frac{M_1}{M_2} \left(\frac{1 + \frac{\gamma - 1}{2} M_2^2}{1 + \frac{\gamma - 1}{2} M_1^2} \right)^{\frac{1}{2}} \dots\dots\dots \text{Eqn. I.9}$$

where M_1 is the Mach Number at Station 1.

When Equation I.9 is substituted in Equation I.7 we obtain -

$$\lambda \frac{\gamma}{2} M_1^2 = 1 - \frac{M_1}{M_2} \left(\frac{1 + \frac{1}{2} (\gamma - 1) M_1^2}{1 + \frac{1}{2} (\gamma - 1) M_2^2} \right)^{\frac{1}{2}} \dots\dots \text{Eqn. I.10}$$

This gives the relationship between the Baffle Loss Coefficient and the Mach Numbers at Stations 1 and 2.

Air Specific Impulse and Theoretical Fuel/Air Ratio.

As defined in Equation I.1

$$S_a = \frac{P_3 A + \frac{u_3}{g} m_3}{m_2}$$

The mass flow rate at Station 3, m_3 is related to the mass flow rate at Station 2, m_2 , by the expression

$$m_3 = m_2 (1 + \alpha) \dots\dots\dots \text{Eqn. I.11}$$

where α is the fuel/air ratio by weight.

Thus

$$S_a = \frac{(1 + \alpha) P_3 A}{m_3} + \frac{(1 + \alpha) u_3}{g} \dots\dots \text{Eqn. I.12}$$

Applying the Continuity Equation to Station 3 gives -

$$m_3 = A u_3 \frac{P_3}{R_3 T_3} \dots\dots \text{Eqn. I.13}$$

where R_3 is the Gas Constant for the combustion products at Station 3 and T_3 is the static temperature at Station 3.

Substituting Equation I.13 in Equation I.12 leads to -

$$S_a = (1 + \lambda) \left(\frac{u_3}{g} + \frac{R_3 T_3}{u_3} \right) \dots\dots\text{Eqn. I.14}$$

The gas velocity, u_3 , is given by -

$$u_3^2 = 2 g J \Delta H \dots\dots\text{Eqn. I.15}$$

where J is the mechanical equivalent of heat, and ΔH is the drop in enthalpy from stagnation conditions.

To calculate the Air Specific Impulse from Equations I.14 and I.15, the enthalpy drop and the gas constant and temperature at Station 3 must be known. Beeton (1949) has evaluated these quantities for a hydrocarbon fuel, and using the equations above has calculated the Air Specific Impulse over a range of fuel/air ratios. The fuel on which the calculations were based had a Lower Calorific Value of 10,300 C.H.U./lb. and a composition by weight of carbon 85% and hydrogen 15%, which is a fair representation of the fuel used in the experiments reported in Chapters 2 and 3.

The results of Beeton's calculations of Air Specific Impulse from the fuel/air ratio assuming complete combustion have been published by Morley (1953, p.198).

As a demonstration of the method used by Beeton the calculation of the Air Specific Impulse is outlined below for a fuel/air ratio of 0.0667 by weight, and an air inlet temperature of 600°K.

A series of temperature and pressure levels is chosen to cover the range between the total head conditions of the combustion products and the conditions of choked flow at the

tailpipe exit (Station 3). At each set of temperature and pressure conditions the equilibrium concentration of the products of combustion is calculated, the dissociations of carbon dioxide to carbon monoxide and oxygen, and of water vapour to hydrogen and oxygen being considered. The equilibrium constants, K_1 and K_2 , of these dissociations are defined respectively by -

$$K_1 = \frac{p_{CO} (p_{O_2})^{\frac{1}{2}}}{p_{CO_2}} \quad \dots\dots\dots \text{Eqn. I.16}$$

and

$$K_2 = \frac{p_{H_2} (p_{O_2})^{\frac{1}{2}}}{p_{H_2O}} \quad \dots\dots\dots \text{Eqn. I.17}$$

where p_{CO} , p_{O_2} , p_{H_2} and p_{H_2O} are the partial pressures, in atmospheres, of the components indicated.

To give a typical result, it is found that, at a temperature of 2400°K and a pressure of 1 atmosphere, 0.0113 lb./mols. of carbon dioxide and 0.0024 lb. mols. of water vapour dissociate per lb. of fuel.

From the equilibrium composition which is then obtained, the enthalpy and entropy per lb. of products, and the mean gas constant of the products, are calculated. For the example quoted above, these quantities have the values 791.7 C.H.U./lb. mixture, 2.316 entropy units/lb. mixture and 98.06 ft. x lb./lb. x °C. respectively.

From these, and similar results at the other temperature and pressure levels, an enthalpy - entropy graph

carrying lines of constant pressure and constant temperature is prepared for the products. A corresponding graph of Gas Constant against entropy is also drawn.

The total head enthalpy of the products of combustion is then calculated from the inlet air temperature and the fuel calorific value and enthalpy at injection. For an air inlet temperature of 600°K and a fuel/air ratio of 0.0667 by weight, the total head enthalpy of the products is calculated to be 787.6 C.H.U./lb. A total head pressure is then selected, say 3 atmospheres, giving a point on the entropy charts representing the total head conditions. An isentropic is then drawn through this point. The calculation now becomes one of trial and error. A number of heat drops, Δh , are chosen and the temperature and pressure and gas constant at Station 3 corresponding to each of the heat drops are read from the Entropy Charts. The gas velocity u is calculated from the heat drop (Equation I.15). These values of velocity, temperature, pressure and gas constant at Station 3 are then substituted in Equation I.14 giving a value of the air specific impulse, S_a , for each of the heat drops initially chosen. The minimum value which is obtained for the air specific impulse is the required one, and corresponds to choked conditions at Station 3. For the example chosen, the

minimum value of the air specific impulse is found to be 175.1 sec.

The value of the air specific impulse calculated in this way is, for practical purposes, independent of the value of stagnation pressure initially selected.

APPENDIX II.FLOW THROUGH A CAPILLARY METER

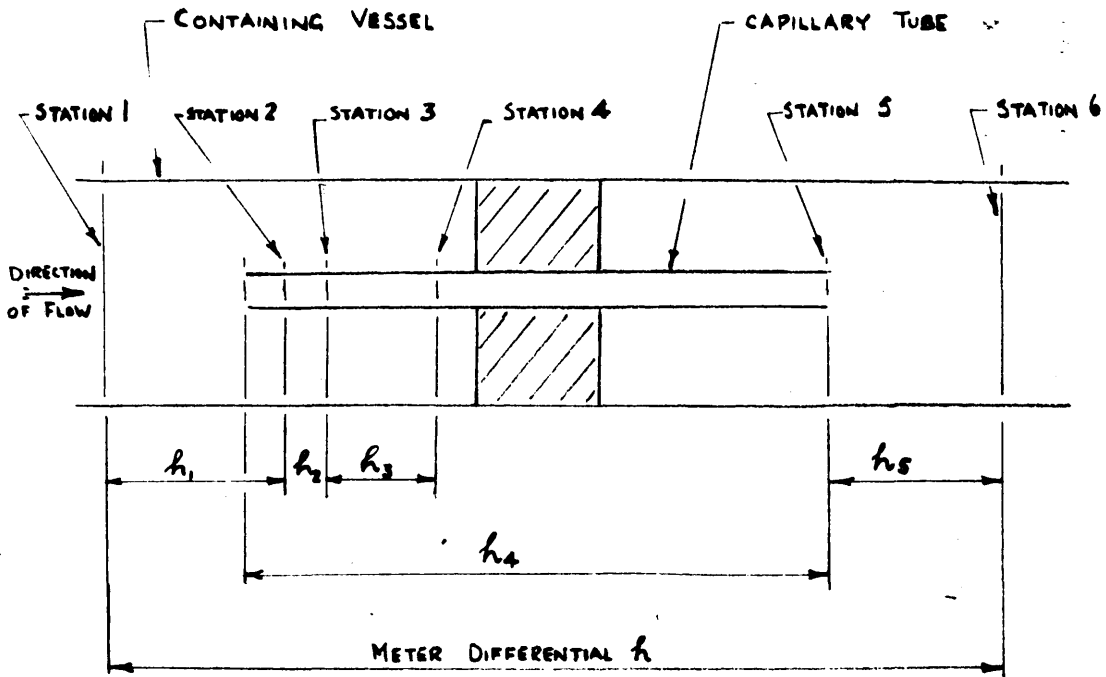
Capillary meters have been used to measure the flow rates of butane and air in the small scale experiments described in Chapters 4 and 5. Expressions are derived below which predict the volume flow rate through the meter in terms of the meter differential, the capillary tube length and bore, and the properties of the fluid. On calibrating these capillary meters against a standard such as a soap bubble meter it has been found that the relations obtained below may be in error by 10%. Thus the expressions do not yet provide a substitute for the time consuming calibration of every capillary meter against a standard. However, the expressions are useful as a guide to the dimensions of the meters necessary to cover a given flow range. The relationships also enable one to predict the influences of pressure and temperature changes on the calibration of a capillary meter.

Pressure changes along the capillary meter.

As an approximation, the pressure change across a capillary tube may be divided into the following components -

- (i) Pressure drop, h_1 from the inlet vessel conditions to the vena contracta,
- (ii) Pressure rise, h_2 in the expansion from the vena

FIG. 38 COMPONENTS OF PRESSURE DROP ACROSS A CAPILLARY METER



STATION 2 Vena Contracta

STATION 3 Flat Velocity Profile, filling tube bore

STATION 4 End of Transition Length,
ie "fully developed" velocity profile

Symbols h , h_2 , h_3 , h_4 and h_5 are explained in the text

contracta to the full bore of the capillary tube,

- (iii) Pressure drop, h_3 , due to change in the velocity distribution,
- (iv) Pressure drop, h_4 , due to friction along the wall of the capillary tube,
- (v) Pressure rise, h_5 , in the expansion from the capillary tube outlet to the outlet vessel.

The positions of these pressure changes in a typical capillary meter are shown in Fig. 38.

The capillary meter differential h is equal to the algebraic sum of the above components -

$$h = h_1 - h_2 + h_3 + h_4 - h_5 \quad \dots\dots\text{Eqn. II.1}$$

It is assumed in the treatment given below that the fluid is incompressible.

1. Pressure drop from the inlet vessel to the vena contracta.

Applying Bernoulli's theorem between stations 1 and 2 gives -

$$P_1 + \frac{\rho u_1^2}{2g} = P_2 + \frac{\rho u_2^2}{2g} \quad \dots\dots\text{Eqn. II.2}$$

where P_1 and P_2 are the absolute pressures at stations 1 and 2, u_1 and u_2 are the velocities at stations 1 and 2, ρ is the fluid density and g is the acceleration due to gravity.

Thus

$$h_1 = P_1 - P_2 = \frac{\rho}{2g} (u_2^2 - u_1^2) \quad \dots\dots\text{Eqn. II.3}$$

Now by continuity,

$$u_1 \rho \frac{\pi}{4} D^2 = u_2 \rho \frac{\pi}{4} d^2 \alpha = \bar{u} \rho \frac{\pi}{4} d^2 \quad \dots \text{Eqn. II.4}$$

where D is the diameter of the inlet vessel (also the diameter of the outlet vessel), α is the contraction coefficient to the vena contracta, and \bar{u} is the average velocity through the capillary tube.

Combining Equations II.3 and II.4 gives -

$$h_1 = \frac{\rho \bar{u}^2}{2g} \left[\frac{1}{\alpha^2} - \left(\frac{d}{D} \right)^4 \right] \quad \dots \text{Eqn. II.5}$$

For a sharp edged entry, α may be taken as 0.64 (Prandtl, Tietjens, 1934, p 52). Also, for all the meters used $(d/D)^4$ is less than 0.002 and may be omitted.

Thus

$$h_1 = 1.22 \frac{\rho \bar{u}^2}{g} \quad \dots \text{Eqn. II.6}$$

2. Pressure rise in expansion from the vena contracta to the full bore of the capillary tube.

Between stations 2 and 3 the pressure rise is given by -

$$\begin{aligned} h_2 = P_3 - P_2 &= \frac{\rho}{\frac{\pi}{4} d^2 g} \left(u_2^2 \frac{\pi}{4} d^2 \alpha - u_3^2 \frac{\pi}{4} d^2 \right) \\ &= \frac{\rho \bar{u}^2}{g} \left(\frac{1}{\alpha} - 1 \right) \quad \dots \text{Eqn. II.7} \end{aligned}$$

Substituting $\alpha = 0.64$ gives -

$$h_2 = 0.56 \frac{\rho \bar{u}^2}{g} \quad \dots \text{Eqn. II.8}$$

3. Pressure drop due to change in velocity distribution.

The velocity profiles developed in the tube and the laws governing the friction pressure drop are well established for

flows for which the Reynolds Number in the capillary tube is less than 2000, or is greater than 3000. In the intermediate range of Reynolds Numbers the friction pressure drop at any one flow rate is rather uncertain. To avoid this possible cause of irregularities in the calibrations, capillary meters, were never used within the range of Reynolds Numbers of 1800 to 3000.

The pressure drops due to the change in velocity distribution, and due to wall friction are calculated separately for laminar flow meters, and for turbulent flow meters.

(a) Laminar flow meters.

The Transition Length is the length of tube required to transform an initially flat velocity profile into one in which the velocity at the centre of the channel is within 1% of the central velocity for parabolic velocity distribution. The Transition Length X is given by (Prandtl, Tietjens, 1934, p.22) -

$$X = 0.065 d N_{Re} \quad \dots \text{Eqn. II.9}$$

where N_{Re} is the Reynolds Number.

For each of the meters used the Transition Length was less than the length of the capillary tube, and so it may be assumed that for each meter the flow had become parabolic at Station 4 (Fig. 38).

At Station 3, where the velocity profile is flat, the

flow of kinetic energy is given by

$$\frac{\pi}{4} \frac{d^2 \rho \bar{u}^3}{2g}$$

At Station 4, where the velocity profile is almost parabolic, the flow of kinetic energy is given by

$$\int_0^{\alpha/2} 2\pi y \frac{\rho u^3}{2g} dy = \frac{\pi}{4} \frac{d^2 \rho \bar{u}^3}{g}$$

where y is the radius of an elemental ring.

Thus

$$\begin{aligned} \frac{\pi}{4} d^2 (P_3 - P_4) \bar{u} &= \text{increase in flow kinetic energy} \\ &= \frac{\pi}{4} \frac{d^2 \rho \bar{u}^3}{2g} \end{aligned}$$

hence

$$h_3 = P_3 - P_4 = 0.5 \frac{\rho \bar{u}^2}{g} \quad \dots \text{Eqn. II.10}$$

(b) Turbulent Flow Meters.

The pressure drop due to the change from a flat velocity profile to a fully developed turbulent profile is given by (Prandtl, Tietjens, 1934, p.51)

$$h_3 = \frac{0.045 \rho \bar{u}^2}{g} \quad \dots \text{Eqn. II.11}$$

4. Pressure drop due to friction.

As an approximation it is assumed that the actual friction pressure drop is the same as the friction pressure drop with fully developed flow at the inlet to the tube.

(a) Laminar flow meters.

The pressure drop due to viscous drag is given by

(Prandtl, Tietjens, 1934, p 20) -

$$h_4 = \frac{32 \nu \rho \ell \bar{u}}{gd^2} \quad \dots \text{Eqn. II.12}$$

where ν is the kinematic viscosity of the fluid and ℓ is the length of the capillary tube.

(b) Turbulent flow meters.

The pressure drop due to friction in turbulent flow is given by (Lees, 1914) -

$$h_4 = \frac{\rho \bar{u}^2 \ell}{gd} \left[0.0036 + 0.31 \left(\frac{1}{N_{Re}} \right)^{0.35} \right] \quad \dots \text{Eqn. II.13}$$

5. Pressure rise in the expansion from the capillary tube outlet to the outlet vessel.

The gain in pressure in the expansion is given by -

$$h_5 = \frac{\rho \bar{u}^2}{g} \frac{d^2}{D^2} \left(1 - \frac{d^2}{D^2} \right) \quad \dots \text{Eqn. II.14}$$

The highest value of the multiplying factor $\frac{d^2}{D^2} \left(1 - \frac{d^2}{D^2} \right)$

encountered in the capillary meters is 0.03 and consequently this term may be omitted.

6. Meter differential

The meter differential h is given by

$$h = h_1 - h_2 + h_3 + h_4 - h_5 \quad \dots \text{Eqn. II.1}$$

For laminar flow meters Equation II.1 becomes

$$h = 1.22 \frac{\rho \bar{u}^2}{g} - 0.56 \frac{\rho \bar{u}^2}{g} + 0.50 \frac{\rho \bar{u}^2}{g} + \frac{32 \nu \rho \ell \bar{u}}{gd^2}$$

$$\text{i.e. } h = 1.16 \frac{\rho \bar{u}^2}{g} + 32 \frac{V \rho l \bar{u}}{g d^2} \dots \text{Eqn. II.15}$$

and for turbulent flow meters -

$$h = 1.22 \frac{\rho \bar{u}^2}{g} - 0.56 \frac{\rho \bar{u}^2}{g} + 0.045 \frac{\rho \bar{u}^2}{g} + \frac{\rho \bar{u}^2 l}{g d} \times$$

$$\text{i.e. } h = 0.70 \frac{\rho \bar{u}^2}{g} + \frac{\rho \bar{u}^2 l}{g d} \left[0.0036 + 0.31 \left(\frac{1}{N_{Re}} \right)^{0.35} \right] \dots \text{Eqn. II.16}$$

7. Application of meter equations for air and butane.

A fluid temperature of 20°C. and pressure of 76 cm. Hg. is representative of the average conditions met in a capillary meter. At that temperature and pressure, air and butane have the properties given below -

	Density gm/cm ³	Kinematic Viscosity cm ² /sec.
Air	1.204 x 10 ⁻³	0.151
Butane	2.49 x 10 ⁻³	0.034

Substituting these properties in Equations II.15 and II.16, and expressing the average velocity, \bar{u} , in terms of the volume flow rate, V, gives -

Laminar range.

$$\text{For air } h = 2.3 \times 10^{-6} \frac{V^2}{d^4} + 7.55 \times 10^{-6} \frac{lV}{d^4} \dots \text{Eqn. II.17}$$

$$\text{For Butane } h = 4.8 \times 10^{-6} \frac{V^2}{d^4} + 3.5 \times 10^{-6} \frac{\ell V}{d^4} \dots \text{Eqn. II.18}$$

Turbulent Range

$$\text{For Air } h = 1.40 \times 10^{-6} \frac{V^2}{d^4} + \frac{\ell V^2}{d^5} \times 10^{-6} \times$$

$$\left[0.0072 + 0.29 \left(\frac{d}{V} \right)^{0.35} \right] \dots \text{Eqn. II.19}$$

$$\text{For Butane } h = 2.9 \times 10^{-6} \frac{V^2}{d^4} + \frac{\ell V^2}{d^5} \times 10^{-6} \times$$

$$\left[0.015 + 0.35 \left(\frac{d}{V} \right)^{0.35} \right] \dots \text{Eqn. II.20}$$

8. Comparison with Benton's empirical correlation.

Benton (1919) found his results for air in laminar flow to be correlated by -

$$h = 2.44 \times 10^{-6} \frac{V^2}{d^4} + 7.57 \times 10^{-6} \frac{\ell V}{d^4} \dots \text{Eqn. II.21}$$

This expression is in very good agreement with the theoretical relationship derived above for air in laminar flow (Equation II.17).

APPENDIX IIITHE CALIBRATION AND USE OF SOAP BUBBLE METERS;WET GAS METERS AND DRY GAS METERS.

It has been found that the calibration of a capillary meter given by the theoretical expressions derived in Appendix II may be in error by about 10%. To give a more accurate calibration the capillary meter is calibrated against a standard meter. The standard meters used in this work are Soap Bubble Meters, Wet Gas Meters and a Dry Gas Meter. Before these standards were used they were themselves calibrated.

Calibration and use of standard meters.1. Soap Bubble Meters.

In a Soap Bubble Meter the volume flow rate is measured by the time taken for a soap film, placed across the gas flow, to travel from one scribed mark to another, the volume contained between the two scribed marks being known. This volume was determined by filling the Soap Bubble Meter with water up to the lower scribed mark, and adding water from a burette until the water level reached the upper mark, the volume between the scribed marks being given by the burette readings. The value of the volume between the scribed marks quoted by the manufacturers was found to be accurate for most of the meters when checked in this way. The maximum error found

was of 0.4% in the volume of one of the smaller Soap Bubble Meters.

When a Soap Bubble Meter is being used to measure a gas flow rate and so calibrate a capillary meter, the gas entering the Soap Bubble Meter generally has a relative humidity of less than 100%. It has been found, by dew point observations, that as the gas passes through the Soap Bubble Meter the relative humidity rises rapidly to a value above 90%. This causes a decrease in the partial pressure of the dry air, and consequently the volume flow rate at the Soap Bubble Meter is greater than that at the capillary meter. Thus the indicated volume flow rate given by the Soap Bubble Meter readings has to be corrected to give the true volume flow rate at the capillary meter. Graphs giving this correction have been prepared for various values of capillary meter humidity, and covering a range of capillary meter temperatures and of Soap Bubble Meter temperatures. An average relative humidity within the Soap Bubble Meter of 90% was assumed in calculating the correction.

It is important that the temperature of the gas within the Soap Bubble Meter should be close to the temperature of the gas at the capillary meter. While corrections can be made for temperature differences when known, the difficulty exists of estimating the average temperature within the Soap Bubble Meter. For this reason a Soap Bubble Meter should not be used when

under the direct rays of the sun.

The volumes of the Soap Bubble Meters used in this work ranged from 5 to 2000 ml. These meters were employed to measure flow rates ranging from 0.04 to 100 ml/sec.

2. Wet Gas Meters.

The Wet Gas Meters were used to measure flow rates higher than those that could be measured by Soap Bubble Meters.

It has been found that, when gas flows through a Wet Gas Meter, the Wet Gas Meter registers the flow of the gas when it is at the temperature of the water within the Wet Gas Meter and saturated with water vapour. This was shown in the following way. A steady flow of air was passed through two Wet Gas Meters connected in series. Care was taken to ensure that the water in both meters was at the same temperature. Assuming that the indicated volume per revolution of the first Wet Gas Meter was correct, the volume of gas passing per revolution of the second meter was determined. The water in the second Wet Gas Meter was then drained off, and the Meter refilled with water at a temperature about 10°C . higher than that of the water in the first Wet Gas Meter. The air flow connections were remade, and the revolution speeds of the two Wet Gas Meters were again observed. The results of this second test could only be brought into agreement with the results of the uniform temperature test by assuming that, in each case, the Wet Gas Meter measured the flow rate of air at the

temperature of the water in the Wet Gas Meter and saturated with water vapour.

This hypothesis that a Wet Gas Meter measures the gas flow rate when the gas is at the temperature of the water in the Meter, and is saturated with water vapour, was supported by readings of thermometers placed at several positions in the second Wet Gas Meter. These readings confirmed that the air reached the temperature of the water in the Meter. Also, observations of the dew point of air leaving a typical Wet Gas Meter showed that the air was, within experimental error, saturated with water vapour.

The Wet Gas Meters were calibrated in the following manner. A Wet Gas Meter having a nominal volume per revolution of 2.5 litres was selected. This Meter was calibrated by two methods. Firstly it was calibrated against a standard Soap Bubble Meter by connecting the Soap Bubble Meter to the outlet from the Wet Gas Meter and passing a steady flow of air through both Meters. No humidity corrections were necessary in this experiment since the air which entered the Soap Bubble Meter had already been saturated with water vapour in the Wet Gas Meter. The volume of gas passed per revolution of the Wet Gas Meter was calculated from this calibration to be 2.484 litres. In the second calibration test, a known volume of air, saturated with water vapour, was displaced by water from a vessel, and passed through the Wet Gas Meter. From the movement of the pointers, the volume passing per revolution was calculated to be 2.476

litres. The results of these two methods of calibration are seen to agree to within 0.3%. The Meter thus calibrated was then used to calibrate a Wet Gas Meter having a nominal capacity of 10 litres per revolution. This 10 litre Meter was then used to calibrate a 25 litre Wet Gas Meter.

When a Wet Gas Meter is being used to calibrate a capillary meter the gas entering the Wet Gas Meter from the capillary meter normally is not saturated with water vapour. A correction has to be applied to the volume flow rate indicated by the Wet Gas Meter to give the true volume flow rate at the capillary meter. Another correction is also necessary if a difference exists between the temperatures of the capillary meter and of the Wet Gas Meter. Graphs have been prepared from which these corrections can be read for a range of temperature conditions, and of relative humidities at the capillary meter.

The error which can exist in the setting of the water level within the Wet Gas Meter imposes a limitation on the accuracy that can be achieved with Wet Gas Meters. For example, in the case of the 2.5 litre Wet Gas Meter, an error of 0.02 inch may be present in the setting of the water level, and this causes an error of 0.4% in the volume of gas passed per revolution of the meter.

Wet Gas Meters were used for calibrating capillary meters in the flow range 40 to 800 ml/sec.

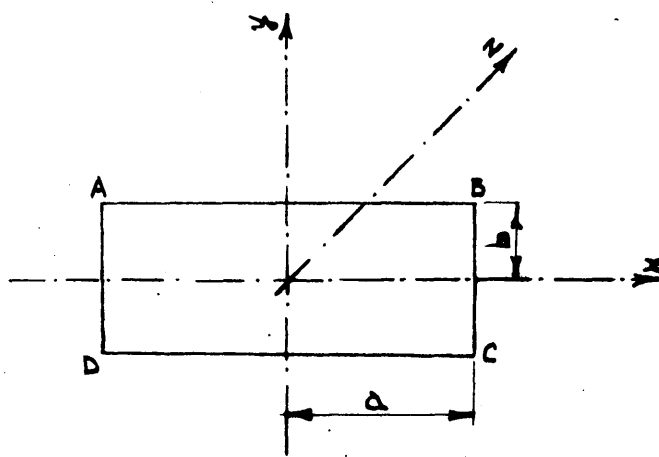
Dry Gas Meter.

A Dry Gas Meter was used for measuring flows in the range 600 to 1200 ml/sec.

The Dry Gas Meter was calibrated by connecting the Meter to the outlet of the 25 litre Wet Gas Meter and passing a steady flow of air through both meters. No evaporation takes place within the Dry Gas Meter, and as the temperature in the Dry Gas Meter exceeded the temperature of the water in the Wet Gas Meter, only temperature corrections were necessary in determining the volume per revolution of the Dry Gas Meter.

When the Dry Gas Meter is being used to calibrate a capillary meter the only correction required is for differences between the temperatures of the capillary meter and of the Dry Gas Meter.

FIG. 39 DIMENSIONS OF CHANNEL HAVING RECTANGULAR CROSS-SECTION



APPENDIX IV.LAMINAR FLOW IN A CHANNEL OF RECTANGULAR CROSS-SECTION.

The velocity distribution in fully developed laminar flow in a channel of rectangular cross-section has been solved by Cornish (1928). The derivation of the equation giving the local velocity is given below. This expression was used in paragraphs 5.3 and 5.4 of Chapter 5.

Consider flow in a channel of rectangular cross-section, as shown in Fig. 39. Let a be the half cross-sectional length (in the x direction), b the half cross sectional width (in the y direction), and u the velocity (in the z direction) at the point (x, y) .

The general equations of motion in viscous flow reduce to:-

$$\frac{\partial p}{\partial x} = 0 \quad \dots\dots\text{Eqn. IV.1}$$

$$\frac{\partial p}{\partial y} = 0 \quad \dots\dots\text{Eqn. IV.2}$$

$$\text{and } \frac{\partial p}{\partial z} = \tau \left(\frac{\partial^2 u}{\partial x^2} + \frac{\partial^2 u}{\partial y^2} \right) \quad \dots\dots\text{Eqn. IV.3}$$

where $\frac{\partial p}{\partial z}$ is the pressure gradient and τ is the absolute viscosity.

$$\text{Let } \tau = - \frac{1}{2\eta} \frac{\partial p}{\partial z} \quad \text{and } u = \chi + \tau (b^2 - y^2)$$

Equation IV.3 then becomes -

$$\frac{\partial^2 \chi}{\partial x^2} + \frac{\partial^2 \chi}{\partial y^2} = 0 \quad \dots\dots\text{Eqn. IV.4}$$

At the boundary $u = 0$ i.e. $\chi + \tau (b^2 - y^2) = 0$

Along AB and DC $\chi = 0$ Eqn. IV.5

and along AD and BC $\chi + \tau (b^2 - y^2) = 0$Eqn. IV.6

From Equation IV.5, the terms which form the function χ must vanish when $y = \pm b$. This condition is satisfied if χ consists of terms such as $\epsilon \psi \cos \frac{2n+1}{2b} \pi y$, where ϵ is a function of τ only, and ψ is a function of x only. n is an integer.

For simplicity at this stage, m is substituted for $\pi(2n+1)/2b$.

Thus $\chi = \sum \epsilon \psi \cos m y$.

Substituting in Equation IV.4 gives -

$$\frac{\partial^2 \psi}{\partial x^2} - m^2 \psi = 0 \quad \text{.....Eqn. IV.7}$$

This equation is satisfied by the solution -

$$\psi = A_n \cosh mx + B_n \sinh mx$$

where A_n and B_n are constants.

By symmetry about the y axis, $B_n = 0$, so the solution becomes -

$$\psi = A_n \cosh mx \quad \text{.....Eqn. IV.8}$$

Hence χ consists of terms such as $\epsilon A_n \cosh mx \cos m y$

$$\text{where } m = \frac{2n+1}{2b} \pi$$

To simplify the application of this type of term to the second boundary condition (Equation IV.6) a new variable, θ , is introduced to replace y , where

$$y = \frac{2b \theta}{\pi} \quad \text{.....Eqn. IV.9}$$

$$\text{Thus } \chi = \sum_{n=0}^{\infty} C_n A_n \text{ Cosh } \frac{(2n+1)\pi x}{2b} \text{ Cos } (2n+1) \theta \quad \dots \text{Eqn. IV.10}$$

Substituting Equation IV.9 in the second boundary condition (Equation IV.6) gives -

$$\chi = \frac{\tau_0 b^2}{\tau^2} \left(\theta^2 - \frac{\pi^2}{4} \right) \quad \dots \text{Eqn. IV.11}$$

Equation IV.11 must agree with Equation IV.10 when $x = \pm a$, i.e. with

$$\chi = \sum_{n=0}^{\infty} C_n A_n \text{ Cosh } \frac{(2n+1)\pi a}{2b} \text{ Cos } (2n+1) \theta \quad \dots \text{Eqn. IV.12}$$

Equation IV.11 may be expanded in the Fourier Series -

$$\chi = - \frac{32\tau_0 b^2}{\pi^3} \left[\text{Cos } \theta - \frac{1}{3^3} \text{Cos } 3\theta + \frac{1}{5^3} \text{Cos } 5\theta \dots \right] \quad \dots \text{Eqn. IV.13}$$

Comparison of the coefficients in Equations IV.12 and IV.13 gives A_0, A_1 etc. whence -

$$\chi = - \frac{32\tau_0 b^2}{\pi^3} \left[\frac{\text{Cosh } \frac{\pi x}{2b}}{\text{Cosh } \frac{\pi a}{2b}} \text{Cos } \frac{\pi y}{2b} - \frac{1}{3^3} \frac{\text{Cosh } \frac{3\pi x}{2b}}{\text{Cosh } \frac{3\pi a}{2b}} \text{Cos } \frac{3\pi y}{2b} + \dots \right]$$

.....Eqn. IV.14

Bringing the original terms of velocity, pressure gradient and viscosity into Equation IV.14 gives -

$$u = - \frac{1}{2\gamma} \frac{dp}{dz} \left[(b^2 - y^2) + \frac{32b^2}{\tau^3} \sum_{n=0}^{\infty} \frac{(-1)^{n+1} \text{Cosh } \frac{(2n+1)\pi x}{2b} \text{Cos } \frac{(2n+1)\pi y}{2b}}{(2n+1)^3 \text{Cosh } \frac{(2n+1)\pi a}{2b}} \right]$$

.....Eqn. IV.15

This equation gives the velocity at the point (x, y) in terms of the pressure gradient, the viscosity, and the geometry of the channel cross-section, and is used in this form in Chapter 5.

BIBLIOGRAPHY.

- BARRERE, M., and
MESTRE, A. (1954) "Stabilization des
Flammes par des
Obstacles." Selected Combustion
Problems, p.426,
AGARD, London,
Butterworths Scienti-
fic Publications.
- BEETON, A.B.P.,
(1949) Unpublished work at the Royal Aircraft
Establishment, Farnborough.
- BENTON, A.F.,
(1919) "Gas flow meters for small rates of
flow" Industr. Engng. Chem.,
Vol. II, p.623
- BERL, W.G.,
RICE, J.L., and
ROSEN, P. (1955) "Flames in Turbulent
Streams". J.Amer. Rocket Soc.
Vol. 25, p.341.
- BOLLINGER, L.M.,
and
WILLIAMS, D.T.
(1947) "Experiments on
Stability of Bunsen
Burner flames for
turbulent flow." Natl. Advisory Comm.
Aeronaut. Tech. Note
1234.
- BROEZE, J.J.,
(1949) "Theories and
phenomena of flame
propagation." Third Symposium on
Combustion, Flame
and Explosion
Phenomena, p.146,
Baltimore, Williams
& Wilkins.
- CORNISH, R.J.,
(1928) "Flow in a pipe of
rectangular cross-
section." Proc. Roy. Soc. A120,
p.691.
- DAMKOHLER, G.
(1947) "The effect of
turbulence on the
flame velocity in
gas streams." Translated in Natl.
Advisory Comm.
Aeronaut. Tech. Memo.
1110 (1947)
- DEZUBAY, E.A.
(1950) "Characteristics of
disc controlled
flame". Aero Digest, Vol. 61.
No. 1 p.54.
- DIXON-LEWIS, G.
and
WILSON, M.J.G.
(1951) "A method for the
measurement of the
temperature distri-
bution in the inner
cone of a bunsen
flame." Trans. Faraday Soc.
Vol. 47., p. 1106.

- DUNLAP, R.A.
(1950) "Resonance of a flame in a parallel walled combustion chamber". University of Michigan, Aeronautical Research Center, UMM-43.
- ERGUN, S.
(1953) "Precision measurements of gas flow rates." Analytical Chemistry, Vol. 25, p.790
- FENN, J.B.
(1955) Private communication, August, 1955.
- FRIEDMAN, R.
(1953) "Kinetics of the combustion wave". J.Amer. Rocket Soc. Vol. 25, p.276.
- GAYDON, A.G.,
and
WOLFARD, H.G.
(1948) "The influence of diffusion on flame propagation." Proc. Roy. Soc. A196, p.105.
- GRUMER, J.,
HARRIS, M.E.,
and SCHULTZ, H.
(1953) "Flame stabilization on burners with short ports or non-circular ports". Fourth Symposium on Combustion, p.695, Baltimore, Williams & Wilkins.
- KARLOVITZ, B.
(1954) "A turbulent flame theory derived from experiments." Selected Combustion Problems. p.248, AGARD, London, Butterworths Scientific Publications.
- KARLOVITZ, B.,
DENNISTON, D.W., Jr.
KNAPSCHAEFFER, D.H.
& WELLS, F.E.
(1953) "Studies on turbulent flames." Fourth Symposium on Combustion, p.613, Baltimore, Williams & Wilkins.
- KARLOVITZ, B.,
DENNISTON, D.W.Jr.
& WELLS, F.E.
(1951) "Investigation of turbulent flames." J.Chem. Phys. Vol. 19, p.541
- LEES, C.H.
(1914) "On the flow of viscous fluids through smooth circular pipes". Proc. Roy. Soc. A91, p.46.
- LEES, I.
(1954) "Fluid-mechanical aspects of flame stabilization." J.Amer. Rocket Soc. Vol. 24, p.234.
- LEWIS, B. and
von EIBE, G.
(1943) "Stability and structure of burner flames". J.Chem. Phys. Vol. II, p.75.

- LEWIS, B. and
von ELBE, G.
(1951) "Combustion, flames
and explosions of
gases." 1st Edition, New
York, Academic Press
Inc.
- LINNETT, J.W.
(1954) "Some experimental
results relating to
laminar flame
propagation." Selected Combustion
Problems, p.92,
AGARD, London.
Butterworths
Scientific Public-
ations.
- LLOYD, P.
(1948) "Determination of gas
turbine combustion
chamber efficiency by
chemical means." Trans. Amer. Soc.
Mech. Engrs. Vol.70,
p.335.
- LONGWELL, J.P.,
(1953) "Flame stabilization by
bluff bodies and
turbulent flames in
ducts." Fourth Symposium on
Combustion, p.90,
Baltimore, Williams
& Wilkins.
- LONGWELL, J.P.
(1955) "Flame stabilization
and flame propagation
in ramjet combustors." Combustion Researches
and Reviews, 1955,
p.58, AGARD, London,
Butterworths
Scientific Publica-
tions.
- LONGWELL, J.P.,
CHENEVEY, J.E.,
CLARK, W.W., and
FROST, E.E.
(1949) "Flame stabilization by
baffles in a high
velocity gas stream." Third Symposium on
Combustion, Flame
and Explosion
Phenomena, p.40,
Baltimore, Williams
& Wilkins.
- LONGWELL, J.P.,
FROST, E.E. and
WEISS, M.A. (1953) "Flame stability in
bluff body recircul-
ation zones", Industr. Engng. Chem.
Vol. 45, p.1629
- McADAMS, W.H.
(1942) "Heat Transmission" 2nd Edition, New York,
McGraw-Hill.
- MORLEY, A.W.
(1953) "Aircraft Propulsion". 1st Edition, London,
Longmans, Green & Co.
- MULLEN, J.W. II.
FENN, J.B. and
GARMON, R.C.
(1951) "Burners for supersonic
ramjets." Industr. Engng. Chem.
Vol. 43. p. 195.

- OLSEN, F.L. and
GAYHART, E.L.
(1955) "Incipient flame
propagation in a
turbulent stream." J.Amer. Rocket Soc.
Vol. 25, p.276
- PRANDTL, L.,
TIETJENS, O.G.
(1934) "Applied Hydro and
Aeromechanics." 1st Edition, New
York, McGraw-Hill.
- PROBERT, R.P.
(1955) "Application of Research
to Gas Turbine combust-
ion problems." Jt. Conference on
Combustion, I.Mech.
E., and A.S.M.E.,
1955.
- SCURLOCK, A.C.
(1948) "Flame stabilization and
propagation in high
velocity gas streams". Massachusetts Inst.
Tech. Meteor Report
No. 19
- SMITH, R.W. Jr.
EDWARDS, H.E., and
BRINKLEY, S.R. Jr.
(1952) "Velocity distribution
in rectangular
channels." U.S. Bureau of Mines
Report of
Investigations 4885.
- SPALDING, D.B.
(1953) "Theoretical aspects of
flame stabilization." Aircr. Engng.
Vol. 25, p.264
- SPALDING, D.B.
(1954) Discussion on "Technical
Combustion Problems." Selected Combustion
Problems, p.517,
AGARD, London,
Butterworths Scient-
ific Publications.
- SPALDING, D.B.
and
TALL, B.S.
(1954) "Flame stabilization in
high velocity gas
streams and the effect
of heat losses at low
pressures." Aero. Quart. Vol. 5,
p.195
- SUMMERFIELD, M.,
REITER, S.H.,
KEBELY, V., and
MASCOLO, R.W.
(1955) "The structure and
propagation mechanism
of turbulent flames in
high speed flow." J. Amer. Rocket Soc.
vol. 25, p.377.
- TANFORD, C.
(1947) "Theory of burning velocity I.
Temperature and free
radical concentrations
near the flame front,
relative importance of
heat conduction and
diffusion." J.Chem. Phys.
Vol. 15,
p.433

- TANFORD, C.
(1949) "The role of free atoms and radicals in burner flames." Third Symposium on Combustion, Flame and Explosion Phenomena, p.140 Baltimore, Williams & Wilkins.
- TANFORD C,
and
PEASE, R.N.
(1947a) "Equilibrium atom and free radical concentrations in carbon monoxide flames, and correlation with burning velocity". J. Chem. Phys. Vol. 15, p.431
- TANFORD, C. and
PEASE, R.N.
(1947b) "Theory of burning velocity II. The square root law for burning velocity." J.Chem. Phys. Vol.15 p.861.
- THOMSON, J.J.
and
THOMSON, G.P.
(1928) "Conduction of electricity through gases." 3rd Edition, Vol. 1, Cambridge University Press.
- TSIEN, H.S.
(1951) "Influence of flame front on the flow field." J.App. Mech. Vol.18 p.188.
- WILKERSON, E.C.
and
FENN, J.B.
(1953) "The effect of flame holder geometry on combustion efficiency in ducted burners." Fourth Symposium on Combustion, p.749, Baltimore, Williams & Wilkins.
- WILLIAMS, G.C.
and
SHIPMAN, C.W.
(1953) "Some properties of rod-stabilized flames of homogeneous gas mixtures." ibid, p.733
- WILSON, H.A.
(1931) "Electrical conductivity of flames." Reviews of Modern Physics, Vol. 3, p.156
- WOHL, K.
(1953) "Quenching, Flash-back, Blow-off - Theory and Experiment." Fourth Symposium on Combustion, p.68, Baltimore, Williams & Wilkins.
- WOHL, K.,
KAPP, N.M.
and
GAZLEY, C.
(1949) "The stability of open flames." Third Symposium on Combustion, Flame and Explosion Phenomena, p.3, Baltimore, Williams & Wilkins.

WOHL, K.,
SHORE, L.
von ROZENBERG, H.
& WEIL, C.W.
(1953)

"The burning velocity
of turbulent flames."

Fourth Symposium
on Combustion,
p.620, Baltimore,
Williams & Wilkins.

ZUKOSKI, E.E.
& MARBLE, F.E.,
(1955)

"The role of wake
transition in the process
of flame stabilization by
bluff bodies."

Combustion Researches
and Reviews, 1955,
p.167, AGARD,
London, Butterworths
Scientific
Publications.

LIST OF TABLES.

<u>Table.</u>	<u>Title.</u>	<u>Opposite Page.</u>
1	Results of sampling tests.	39
2	Spreader arrangements and tailpipes used in combustion efficiency measurements.	50
3.	Combustion efficiencies in 1.875 inch diameter ramjet.	61
4.	Analysis of a typical sample of "Stenched Butane"	66
5	Ionisation Probe Calibrations - Ranges of conditions.	82
6	Blow off velocities predicted by method of Grumer et al (1953)	92
7	Values of functions P and Q	98

LIST OF FIGURES.

<u>Figure No.</u>	<u>Title.</u>	<u>Opposite Page.</u>
1	Flame propagation.	5
2	Stabilisation of a fuel-weak flame on a bunsen burner	9
3	Stabilisation of a fuel-rich flame on a bunsen burner	11
4	Flame stabilization by a can	17
5	Influence of mixing and of pilot heat on combustion efficiency	26
6a, 6b.	Open Jet Apparatus: Pilot Stability Limits	30
7	Flame Appearance in flame spreading systems.	33
8	Tailpipe Apparatus	40
9	Ideal ramjet combustion system	40
10	Theoretical fuel/air ratio as a function of Air Specific Impulse	42
11	Influence of spreader on combustion efficiency	42
12	Influence of pilot fuel/air ratio on combustion efficiency	51
13	Influence of tailpipe length on combustion efficiency	53
14	Influence of number of fingers and width of fingers on combustion efficiency	54
15	Influence of finger inclination on combustion efficiency	57
16	Influence of spreader position on combustion efficiency	57

<u>Figure No.</u>	<u>Title.</u>	<u>Opposite Page.</u>
17	Influence of spreader shape on combustion efficiency	59
18	Overall stability limits	59
19	Volume flow rate through a capillary meter	67
20	Blow off from wire stabilisers.	71
21	Apparatus for testing inclined wire stabiliser	72
22	Blow off from wire stabilisers with flame pilot	73
23	Preliminary Ionisation Probe circuit	77
24	Influence of probe polarity on signal	77
25	Sketch of Ionisation Probe	79
26	Electronic Circuits - Ionisation Probe	79
27	Laminar burners for calibration of Ionisation Probe	80
28	Apparatus used in the calibration of the Ionisation Probe	82
29	Typical schlieren image of a laminar flame	82
30	Comparison of direct and schlieren images of a laminar flame.	82
31	Calibration of Ionisation Probe in Laminar Flames.	83
32	Flame Blow-off Photographs	95
33	Blow off from rectangular burners	98
34	Stability limits of rectangular burners	99
35	Velocities at blow off from 2.00 x 0.125 inch burner	101

<u>Figure No.</u>	<u>Title</u>	<u>Opposite Page.</u>
36	Blow off from rectangular burners	101
37	Friction Coefficient in rectangular channels	102
38	Components of pressure drop across a capillary meter	121
39	Dimensions of channel having rectangular cross section.	134

LIST OF SYMBOLS.

<u>SYMBOL.</u>	<u>Pages.</u>
a	97, 134
A	17, 113
b	93, 134
B	25
c_p	6
C	25
d	67, 92, 121
d_L	22
d_T	22
D	15, 122
E	25
g	66, 92, 113, 121
ϵ_{av}	101
ϵ_c	98
h	25, 66, 121
J	116
k	6
K	25, 117
l	67, 125
L	7
m	113, 135
M_1 M_2	41, 114
n	15, 135

Number of page on which first defined.

<u>Symbols.</u>	<u>Pages.</u>
N_{Re}	67, 92, 125
p	117
P	17, 98, 113, 121
q	17
Q	7, 102
R	42, 113
\bar{R}	25
S_a	41, 112
S_L	6
S_T	20
S_u	95
T	113
T_t	42, 114
T_1	6
T_u	6
T_b	6
u	97, 113, 121, 134
\bar{u}	93, 122
u'	20
U_{BO}	15
V	17, 66, 92, 126
x	134
X	94, 123
y	124, 134
z	134

<u>Symbols.</u>	<u>Pages.</u>
α	115, 122
γ	41
ϵ	20, 135
η	67
η_c	25
θ	135
λ	41, 92, 114
ν	20
ρ	6
τ	134
χ	134
ψ	135
$\frac{dp}{dz}$	97, 134
ΔH	116